6-11-2015

Accentuating Death Signaling in Colon Cancer Cells: A Chemical Biology Approach

Avijeet S. Chopra
University of Connecticut - Storrs, aschopra89@gmail.com

Accentuating Death Signaling in Colon Cancer Cells: A Chemical Biology Approach

Avijeet Singh Chopra, PhD

University of Connecticut, 2015

Colon cancers harbor a variety of mutations that result in uncontrolled proliferation and suppression of apoptotic pathways. The initial objective of our work was to understand how colon cancer cells survive their inflammatory micro-environment, including high levels of TNF and other death ligands. Towards this goal, we identified a series of mitotically acting piperazine-based compounds that sensitized colon cancer cells to TNF-dependent apoptosis. The most potent of these compounds, 1-(3-chlorophenyl)-4-(2-ethoxybenzoyl)piperazine or AK301, arrested cells in a mitotic state ($EC_{50} \approx 115$ nM) in which the TNF receptor was efficiently coupled to caspase-8 activation. Our structure-activity relationship studies predicted AK301 binding to β-tubulin in a novel orientation that reduced the rate of tubulin polymerization. These data suggested that targeting mitosis may be an effective approach for sensitizing cancer cells to their inflammatory microenvironment. Further study of the activity of AK301 showed that p53-normal colon cancer cells efficiently underwent apoptosis in the absence of death ligands following release from their mitotic arrest. Study of this effect indicated that AK301-treated cells showed high levels of ATM signaling during mitotic arrest and exit from mitosis, following compound withdrawal, resulted in a p53-dependent apoptosis. Interestingly, the apoptotic activity of AK301 was more apparent in *APC* mutant cells, suggesting that AK301 exacerbated the mitotic defects associated with an *APC* mutation. This work details the identification and structure-activity relationship studies of a new class of small molecule compounds and explores their anti-mitotic activity and provides a paradigm for exploiting molecular alterations in mutated cells. These findings could serve as a basis for the development of agents that target the

molecular alterations in mutated colon cancer cells and augment the apoptotic actions of their inflammatory microenvironment, for robust activation of apoptotic signaling. Understanding the mechanisms cancer cells use to suppress apoptosis may ultimately facilitate in the development of novel approaches to colon cancer treatment and prevention.

Accentuating Death Signaling in Colon Cancer Cells: A Chemical Biology Approach

Avijeet Singh Chopra

B.S., University of Kansas, 2011

A Dissertation

Submitted in Partial Fulfillment of the

Requirements for the Degree of

Doctor of Philosophy

at the

University of Connecticut

2015

APPROVAL PAGE

Doctor of Philosophy Dissertation

Accentuating Death Signaling in Colon Cancer Cells: A Chemical Biology Approach

Presented by

Avijeet Singh Chopra, B.S.

Major advisor

_____

Charles A. Giardina

Associate advisor

_____

Daniel W. Rosenberg

Associate advisor

_____

Brian Aneskievich

University of Connecticut
2015

ACKNOWLEDGEMENTS

I would have never been able to finish my dissertation without the help from my committee members and support of my family. I am grateful for all of their efforts, over the years, in shaping the individual I am today. First, I would like to express my deepest gratitude to Charles Giardina for being not only being an advisor and a mentor, but also a friend. I thank him for giving me an opportunity to work in his laboratory and helping me develop as a scientist. I have always looked up to him for his keen insight, encouragement, and motivation, which has helped me realize my goals.

I would like to thank my parents, Satinder and Tarvinder, and my sister, Ishveen, for their encouragement, love, and support from my childhood through my entire graduate school. I dedicate this degree to them. A special thanks to my sister for her intellectual support and guidance, and for being there through my hardships and my successes.

I would also like to thank members of my committee, Dr. Daniel Rosenberg for his feedback, encouraging remarks, and guidance, Dr. Brian Aneskievich for his insightful feedback, Dr. Amy Anderson for taking time and patiently explaining things multiple times, and Dr. Dennis Wright for his continual support and a great collaboration. Each of you have truly contributed to making this project a possibility and my graduate school a memorably collaborative experience. Last, but not the least, I would like to express my sincere gratitude to Dr. Carol Norris, who spent time training me and helping me setup and troubleshoot various microscopy and flow cytometry experiments. It’s hard to imagine completion of any of these projects without her assistance.

Finally, I would like to thank present and past members of the Giardina lab, who have taught me techniques and helped troubleshoot various protocols. I would, especially, like to

thank our undergraduate research assistant, Michael Bond, who helped me with managing some of my experiments as well as for all the fruitful conversations that have opened doors to new projects. I have learned and re-learned a lot of basic science through our conversations.

TABLE OF CONTENTS

LIST OF TABLES

LIST OF FIGURES

LIST OF ABBREVIATIONS

5-ASA	5-aminosalicylic acid
AD Vina	AutoDock Vina
ANOVA	analysis of variance
AOM	azoxymethane
APC	Adenomatous polyposis coli
ARF	Alternative Reading Frame
ATM	ataxia telangiectasia mutated
AukA	Aurora kinase A
BUB1B	Budding uninhibited by benzimidazoles 1 homolog beta
BIRC	Baculoviral IAP repeat-containing
CASPASE	cysteine aspartate-directed protease
CBQCA	3-(4-carboxybenzoyl)-2-quinolinecarboxaldehyde
CDK	Cyclin-dependent kinase
CHAPS	3-[(3-cholamidopropyl)dimethylammonio]-1-propanesulfonate
CHFR	Checkpoint with forkhead and ring finger domains
CIN	chromosomal instability
CRC	colorectal cancer
CTLs	cytotoxic T cells
Cy3	indocarocyanine 3
DAPI	4’,6-diamidino-2-phenylindole
DEVD-AMC	acetyl-Asp-Glu-Val-Asp-7-Amino-4-methylcouramin
DNA	deoxyribonucleic acid

DISC	Death-inducing signaling complex
DR	Death receptor
DSS	dextran sulfate sodium
DTT	dithiothreitol
EB1	End binding protein 1
EC_{50}	half maximal effective concentration
ED_{50}	half maximal effective dose
EDTA	ethylenediaminetetraacetic acid
EGFP	enhanced green fluorescent protein
EGTA	ethylene glycol tetraacetic acid
FAP	familial adenomatous polyposis
Fas	Fatty acid synthase
FasL	Fatty acid synthase ligand
FITC	fluorescein isothiocyanate
FOLFOX	folinic acid, fluorouracil (5-FU), and oxaliplatin
GFP	green fluorescent protein
GM-CSF	granulocyte-macrophage colony-stimulating factor
GTP	guanosine triphosphate
HDAC	histone deactylase
HNPCC	hereditary non-polyposis colorectal cancer
IAP	inhibitor of apoptosis
IC_{50}	half maximal inhibitory concentration
IMCEs	Immorto-Mouse Colonic Epithelial [cells]

IL2	Interleukin 2
IL6	Interleukin 6
INK4A	Inhibitor of CDK4A
LD_{50}	Half maximal lethal dose
MAPs	Microtubule associated proteins
MFI	mean fluorescence intensity
$MgCl_2$	magnesium chloride
MHC	major histocompatibility complex
MLH1	MutL homolog 1
MTOC	microtubule organizing center
MTSB	microtubule stabilizing buffer
MVD	Molegro Virtual Docker
$NaBH_4$	sodium borohydride
NaCl	sodium chloride
NFκB	Nuclear factor kappa-light-chain-enhancer of activated B cells
NMR	nuclear magnetic resonance
NK cells	natural killer cells
NP40	nonidet P40
NSAIDs	nonsteroidal anti-inflammatory drugs
OD	optical density
PBS	phosphate buffered saline
PCR	polymerase chain reaction
PDB	Protein Data Bank

p-HH3 Ser 28	phospho-histone H3 serine 28
PFA	paraformaldehyde
PI	propidium iodide
PIPES	piperazine-N,N'-bis(2-ethanesulfonic acid)
PLK1	Polo-like kinase 1
RIPA	radioimmunoprecipitation assay
RNA	ribonucleic acid
RT	room temperature
SAC	spindle assembly checkpoint
SAHA	suberanilohydroxamic acid
SAR	structure-activity relationship
SEM	standard error of mean
TCR	T cell receptor
TNF	Tumor necrosis factor
TNFR1	Tumor necrosis factor receptor 1
TRAIL	Tumor necrosis factor-related apoptosis-inducing ligand
TRAIL-R	TRAIL receptor
TRIS-HCl	2-amino-2-hydroxymethylpropane-1,3-diol hydrochloride
UC	ulcerative colitis
YAMCs	Young Adult Mouse Colonocytes

CHAPTER 1

Introduction

1.1. Colorectal cancer – prevalence and significance

Colorectal cancer is the third most common cancer in the United States with an estimated 1.3 million people being afflicted in the US alone in 2014 [1, 2]. It is the second leading cause of cancer-related deaths in the US, with an estimated 50,000 deaths in 2014 [2]. Periodic colon cancer screening and the removal of early polyps and other lesions has been demonstrated to reduce the risk of death from colon cancer by up to 53% [3, 4]. Screening exams can also find early cancers, which increases the likelihood of survival—five-year survival for patients diagnosed with colon cancer at an early stage is 74%, but drops to only 6% for metastatic colon cancer [3, 5]. For early (stage 1 lesions), surgery is usually sufficient to cure the disease. Some drug combinations, such as FOLFOX, are used along with surgery to treat more advanced colon cancers [6]. Unfortunately, these regimens have sere side effects and may not completely eliminate colon cancer.

The U.S. Preventive Services Task Force (USPSTF) recommends regular screening for colorectal cancer beginning at age 50, by fecal occult blood testing, sigmoidoscopy, or colonoscopy [7]. Patients with familial adenomatous polyposis (FAP), hereditary non-polyposis colorectal cancer (HNPCC), or a family history of colon cancer are advised to undergo colon cancer screening earlier and more frequently (before the age of 50) [8, 9]. However, even with careful screening and treatment, the rate of colon polyp recurrence can be high. After three years, almost one third of the patients showing a polyp on an initial screening exam will have already developed another; after 5 years, this probability increases to ~50% [10]. These data indicate that

some individuals may be advised to undergo examinations even more frequently than every five years. These data have also prompted the search for strategies that can reduce the frequency of polyp development and progression to more advanced lesions. One such strategy is the use of chemopreventive agents. These agents could be administered to high risk individuals to complement cancer prevention provided by routine colonoscopy.

Potential chemopreventive agents for colon cancer are often identified in epidemiological studies and then assessed in rodent models and human intervention studies by associating intake of a particular agent with reduced colon cancer risk [11-13]. This approach led to the identification of NSAIDs as chemopreventive agents for colon cancer [14, 15]. However, such studies are time-intensive and costly, and the results of these studies vary greatly based on an individual's diet and lifestyle. An alternative approach to identifying chemopreventive agents would be to target aberrant pathways in mutated cells and select compounds that selectively induces apoptosis of mutated cells in culture. This approach could utilize specific oncogene and kinase inhibitors that selectively target cancer cells. Whether this approach will be safe and effective *in vivo* is not clear. The work in this dissertation focuses on understanding specific vulnerabilities of colon cancer cells and their precursors. We envision this knowledge leading to a better understanding of apoptotic signaling in colon cancer cells, which may in the long run lead to new strategies for treatment and prevention.

Table 1.1. Stage-wise five-year survival rates for colon cancer.

The five-year survival at stage I colon cancer is high; the survival rates reduce dramatically with each subsequent stage (with the exception of stage IIIA [16].

Stage of colon cancer	5-year relative survival rate
Stage I	92%
Stage IIA	87%
Stage IIB	63%
Stage IIIA	89%
Stage IIIB	69%
Stage IIIC	53%
Stage IV	11%

1.2. Apoptosis *versus* survival

Apoptosis is vital for the development and homeostasis of metazoans, whereby damaged or infected cells are sacrificed for the integrity of the whole organism [17, 18]. It is component of normal cell turnover in tissues and is characterized by distinct morphological changes [18, 19]. Apoptosis is a highly coordinated and energy-dependent process with characteristic blebbing of the plasma membrane, distinct from other forms of cell death (necrosis and autophagy) [19-21]. This is followed by separation of apoptotic bodies by *budding* [19]. Apoptosis can be induced by immune system in response to damaged or diseased cells. However, different cells may respond differently to the same stimuli and conditions that invoke apoptosis. Apoptosis is critical for the survival of neighboring cells by eliminating damaged or infected cells [19]. Evasion of apoptotic signals through suppression of internal regulatory controls is one of the hallmark of cancers [22]. Suppression of apoptotic responses in transformed cells facilitates the growth and progression of neoplastic lesions [23, 24]. Several apoptotic proteins and pathways have been shown to be defective or suppressed in colon cancers, as a result of mutations as well as micro-environmental conditions within the lesion [25-28].

1.2.1. Extrinsic versus intrinsic apoptosis

In mammalian cells, apoptosis can be subdivided into two categories – extrinsic and intrinsic apoptosis, depending on the origin of the death stimulus [19]. Extrinsic apoptosis is mediated by the death receptor/ligand coupling of the tumor necrosis factor receptor (TNFR) superfamily on the cell surface, such as TNFR1/TNF (TRADD), TRAIL/TRAIL-R (DR4 and DR5), and Fas/FasL (FADD) . Upon receptor-ligand complex formation, the death receptors can initiate signaling via receptor oligomerization. This results in recruitment of adaptor proteins and

activation of a cascade of caspases that culminates in the final demise of a cell [19, 27] (Figure 1.1). Suppression of this pathway results in aberrant growth and survival signaling, leading to tumorigenesis [18, 26, 29]. Intrinsic apoptosis, on the other hand, is triggered in response to a wide variety of intracellular death stimuli, such as DNA damage and oncogene activation [19, 27]. Intrinsic apoptosis is distinct from extrinsic apoptosis not only with respect to the death stimulus, but also in the mechanisms that carry out apoptosis. The intrinsic pathway is mediated by mitochondria; several proteins, including cytochrome c, are released from the mitochondrial intermembrane space. Cytochrome c activates and binds to APAF1, which allows for the formation of apoptosome and activation of caspase-9 and other downstream effector caspases [19] (Figure 1.1). It is important to note that even though the two apoptotic pathways operate by distinct mechanisms, they can crosstalk. For instance, caspase-8 (an extrinsic initiator caspase) can mediate the cleavage and activation of BID, a pro-apoptotic mitochondrial BCL2 family protein, which triggers the release of mitochondrial proteins and the activation of intrinsic apoptosis [18, 19].

1.2.2. Role of caspases in apoptosis and their regulation

Cysteine aspartate-directed proteases (caspases), a conserved family of enzymes, are central to the process of apoptosis [30, 31]. Typically, activation of caspases is a regulated process and can be divided into two classes – initiator or apical caspases (caspase-8 and -10) and effector or executioner caspases (caspase-3 and -6). Initiator caspases are activated by recruitment to the adaptor proteins and death receptor-ligand complex at the cell surface. Initiator caspases, in turn, activate effector caspases, which work to cleave cellular proteins [31, 32]. All eukaryotic caspases are produced as inactive zymogens and have to undergo proteolytic cleavage

during apoptosis [31]. Caspase activation is tightly regulated at different levels in order to illicit a fine-tuned response to a death signal and to avoid inadvertent cell death. First, caspases are subject to transcription regulation and post-translational modifications. For instance, mRNA levels of caspase-2 are regulated in a p53/p21-dependent manner and are upregulated only in the case of DNA damage [33]. Similarly, previous studies have shown that caspase-8 is phosphorylated by a number of serine/threonine and tyrosine kinases (including Cyclin B/Cdk1 and p38 MAPK) that have been linked with the inhibition of caspase-8 cleavage and activation [33, 34]. Second, caspase activation, especially in the extrinsic pathway, strictly requires the recruitment of procaspases to active death signaling complexes at the cell surface (*e.g.*, procaspase-8 recruitment by adaptor proteins bound to TNF/TNFR1 death signaling complex) [34, 35]. Third, caspase activation is finely regulated through a cascade of initiator and effector caspases to prevent inadvertent apoptosis [30, 33]. Fourth, cell survival and apoptosis are regulated by several intermediary proteins, such as c-FLIP that compete with procaspases for binding to death inducing silencing complex (DISC), thereby preventing caspase activation and apoptosis [33, 35]. Lastly, the conserved inhibitor of apoptosis (IAP) family of proteins can potently inhibit the activity of caspases and can degrade them through ubiquitination-mediated proteasome pathway [36-38].

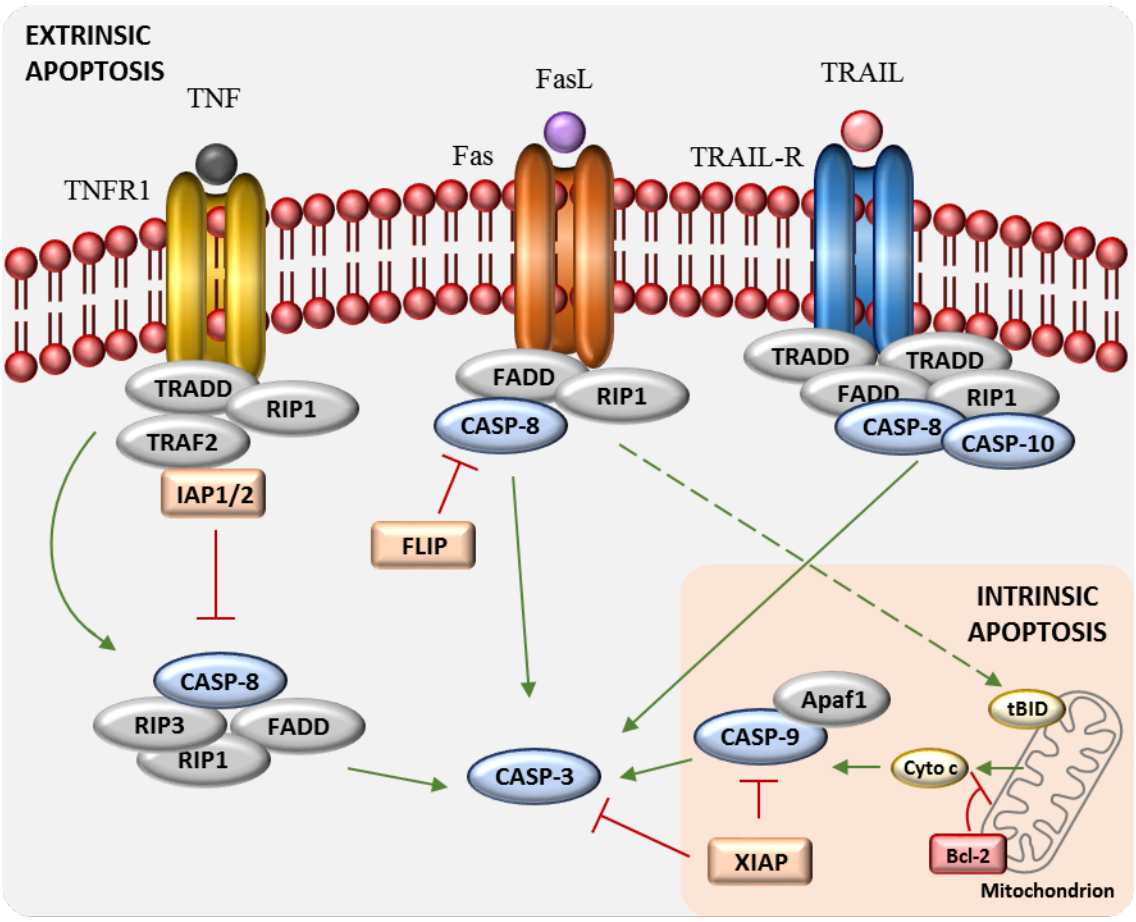

Figure 1.1. Schematic of extrinsic and intrinsic apoptosis.

Extrinsic apoptosis is induced by coupling of death receptors with their ligands at the cell surface. The signal is then transduced to the inside of the cell via several adaptor proteins that are recruited by the death receptors. This initiates recruitment and activation of caspase-8 (an initiator caspase), which leads to the activation of caspase-3 (an effector caspase). The activation of caspases is repressed by anti-apoptotic proteins, such as IAPs and FLIP (shown as rectangles). On the other hand, intrinsic apoptosis initiates with activation of pro-apoptotic Bcl family of proteins (*e.g.*, BID), releasing cytochrome c and activating caspase-9. Similar to anti-apoptotic signaling in extrinsic apoptosis, caspase-9 activation can be repressed by XIAP. There is crosstalk between extrinsic and intrinsic apoptotic pathways as indicated.

1.2.3. Apoptosis and colorectal cancer

Dysregulation of apoptosis leads to a variety of human diseases, such as autoimmune diseases, neurodegenerative disorders, and is a hallmark of cancer [19, 39]. While apoptosis is essential to homeostasis of the colonic epithelium, abnormalities in apoptotic response can contribute to the pathogenesis of colorectal cancer and resistance to chemotherapeutic agents and radiation therapy [27]. Thus, there is great interest in understanding how colorectal cancer cells evade apoptosis and transition to a more uncontrolled proliferation. Since apoptosis is an important mechanism of tumor suppression, there are strong selective pressures to disable apoptosis in cancer cells, with most of the mutations targeting pathways leading into apoptosis, rather than the apoptotic machinery itself. There are two general mechanisms by which apoptosis is suppressed in colon cancers: (1) through the mutation of genes that mediate apoptotic signaling and apoptosis, and (2) through the establishment of a micro-environment that stimulates survival pathways.

Colon cancers harbor mutations that suppress apoptotic signaling or apoptotic execution. Most common of these are mutations of p53 tumor suppressor gene, TGFβ, PTEN, caspase-8, and SMAD4 [40-45]. For instance, p53 is found to be mutated in about 60 percent of colorectal cancers and about 15 percent of the colorectal cancers harbor caspase-8 mutations [40]. Mutations of p53, SMAD4, and PTEN suppress apoptotic signaling [46], mutations in TGFβ1 promote proliferation and survival [42, 47], and mutations in caspase-8 inactivate the apoptotic machinery [43]. In addition, activating mutations of receptor tyrosine kinase (RTK) as well as oncogenes in the MEK/ERK pathway (Kras and Braf) signal for cell survival and proliferation [48-50]. In addition to genetic mutations, colon cancer cells also take advantage of the inflammatory cytokines in their microenvironment by upregulating pro-survival and proliferation

signaling, while suppressing apoptosis [51, 52]. For example, coupling of TNF to TNFR1 can mediate NF-κB activation, which targets the transcription of genes involved in cell survival and proliferation [53]. However, as previously noted, TNF/TNFR1 coupling can also result in caspase-8 activation [34, 54]; cancer cells circumvent this by increasing the cell surface expression of TNFR2, which exclusively signals for NF-κB activation [55, 56] (Figure 1.2). Thus, cancer cells suppress apoptotic signaling through genetic mutations and by using their micro-environment for enhanced survival signaling.

In summary, induction of apoptosis is one of the major mechanisms of tumor suppression and elimination of mutated cells. However, cancer cells develop various mechanisms to evade apoptosis. Moreover, cancer cells upregulate survival pathways to increase the likelihood of their survival and proliferation. Understanding genetic alterations and molecular events that help tumor cells evade apoptosis would establish a paradigm to explain the association between alterations in cancer cells, drug resistance, and evasion of apoptosis. Understanding these associations may aid in the development of novel, targeted therapies that can activate apoptotic signaling in cancer cells and may ultimately help in cancer treatment and prevention.

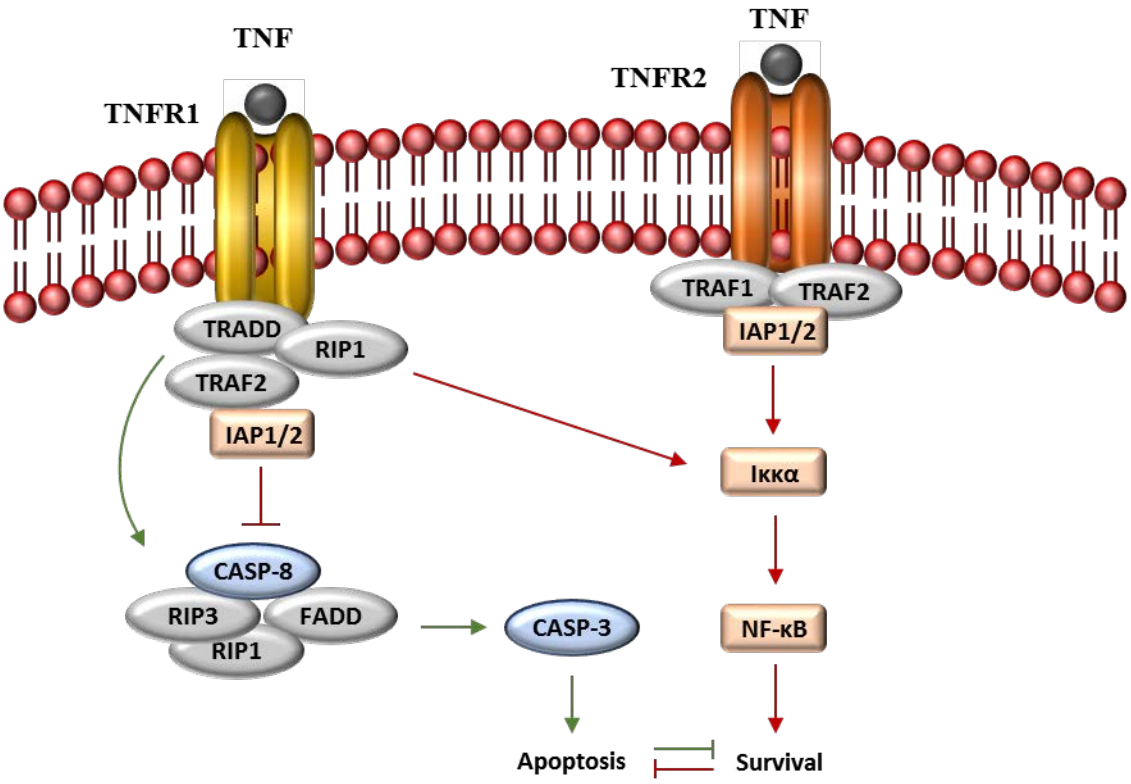

Figure 1.2. Schematic of TNFR1-mediated death and survival signaling.

TNFR1-TNF coupling can mediate extrinsic apoptotic response as well as survival signaling through NF-κB activation. Activation of the NF-κB transcription factor results in the transcription of survival genes. Activation of survival signaling, in turn, suppresses cellular apoptotic signaling. Conversely, activation of apoptosis suppresses cell survival signaling. On the other hand, TNFR2-TNF coupling exclusively signals for cell survival via NF-κB activation, leading to enhanced cell survival and suppressed apoptosis.

CHAPTER 2

Identification of novel compounds that enhance colon cancer cell sensitivity to inflammatory apoptotic ligands

2.1. Abstract

Immune and inflammatory death ligands expressed within neoplastic tissue could potentially target apoptosis to transformed cells. To develop approaches that accentuate the anti-cancer potential of the inflammatory response, the ChemBridge DIVERSet^{TM} library was screened for compounds that accentuated apoptosis in a strictly TNF-dependent manner. We identified a number of novel compounds with this activity, the most active of these, AK3 and AK10, sensitized colon cancer cells to TNF at 0.5 μM and 2 μM, respectively, without inducing apoptosis on their own. The activity of these compounds was structure-dependent and general, as they accentuated cell death by TNF or Fas ligation in multiple colon cancer cell lines. Both AK3 and AK10 arrested cells in mitosis, with live cell imaging indicating that mitotically arrested cells were the source of apoptotic bodies. AK3 accentuated caspase-8 and caspase-9 activation with little effect on NF-κB target gene activation. Enhanced caspase activation corresponded to an increased expression of TNFR1 on the cell surface. To determine the general interplay between mitotic arrest and TNF sensitivity, aurora kinase (MLN8054 and MLN8237) and PLK1 (BI2536) inhibitors were tested for their ability to sensitize cells to TNF. PLK1 inhibition was particularly effective and influenced TNFR1 surface presentation and caspase cleavage like AK3, even though it arrested mitosis at an earlier stage. We propose that AK3 and AK10 represent a new class of mitotic inhibitor and that selected mitotic inhibitors may be useful for treating colon cancers or earlier lesions that have a high level of inflammatory cell infiltrate.

2.2. Introduction

Inflammation can play a central role in cancer promotion in many tissues, one of the best documented being the colon. Extensive ulcerative colitis (UC) has been associated with a significant increase in colon cancer development, and managing inflammation with 5-ASA decreases this risk [57, 58]. Inflammation may also contribute to the development of sporadic colon cancer; nonsteroidal anti-inflammatory drugs (NSAIDs) such as aspirin and ibuprofen can decrease cancer risk in the population at large by close to 50% [59-61]. The interaction between inflammatory signaling and cancer may continue through late stages of the disease, as most cancers maintain elevated levels of TNF, IL6 and other inflammatory mediators [51, 62-65]. The role of inflammation in colon cancer development is multifaceted and includes the increased generation of DNA-reactive molecules, enhanced angiogenesis and activation of the anti-apoptotic transcription factor NF-κB [63, 65-69].

Although inflammation is associated with cancer development, immune and inflammatory cells produce a range of molecules with potent death-inducing capabilities that have the potential to limit lesion growth. Evidence suggests that early tissue lesions are kept at bay by the immune response [70, 71]. Cancers are in fact found to be “immune-edited,” consistent with the active elimination of immunogenic cells from the developing lesion [72, 73]. In this regard, the adaptive immune response is likely to be anti-tumorigenic. The contribution of innate immunity to cancer development is less clear. Generalized inflammation has been implicated in cancer promotion [74]. However, the influence of innate immune cells on cancer development may be stage-specific. In the case of advanced colon cancer, macrophage density at the tumor margin is strongly associated with a better patient outcome, which may result from their ability to generate apoptosis-inducing factors [75].

The death-inducing capabilities of immune cells serves as the basis for cancer therapies utilizing vaccines or immune stimulants. For example, the inclusion of Aldesleukin and granulocyte- macrophage colony-stimulating factor (GM-CSF) with traditional chemotherapeutic agents has been shown to improve the outcome of colon cancer patients [76, 77]. Evidence suggests that immune stimulants activate both the innate and adaptive arms of the immune response to induce lesion regression [78-80]. The anticancer activities of the immune response can be counteracted by a range of phenotypic changes in cancer cells. The cell killing actions of the adaptive immune response can be mitigated by the decreased expression of MHC molecules on cancer cells [81-83]. A more general resistance to immune cell killing may also be achieved by the increased expression of anti-apoptotic proteins, such as survivin and other IAPs, by cancer cells [84, 85]. To obtain insight into cellular pathways that are associated with an increased resistance to immune cells, we screened a compound library for agents that sensitize colon cancer cells to TNF induced apoptosis, without affecting cell viability on their own.

The majority of compounds obtained through this screen worked through a mitotic arrest mechanism. We propose that agents that target mitosis may be well-suited for enhancing the anticancer actions of the immune and inflammatory response. We also discuss the possibility that the mitotic proteins that are frequently upregulated in colon cancers serve (in part) to ensure that cancer cells proceed efficiently through mitosis so that they evade elimination by apoptotic ligands.

2.3. Materials and Methods

2.3.1. Cell culture

HT29 and HCT 116 colon cancer cell line were obtained from the American Type Culture Collection. These cell lines were cultured in McCoy's 5A medium with 10% fetal bovine serum, non-essential amino acids and antibiotic/antimycotic (Life Technologies). The AJ02-NM_0 cell line was isolated from an AOM-induced tumor from the A/J mouse strain and were cultured in RPMI 1640 with Glutamax (Life Technologies) supplemented with 5% (v/v) fetal bovine serum (Lonza), 5% (v/v) heat-inactivated horse serum, 1% (v/v) insulin-transferrin-selenium (Gibco), 100 mM non-essential amino acids (Invitrogen) and antibioticantimycotic (Life Technologies) [86]. The compounds tested were obtained from the ChemBridge DIVERSet^{TM} library. BI2536, MLN8054 and MLN8237 were obtained from Selleck Chemicals. Drug treatments were performed approximately 24 h after passage for 18 h, unless otherwise indicated. TNF was obtained from Pierce Protein Research Productsand the activating Fas antibody (clone CH11) was purchased from Millipore.

2.3.2. Caspase-3 activity

Caspase activity was determined as previously described [87]. Briefly, cells were scraped off into a new tube, centrifuged at full speed in a microcentrifuge at 10,000 × g for 5 min and washed once with PBS. Pelleted cells were lysed by two rounds of freeze-thaw in lysis buffer containing 10 mM TRISHCl (pH 7.5), 0.1 M NaCl, 1 mM EDTA and 0.01% Triton X-100 and centrifuged at 10,000 × g for 5 min. The assays were performed on 96-well plates by mixing 50 ml of cell lysis supernatant with 50 ml of 2× reaction mix [10 mM PIPES (pH 7.4), 2 mM EDTA, 0.1% CHAPS, 10 mM DTT] containing 200 nM of the fluorogenic substrate Acetyl-Asp-

Glu-Val-Asp-7-Amino-4-methylcoumarin (DEVD-AMC; Enzo Life Sciences). The fluorescence was quantified using a microplate reader (excitation/ emission 360/460 nm) at the start of the reaction and after 30 min. Protein concentrations were determined using CBQCA Protein Quantification Kit (Life Technologies). Caspase activity was determined by dividing the change in fluorescence after 1 h by the total protein content of the reaction mixture.

2.3.3. Immunoflurorescence microscopy.

Treated cells cultured on coverslips were fixed with 4% paraformaldehyde or methanol and then permeabilized with 0.5% Triton X-100 in PBS. Cells were blocked in 5% serum (in PBS) and then incubated for 1 h at room temperature on the shaker with the primary antibody (in 5% serum) against cleaved caspase-3 (9961, Cell Signaling Technology), phospho-histone H3 Ser 28 (sc-12927, Santa Cruz Biotechnology) or β-tubulin (E7 monoclonal antibody, Developmental Studies Hybridoma Bank). TNFR1 antibody (H-5, Santa Cruz Biotechnology) incubation was performed overnight at 4°C. Appropriate secondary antibodies (Jackson ImmunoResearch) were used for 45 min incubation. Nuclei were visualized using DAPI (5 mg/ml in H2O) (D1306, Life Technologies). Coverslips were mounted on slides using ProLong® Gold AntiFade Reagent (Life Technologies). Images were acquired using Nikon A1R Confocal Microscope (v. 2.11) and NIS-Elements Advanced Research Software (version 3.2). Quantification of immunostaining was performed using ImageJ image analysis software (http://rsb.info.nih.gov/ij/) as previously described [88]. Following background subtraction, both DAPI and immunofluorescent images were converted to binary using the convert to mask function. To remove any false positive signal, a binary image of the colocalized points was generated using the colocalization plugin of Bourdoncle

(http://rsbweb.nih.gov/ij/plugins/colocalization.html). The integrated densities of the total area of the colocalized binary image and the corresponding DAPI image were then measured to generate staining index.

2.3.4. Time lapse imaging

HT29 cells stably expressing histone H2B-GFP were used for live cell imaging. Images were taken with Nikon A1R Confocal Microscope every 16 min as Z-stacks of 30 images, each 1 μm apart. Images were restacked using Fiji/ ImageJ (National Institute of Health).

2.3.5. Cell cycle analysis

HT29 and HCT116 cells were analyzed for DNA content by ethanol fixation and staining with propidium iodide as previously described [89]. Floating and adherent cells were combined and analyzed by flow cytometry. Adherent cells were harvested using a trypsin-EDTA solution, centrifuged together with the floating cells at 100 × g for 5 min and resuspended in 1 ml of cold saline GM. Cells were then fixed by adding 3 ml of cold 100% ethanol while gently vortexing and stored at -20°C for at least 2 h. Cells were then pelleted and washed once with PBS containing 5 mM EDTA. Pelleted cells were stained with 30 μg/ml propidium iodide (Sigma-Aldrich) and 0.3 mg/ml RNase A in 1 ml PBS solution for 1 h in the dark at RT. The stained cells were filtered prior to analysis on FACSCalibur flow cytometer (BD Biosciences) using Cell Quest software (BD Biosciences). The data were analyzed using FlowJo (TreeStar Inc.).

2.3.6. Western blot

RIPA buffer was employed for protein extraction and 30 μg of protein was denatured under reducing conditions [90, 91]. Proteins were separated on 4–20% gradient gels (Bio-Rad) and transferred to nitrocellulose by voltage gradient transfer. The resulting blots were blocked with 5% (w/v) non-fat dry milk in PBS + 0.1% (v/v) Tween-20. Specific proteins were detected with appropriate antibodies using enhanced chemiluminescence detection (Santa Cruz Biotechnology) as recommended by the manufacturer. Immunoblotting antibodies were survivin (71G4B7, Cell Signaling Technology), phospho-survivin (Thr34) (D2E11, Cell Signaling Technology), cleaved caspase-8 (18C8, Cell Signaling), caspase-9 (human specific, Cell Signaling), pro-caspase-8 (8CASP03, Santa Cruz Biotechnology), TNFR1 (H-5, Santa Cruz Biotechnology) and β-actin antibody (I-19, Santa Cruz Biotechnology).

2.3.7. RNA quantification

Total RNA extraction was performed using Trizol reagent (Life Technologies) following the manufacture's instruction. RNA was quantified by reverse transcription and quantitative PCR analysis using Taqman reagents (Life Technologies), as previously described [90].

2.3.8. Compound synthesis

Starting from commercially available tert-Butyl piperazine-1-carboxylate, a Buchwald coupling (palladium cross coupling reaction between an amine and an aryl halide) was performed to append the dimethylbenzene ring to the free amine. Deprotection of the carbamate was achieved using 20% HCl in methanol. Subsequent amidation using trimethylamine and

various acyl chlorides yielded the final compounds that were tested after purification by column chromatography and structure validation using proton and carbon NMR.

2.3.9. Statistical analyses

All results are reported in triplicates as mean ± standard error of mean, unless specified otherwise. One-way analysis of variance (ANOVA) was used when comparing two groups with Tukey's post hoc test. For more than two groups, two-way ANOVA was used with Bonferroni correction. Significance was calculated at an alpha of 0.05.

2.4. Results

2.4.1. Compound screen for the induction of TNF sensitivity

Four hundred compounds from the ChemBridge DIVERSet^{TM} library were assessed for their ability to increase the sensitivity of the HT29 colon cancer cell line to TNF-induced apoptosis (Figure 2.1A). For this screen, duplicate 96-well plates were generated and treated in parallel with 40–50 μM of compound with one of the plates containing 50 ng/ml TNF. After 18 h, the plates were visually inspected for cell death and cellular extracts were prepared for an enzymatic caspase-3 assay (using the DEVD-AMC fluorogenic substrate). From this initial screen, six compounds were selected for further analysis, based on the level of caspase activation in the presence of TNF. These compounds were retested on HT29 cells, with active caspase-3 staining employed as a test of apoptosis. Quantification of this staining showed that the six compounds identified in the primary screen increased active capsase-3 in HT29 cells in a strictly TNF-dependent manner (Figure 2.1B). The structures of these compounds are shown in Figure A1.

Two of the most active compounds from the screen, AK3 and AK10, were taken for further analysis. Figure 2.2A shows their chemical structure; both have a central piperazine group with a phenyl and a benzoyl group attached to the two piperizane nitrogens. HT29 cells treated with TNF in combination with AK3 or AK10 showed an increase in the proportion of cells expressing active caspase-3, with positively staining cells frequently showing an apoptotic morphology (Figure 2.2B). A titration of the compounds for activation of caspase-3 (DEVDase) in the presence and absence of TNF is shown in Figure 2.2C. Neither AK3 nor AK10 significantly induced caspase-3 activity on their own, but did so when TNF was present. The level of agent required to stimulate apoptosis when TNF was present was in the low micromolar range for both AK3 and AK10, with an LD_{50} of 0.5 μM for AK3 and 2 μM for AK10.

Since both AK3 and AK10 compounds have a similar chemical structure, we generated a number of related compounds to determine whether their TNF sensitizing activity was dependent on their structure or whether it was a property inherent to the central piperazine group. The compounds synthesized are shown in Figure A2A. Application of these compounds to HT29 cells in the presence or absence of TNF showed that AK24 had a significantly higher TNF sensitizing activity than the other derivatives (Figure A2B). AK24 was, however, significantly less potent than AK3, as shown in Figure A2C. These structure-activity studies indicate that the activity of the piperazine-based compounds AK3 and AK10 result from specific structural elements that most likely function by binding to specific target molecules in the cell.

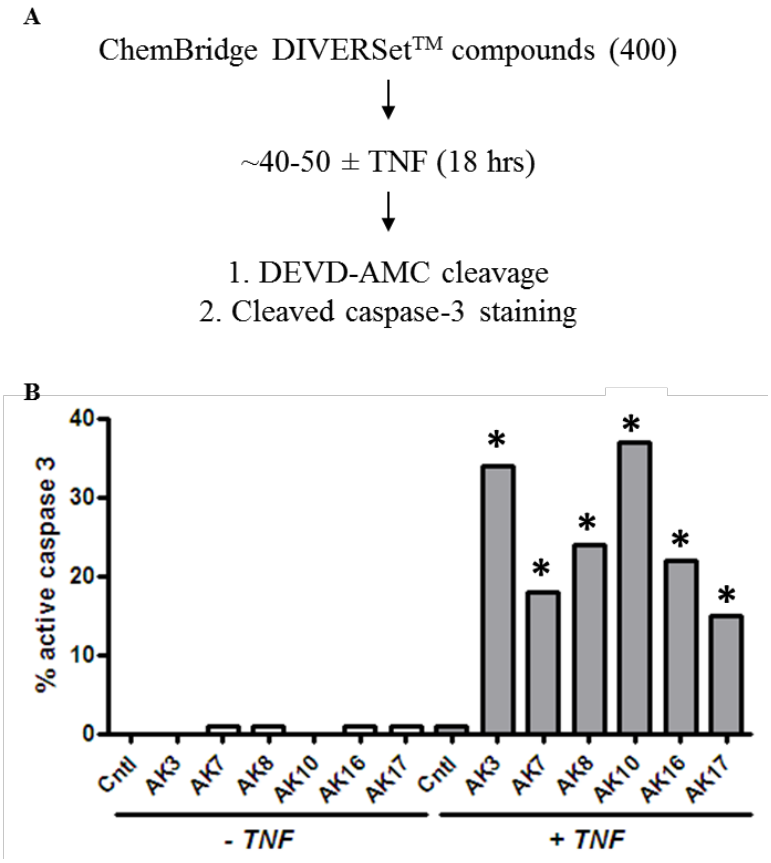

Figure 2.1. Identification of compounds that induce caspase-3 activation in a TNF-dependent manner.

(A) Schematic of the strategy employed for screening compounds from ChemBridge DIVERSet™ library. HT29 colon cancer cells were treated with 5 µM of test compounds for 18 h in the presence or absence of TNF (50 ng/ml). Cell lysates were prepared and tested for caspase-3 activity using the DEVD-AMC fluorogenic substrate. (B) The compound screen identified six compounds that induced caspase-3 activation only in the presence of TNF using a DEVDase assay. As a secondary screen, compounds were tested by immunostaining cells using an antibody specific for cleaved caspase-3. Images were captured and the fraction of cells staining positive for caspase-3 were quantified. AK3 and AK10, two of the most active compounds, were selected for further investigation (*$P < 0.0001$).

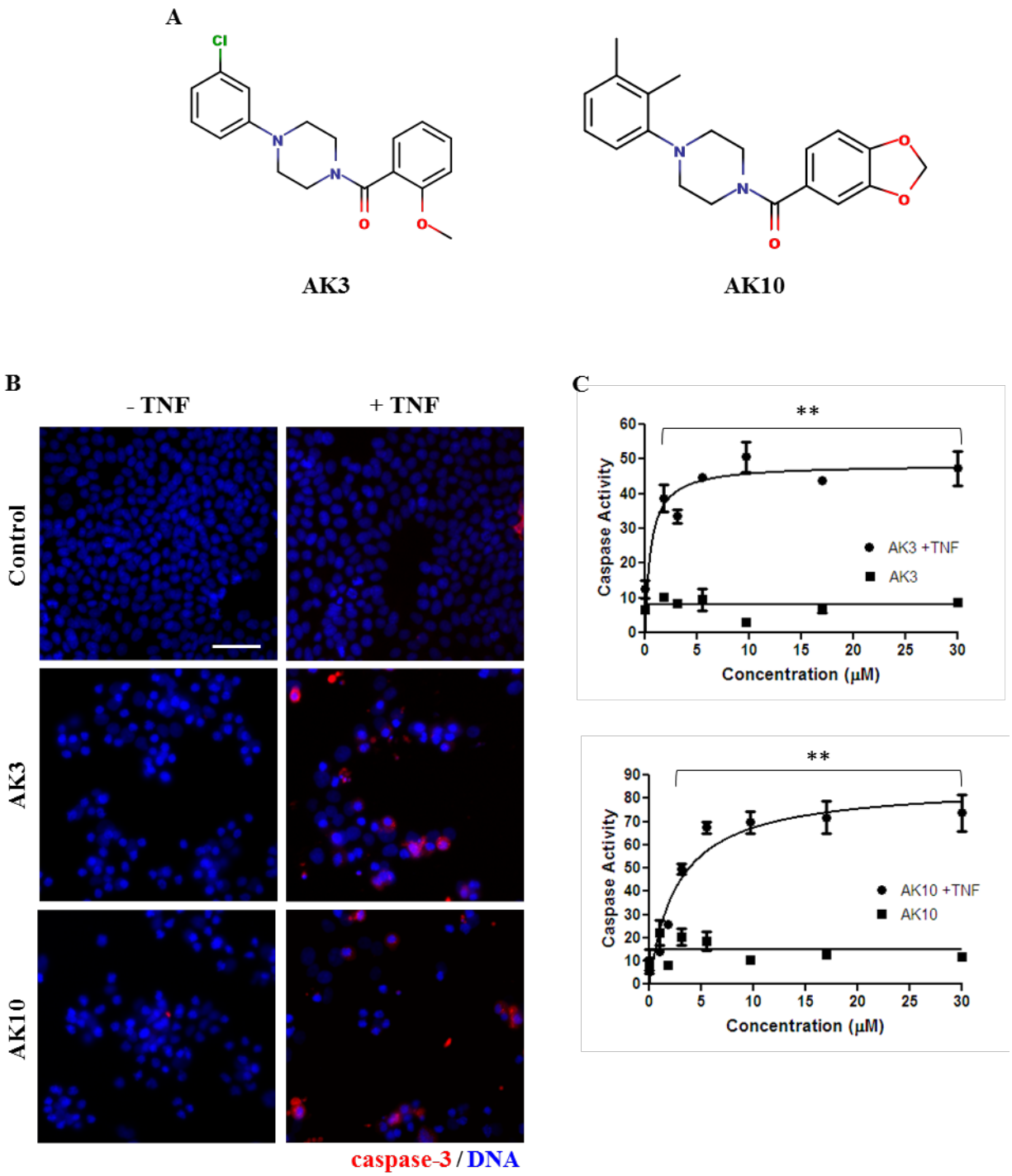
A
Cl
N
N
O
O
AK3
N
N
O
O
O
AK10
B
- TNF
+ TNF
Control
AK3
AK10
caspase-3 / DNA
C
**
Caspase Activity
Concentration (μM)
AK3 +TNF
AK3
**
Caspase Activity
Concentration (μM)
AK10 +TNF
AK10

Figure 2.2. Similarity in structure and TNF-dependent caspase-3 activation between AK3 and AK10.

(A) Similar chemical structure of AK3 and AK10. AK3 and AK10 both have a core piperazine group substituted with phenyl and benzoyl groups at the two piperazine nitrogens. (B) Increased caspase-3 and apoptosis in the combination treatment of AK3 or AK10 with TNF. HT29 cells were treated with AK3 or AK10 in the presence or absence of TNF for 18 h. Cells were fixed, permeabilized, and stained for active caspase-3. Higher proportion of cells stained for active caspase-3 in the combination treatment compared to control or AK3/AK10 treated cells. Positively staining cells displayed an apoptotic morphology. Bar, 100 μm. (C) Representative dose-response curves of caspase-3 activity with increasing concentrations of AK3 or AK10, in the presence or absence of TNF over 18 h. Significant caspase activation was observed only in the combination treatment. The asterisks indicated points where the combination treatment was significantly higher than compound or TNF treatment alone (*$P < 0.01$). LD_{50}s of AK3 and AK10 in the presence of TNF were determined to be 0.5 μM and 2.0 μM, respectively.

2.4.2. Generality of AK3 and AK10 activity

To determine the generality of apoptotic sensitization by AK3 and AK10, these compounds were tested on the HCT116 colon cancer cell line (Figure 2.3A). HCT116 cells are more sensitive to TNF induced apoptosis than HT29 cells (which possibly results from their wild-type p53 status). However, AK3 was capable of further enhancing TNF induced caspase activation in these cells, whereas AK10 was not. AK3 and AK10 were also tested on a mouse colon cancer cell line, AJ02-NM_0 cells (a p53-normal cell line derived from an AOM-induced colon tumor) [92]. TNF induced caspase-3 activation was stimulated in these cells by both AK3 and AK10, with AK3 being more potent (Figure 2.3B). Finally, we determined whether AK3 and AK10 could stimulate caspase-3 activity induced by the Fas pathway. As shown in Figure 2.3C, both AK3 and AK10 stimulated Fas-induced caspase activation, without significantly inducing caspase activity on their own. From these data, we conclude that both AK3 and AK10 are broadly active on different cell lines and with different death ligands, with AK3 being more general in its activity.

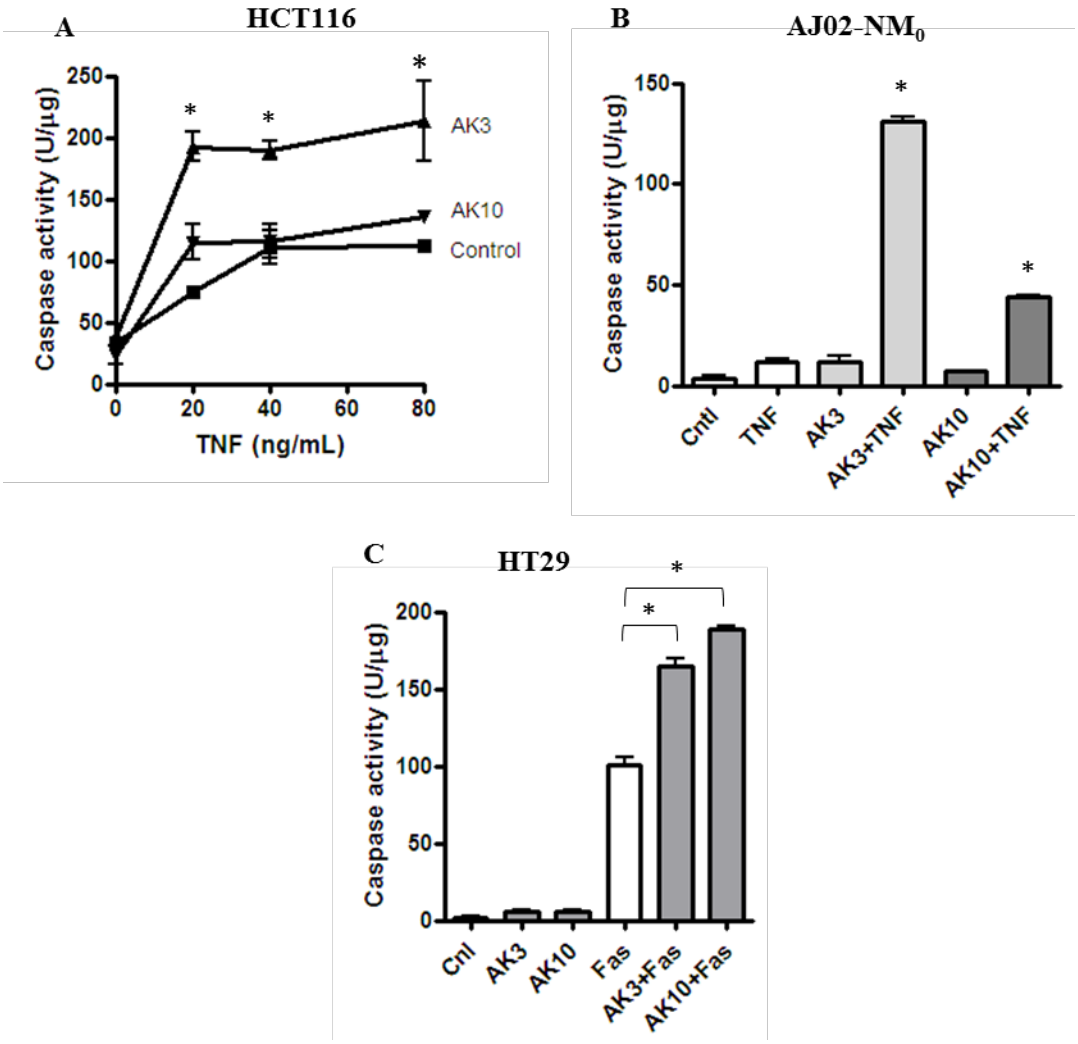

Figure 2.3. Effect of AK3 and AK10 on other colon cancer cell lines and on Fas-mediated cell death.

(A) TNF was titrated on to HCT116 cells in the presence or absence of 20 µM AK3 or AK10 for 18 h. Although these cells are more inherently sensitive to TNF, AK3 significantly increased caspase activity as measured by DEVD-AMC cleavage (*$P < 0.01$). AK10 did not significantly increase caspase activation in this cell line. (B) The mouse colon cancer cell line AJ02-NM_0 cells was treated with AK3 or AK10 and in the presence or absence of murine TNF for 18 h and analyzed for caspase activity. Both AK3 and AK10 increased caspase activity in the presence of

TNF, but not in its absence (*P < 0.001). AK3 was significantly more effective than AK10 (*P < 0.001). (C) AK3 and AK10 accentuated caspase activation by Fas ligation of HT29 cells. Cells were treated with AK3 or AK10 alone or in combination with an anti-Fas antibody (10 μg/ml) for 18 h and analyzed for caspase activation. Although HT29 cells are sensitive to Fas ligation, both AK3 and AK10 significantly enhanced caspase activation (*P < 0.001).

2.4.3. Mitotic arrest and TNF sensitivity

A flow cytometric analysis of propidium iodide (PI)-stained cells was performed to assess the impact of AK3 and AK10 on the generation of subdiploid cells. Co-treatment of HT29 cells with either compound in combination with TNF increased the sub-diploid population approximately 10-fold (Figure 2.4, right column). Treatment with AK3 or AK10 alone increased the fraction of cells in G2/M phase to approximately 70% (Figure 2.4). Interestingly, TNF caused a drop in the G2/M population that corresponded with the increased appearance of sub-diploid cells, suggesting that the G2/M cells were the cells targeted for apoptosis.

To determine if AK3 and AK10 induced a G2 or M phase arrest, immunofluorescent staining for the mitosis marker phospho-histone H3 Ser28 was performed [93, 94]. As shown in Figure 2.5A, both compounds induced a high level of phospho-histone H3 staining, consistent with a mitotic arrest (Figure 2.5A). Confocal analysis of the arrested cells showed similar mitotic structures induced by the compounds: in both cases, chromatin was condensed, but there was no congression of the chromosomes on the metaphase plate (Figure 2.5B). In addition, there were indications of mitotic spindle assembly, with apparent multiple microtubule organizing centers (Figure 5B). Other compounds identified in the screen likewise generated a mitotic arrest, as determined by enhanced histone H3 phosphorylation (Figure 2.5C). The induction of a mitotic arrest therefore appears to be a common mechanism for TNF sensitization.

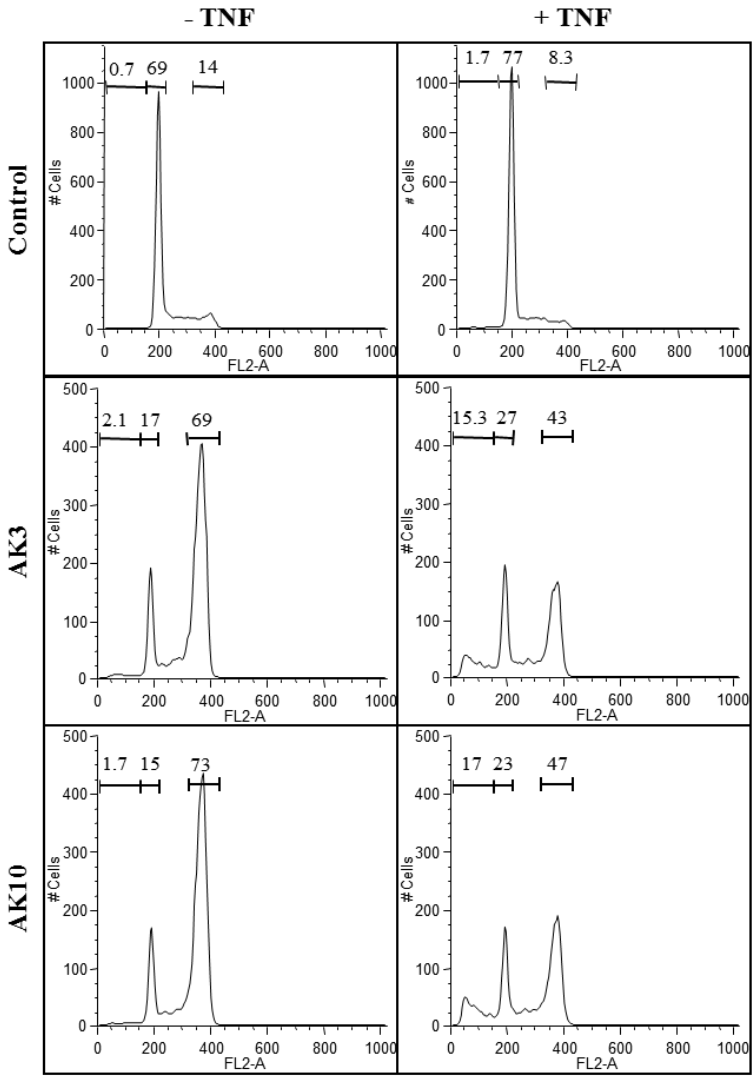

Figure 2.4. AK3 and AK10 induce a G2/M arrest on their own and sub-diploid cell fragments in the presence of TNF.

HT29 cells treated with AK3 or AK10 in the presence or absence of TNF for 18 h were analyzed for DNA content by propidium iodide staining. Flow cytometric analysis of AK3 and AK10 treated cells showed a shift from G1 to G2/M. In the presence of TNF alone, little change in the flow cytometer pattern is observed. Combining TNF with AK3 and AK10 showed a decrease in the G2/M peak and the appearance of a sub-diploid population.

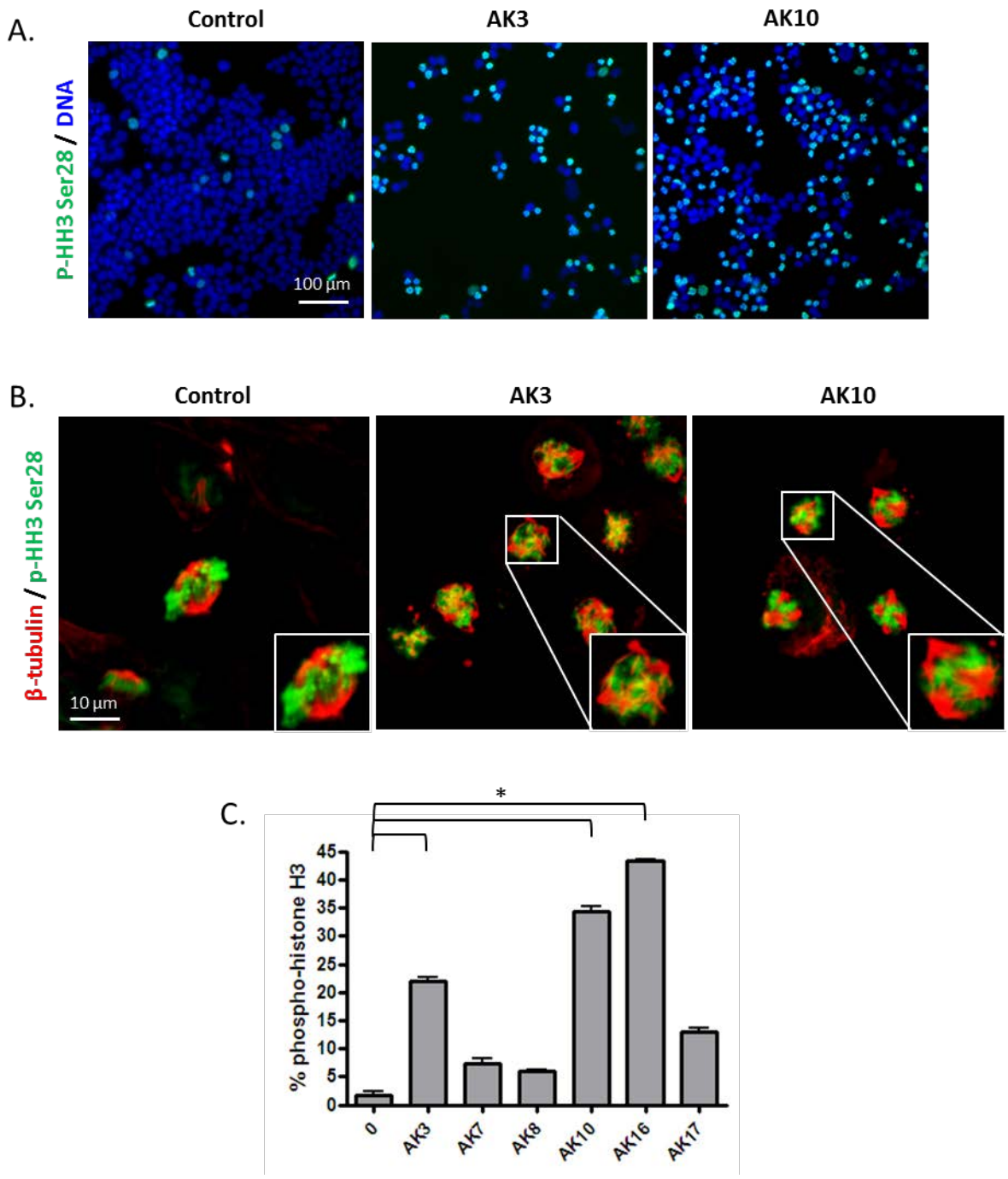

Figure 2.5. AK3 and AK10 induce prophase arrest with the appearance of multiple microtubule organizing centers (MTOCs).

(A) HT29 cells treated with AK3 and AK10 for 18 h were fixed and stained for phospho-histone H3 Serine 28, a marker for chromatin condensation during mitosis. Cells were stained and

examined at 20X magnification by epi-fluorescence. (B) AK3 and AK10 arrest cells in prophase with multiple MTOCs. AK3- and AK10-treated cells were dual stained for phospho-histone H3 (green) and β-tubulin (red) to visualize spindle assembly in arrested cells. Confocal imaging shows prophase arrested cells with spindles arising from multiple poles. Insets show magnified views of the mitotic cells. (C) Many compounds identified in the screen induce mitotic arrest. HT29 cells were treated with the indicated compounds at 25 μM and stained for phospho-histone H3. Images were captured and the mitotic index was quantified as a ratio of number of cell staining positive for histone H3 phosphorylation divided by the total number of cells visualized by DAPI staining (*$P < 0.0001$).

The flow cytometer data suggested that the sub-diploid cells in the co-treated cultures were derived from the arrested M phase population. To address this issue further, time-lapse imaging was performed on HT29 cells expressing a histone H2B-GFP fusion protein. As shown in Figure 2.6, cells treated with AK3 arrested in mitosis as indicated by the condensation of histone H2B-GFP fluorescence. Moreover, cells displaying condensed chromatin ultimately underwent apoptosis when TNF was present, further supporting the sensitivity of mitotically arrested cells.

2.4.4. Effect of AK3 on TNF signaling

Increased sensitivity to TNF-induced apoptosis could arise from an increased signaling through the proximal initiator caspase-8, through the suppression of the anti-apoptotic NF-κB signaling pathways or through a combination of these effects [95-97]. To assess the potential contribution of these pathways to sensitization, we determined the effect of AK3 on TNF-induced gene activation and caspase-8 and -9 cleavage. As shown in Figure 2.7A, gene activation by TNF was largely unaffected by AK3, whereas the activation of the initiator caspase-8 and caspase-9 was increased (Figure 2.7B). Cleavage of pro-caspase-8 showed the largest fold change; its cleavage was undetectable in cells treated with TNF or AK3 alone, but nearly complete when cells were treated with TNF and AK3 for 6 hrs.

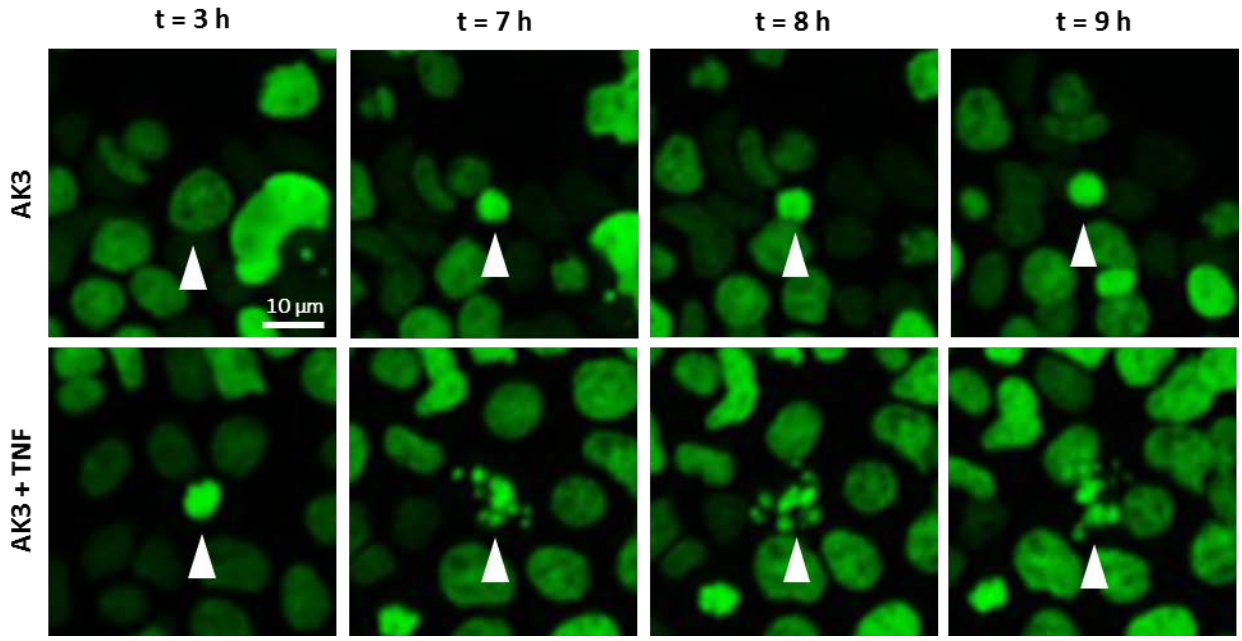

Figure 2.6. AK3-idnuced mitotically arrested cells undergo apoptosis.

Time lapse imaging of histone H2B-GFP expressed in HT29 cells. Cells were treated with either AK3 (top panel) or AK3 plus TNF (bottom panel). Representative images show chromatin condensation in the cells treated with AK3 alone, whereas addition of TNF in combination with AK3 increased apoptosis of the mitotic cells. Arrows point to the cells undergoing mitosis (top panel and bottom panel, t = 3 h) and/or apoptosis (bottom panel, t = 7 h to t = 9 h).

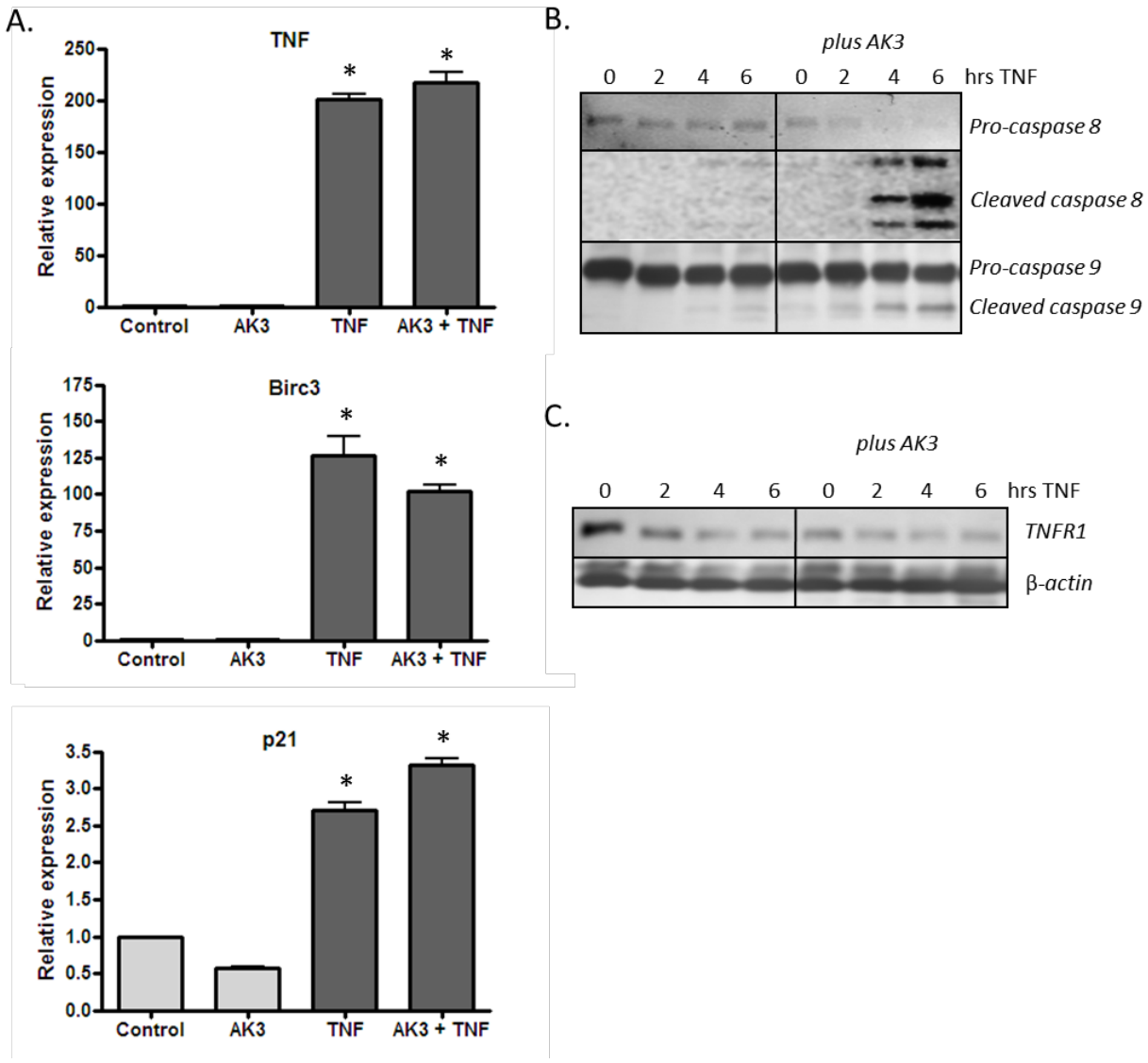

Figure 2.7. Effect of AK3 on gene activation and initiator caspase cleavage by TNF.

(A) HT29 cells were treated with AK3, TNF or AK3 plus TNF for 4 h. RNA was isolated, reverse transcribed, and quantified for expression of TNF, BIRC3, and p21 by real-time PCR. TNF activated the expression of the three genes tested relative to control cells (*P < 0.001), and there was no significant effect of AK3 on this activation. (B) AK3 enhances the TNF induced cleavage of caspase-8 and caspase-9. Cells were treated with TNF for 0, 2, 4, and 6 h in the presence and absence of AK3 and lysates were analyzed by immunoblotting with antibodies

against full length and cleaved caspase-8 and -9. (C) Protein samples were analyzed for TNFR1 by immunoblotting. β-actin was used as the loading control.

A western blot analysis was performed to determine if AK3 altered the expression of the TNF receptor responsible for caspase-8 activation, TNFR1 [98, 99]. Increased caspase-8 cleavage was not associated with an increased expression of total cellular TNFR1 as determined by western blot analysis (Figure 2.7C). In fact, a slight decrease in expression was observed in cells following treatment with AK3 or TNF. To determine whether TNFR1 cellular localization was altered by AK3, cells were examined by immunofluorescent staining. For this experiment, cells were either paraformaldehyde fixed and stained directly for TNFR1 or fixed and permeabilized with Triton X-100 prior to immunostaining. This analysis showed that while permeabilized cells stained uniformly for TNFR1 expression, non-permeabilized cells showed more variable expression (Figure 2.8A). We ascribe these changes in staining to changes in the cellular localization of TNFR1, with the staining of non-permeabilized showing receptors expressed at or close to the cell surface. A higher magnification view showed that cells in mitosis frequently displayed more intense staining than interphase cells under non-permeabilized staining conditions (Figure 2.8B). To determine the relative level of TNFR1 strictly on the cell surface, cells were transferred to ice and stained directly, without fixation or permeabilization (Figure 2.8C). This live cell staining protocol showed a higher level of TNFR1 staining on AK3-treated cells, with the number of cells staining for TNFR1 increased by approximately five-fold (Figure 2.8D). The increased level of cell surface expression of TNFR1 may contribute to the observed increase in TNF induced caspase-8 activation.

2.4.5. Mitosis targeting and TNF sensitivity

A number of pharmacological agents have been developed that can arrest cells in mitosis. We tested a number of these agents for their ability to enhance TNF induced caspase activation

and apoptosis. As shown in Figure 2.9A, two aurora A kinase inhibitors (MLN8054 and MLN8237) and a PLK1 inhibitor (BI2536) were all able to stimulate caspase activation by TNF [100-104]. Of these three agents, BI2536 was the most potent for facilitating caspase activation, even though they all induced mitotic arrest in approximately 70% of the cells. Cell cycle analysis of HT29 cells treated with BI2536 in the presence or absence of TNF showed that the BI2536 induced a G2/M arrest in approximately 70% of the cells and that inclusion of TNF with BI2536 increased the sub-diploid population while decreasing the fraction of cells in G2/M arrest (Figure 2.9B). This result is consistent with apoptosis in the G2/M phase cells being the primary source of the sub-diploid cells. The AJ02-NM_0 mouse colon cancer cell line was likewise sensitized to TNF by BI2536, but less so by the two aurora kinase inhibitors (Figure 2.9C). Figure 2.9D shows that BI2536 and AK3 induce a comparable level of TNF induced caspase activity in HT29 cells, making them roughly equivalent in effectiveness. These data indicate that mitotic arrest can sensitize cells to TNF, but the degree of sensitization can vary depending on the mechanism of arrest.

A critical signaling event that occurs during mitosis linked apoptosis is the phosphorylation of the kinetochore-associated passenger protein survivin by Cdk1-Cyclin B [105]. Survivin phosphorylation at Thr34 promotes mitotic progression and suppresses apoptosis [105, 106]. As shown in Figure 2.10A, AK3 treatment increased survivin phosphorylation, indicating that the cells can proceed past Cdk1 activation in mitosis. Interestingly, cells treated with AK3 and TNF undergo apoptosis even in the face of increased survivin phosphorylation. Figure 10A shows that cells treated with BI2536 have a relatively low level of survivin phosphorylation, which is consistent with its activity as a Plk1 inhibitor, which is upstream of Cdk1-Cyclin B. This analysis is consistent with BI2536 and AK3 arresting mitosis through

distinct mechanisms, even though they can both increase sensitivity to TNF. Like AK3, BI2536 enhances caspase-8 and caspase-9 cleavage (Figure 2.10B) without reducing the activation of TNF target genes (Figure 2.10C). Also like AK3, BI2536 increases the number of cells that express high levels of TNFR1 on their surface, suggesting a possible mechanism of action for cell sensitization with BI2536 (Figure 2.10D).

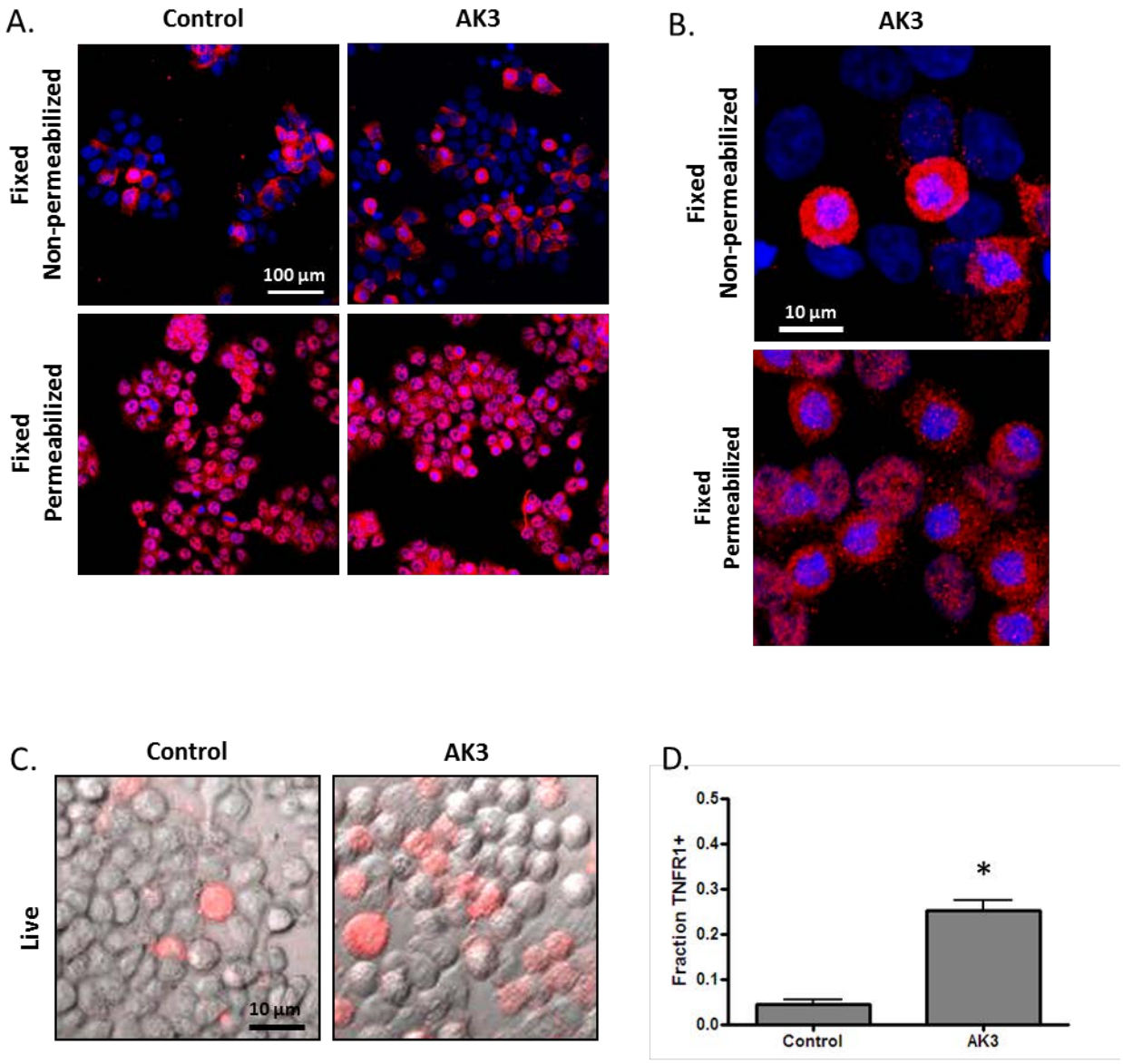

Figure 2.8. Mitotic cells have a higher expression of TNFR1.

(A) HT29 cells were treated with AK3 for 16 h and then fixed with PFA. Fixed cells were either stained directly with a TNFR1 antibody or were stained following permeabilization with Triton X-100. (B) Higher magnification of TNFR1 staining of permeabilized and non-permeabilized AK301-treated HT29 cells. All cells show TNFR1 expression following permeabilization, but staining is more variable in the absence of Triton X-100 permeabilization (as indicated). Mitotic

cells with round morphology and condensed chromatin frequently show elevated TNFR1 expression. (C) Live cells stained for surface expression of TNFR1. HT29 cells were transferred to ice and stained directly for TNFR1 expression. (D) Quantification of the live cells expressing TNFR1 on the surface. Images were captured and quantified for the number of cells staining with the TNFR1 antibody. Significantly more cells cell stained for surface expression of TNFR1 after AK3 treatment (*$P < 0.01$).

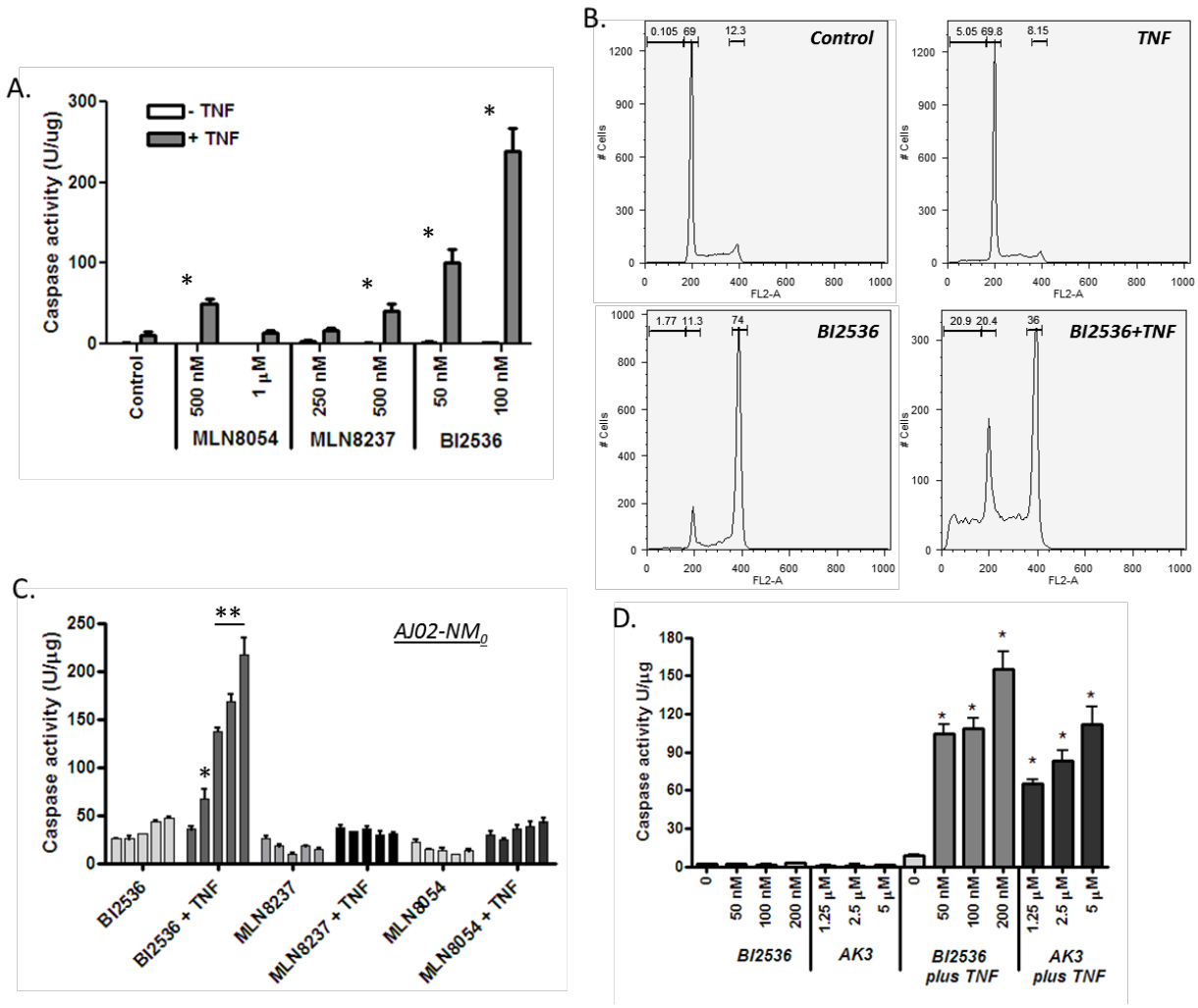

Figure 2.9. Effect of kinase inhibitors on TNF sensitivity of colon cancer cells.

(A) TNF induced caspase-3 activation in the presence of MLN8054, MLN8237 (aurora kinase A inhibitors) and BI2536 (PLK1 inhibitor). HT29 cells were treated with the indicated concentrations of the inhibitors in the presence or absence of TNF for 18 h and tested for caspase-3 activity using DEVD-AMC substrate. BI2536 induced significantly higher level of caspase activation than the aurora kinase A inhibitors (*$P < 0.01$). (B) Cell cycle analysis of HT29 cells treated with BI2536 in the presence or absence of TNF. BI2536 at 100 nM induces a G2/M arrest, and in combination with TNF, causes the appearance of sub-diploid population. (C)

BI2536 enhances TNF induced apoptosis in the mouse AJ02-NM_0 colon cancer cell line more potently than MLN8054 or MLN8237. AJ02-NM_0 cells were treated with the inhibitors in the presence or absence of murine TNF for 18 h and tested for caspase activation using the DEVD-AMC substrate. Inhibitors were used at 0, 125, 250, 500, and 1000 nM (from left to right). BI2536 was a significantly more potent sensitizing agent than aurora kinase A inhibitors at all concentrations tested (*$P < 0.05$, **$P < 0.01$). (D) AK3 and BI2536 induce comparable levels of caspase activation in HT29 cells in the presence of TNF. Cells were treated with the indicated agents and tested for caspase activation using DEVD-AMC substrate. AK3 and BI2536 in combination with TNF induced significantly higher caspase activity than either individual treatment (*$P < 0.01$).

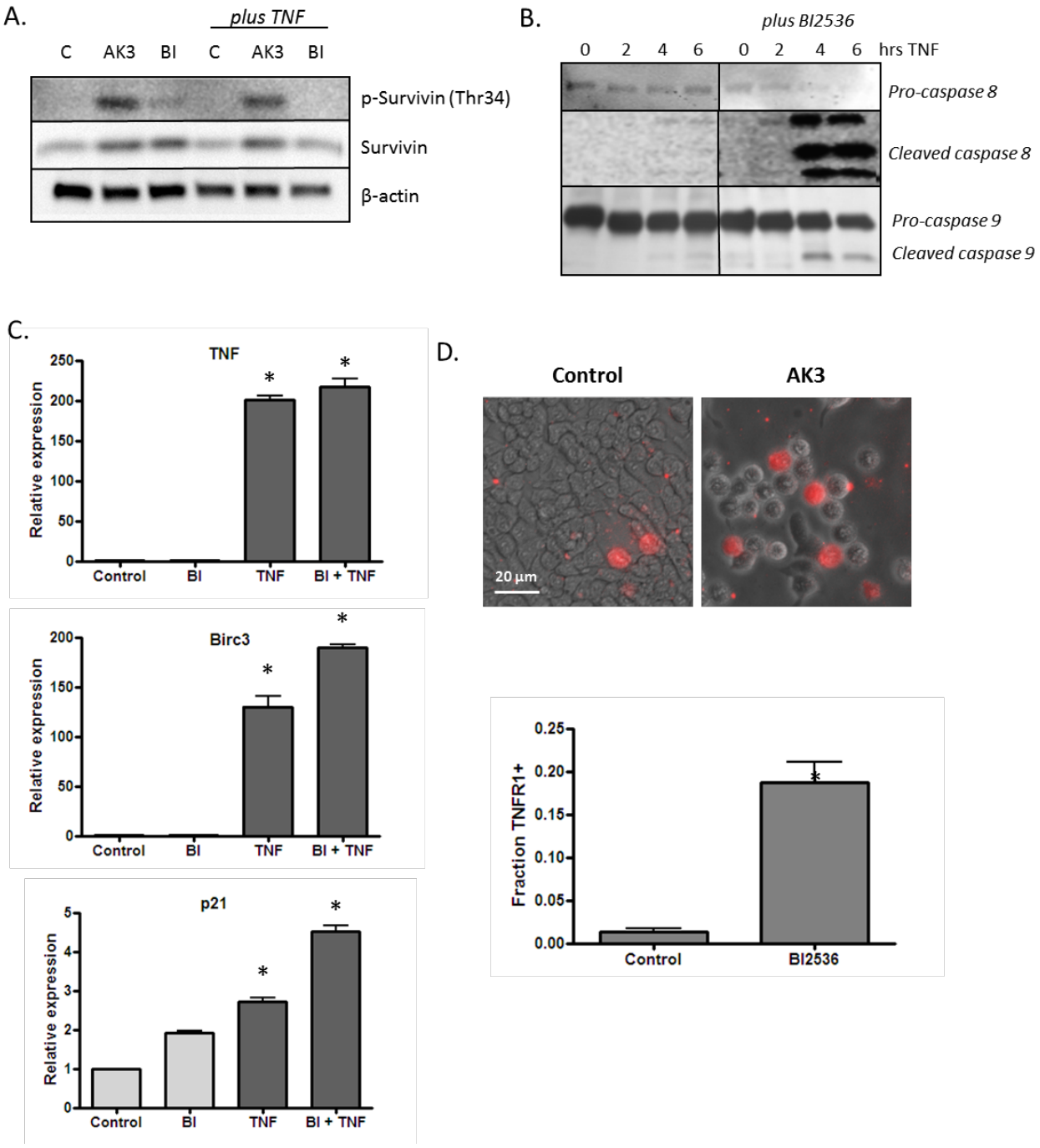

Figure 2.10. AK3 enhances caspase-8 and -9 activation without reducing the activation of surviving or TNF-targeted genes.

(A) Influence of AK3 and BI2536 on mitosis-dependent surviving phosphorylation. HT29 cells were treated with AK3 or BI2536 in the presence or absence of TNF for 18 h, as indicated.

Lysates were analyzed by immunoblotting with antibodies against total surviving and surviving phosphorylated at Thr34. β-actin was run as the loading control. (B) Effect of BI2536 on initiator caspase cleavage. HT29 cells were treated with TNF for the indicated times in the presence or absence of BI2536. Cell lysates were prepared and analyzed caspase-8 and caspase-9 cleavage. (C) Effect of BI2536 on gene activation by TNF> HT29 cells were treated with the TNF in the presence or absence of BI2536 as indicated. RNA was extracted at 4 h and quantified for expression of TNF, BIRC3, and p21 mRNA by reverse transcription/ real-time PCR assay using actin as an internal control. The expression levels shown are relative to the untreated control cells. TNF activated the expression of the three genes tested relative to control cells (*$P < 0.001$), but there was no significant effect of BI2536 on this activation. (D) Quantification of the live cells expressing TNFR1 on the surface. Images were captured and quantified for the number of cells staining with the TNFR1 antibody. Significantly more cells stained for surface expression of TNFR1 after BI2536 treatment (*$P < 0.0.1$).

2.5. Discussion

Colon cancers arise in an inflammatory microenvironment and continue to accommodate elevated levels of infiltrating immune cells as they progress. Although the suppression of inflammation over the long-term is a sensible approach to colon cancer prevention, a complementary approach would be to take advantage of the pro-apoptotic signals associated with an inflammatory response to target transformed cells for apoptosis. A number of natural and pharmacological agents, including NSAIDs, appear to have this ability and have been reported to increase cancer cell sensitivity to TNF, TRAIL or Fas ligand, although it is not clear how this activity functions in cancer prevention [87, 91, 107-109]. We and others have reported that HDAC inhibition is particularly effective at increasing colon cancer cell sensitivity to TNF, Fas and TRAIL [87, 110]. This sensitizing activity may account for the reported ability of SAHA/Vorinostat to selectively enhance apoptosis in AOM-induced colon tumors and suppress their formation and growth [87, 111-113]. It is not clear, however, whether HDAC inhibitors are ideal for this purpose since they also cause changes in histone acetylation and gene expression systemically.

To better understand the mechanisms by which cancer cells can be sensitized to the inflammatory milieu of a lesion, we screened for compounds that increase TNF induced apoptosis of colon cancer cells. Of the 400 compounds screened, 2 of the agents identified AK3 and AK10, had good potency and were structurally related. Interestingly, these and a number of other compounds identified in the apoptosis screen also induced mitotic arrest, with evidence pointing to a higher apoptotic rate of mitotically arrested cells. A number of pharmacological agents that target mitosis were also found to increase cancer cell sensitivity to TNF, but with varying efficacy. For instance, a Plk1 inhibitor (BI2536) was found to function better than two

aurora kinase A inhibitors (MLN8054 and MLN8237) at sensitizing cancer cells to TNF induced apoptosis, even though they all enforced comparable degrees of mitotic arrest. Compounds identified in the library screen likewise showed variations in their ability to induce mitotic arrest and sensitize cells to TNF. For example, AK16 was the most potent mitotic arrest agent but not the best sensitizing agent. The reason for this variation in efficiency is not clear. Nonetheless, our data suggest that selected mitotic inhibitors may effectively target neoplastic lesions because of their elevated rate of cell division, their loss of mitotic checkpoints and because they sensitize cancer cells to their inflammatory micro-environment. Whether this approach would be feasible on its own for clearing lesions from the colonic mucosa will require further study.

Mobilization of the immune response, whether through vaccination, immune stimulatory treatments or inflammatory agents, has long been envisioned as an ideal approach to selectively target cancer cells. Tumor cells have been documented to present epitopes that can be recognized as foreign by the immune response and that well-considered stimulants can direct immune cells to neoplastic lesions. Immune stimulants ideally increase the activity of cytotoxic T cells (CTLs), which function through either Fas ligation or release of perforin/granzyme. The Fas system becomes particularly important for targeting cancer cells with weak TCR-epitope complexes [72, 73]. Since tumors are immune-edited for strongly immunogenic epitopes, enhancing Fas-inducing cell death may be particularly beneficial [114]. We found that both AK3 and AK10 can enhance cell death mediated by Fas ligation, suggesting that these or similarly acting agents might increase the effectiveness of CTLs. The induction of a strong Th1 response by immune stimulants also increases the local concentration of a number of characteristic cytokines, including TNF. AK3, AK10 and similarly acting agents might, therefore, facilitate the TNF-induced cell killing to eliminate cells in the lesion that escape direct CTL detection.

In addition to identifying potential drug targets, compound screens can also generate molecular probes useful for identifying and studying critical pathways in cancer progression. In this regard, the results of our compound screen indicate that mitotic regulators may play an important role in helping cancer cells resist death ligands within the inflammatory milieu of a neoplastic lesion. Colon cancer cells have long been noted for altered expression of proteins involved in mitosis. These proteins include components of the centromeres as well as kinases and ubiquitin ligases that regulate mitotic progression [115, 116]. Proteins in this latter group include Cyclin B, aurora kinases A and B and CHFR [117-121]. CHFR, which regulates entry of cells into prophase is frequently silenced by promoter methylation in colon cancer cells [118]. The altered expression of mitotic proteins in colon cancer cells likely contributes to their chromosomal instability. However, these changes are also observed in colon cancer cells with a mutator phenotype that are chromosomally stable. For example, CHFR silencing is frequently associated with MLH1 silencing and a mutator phenotype [122]. We propose that the altered expression of mitotic regulators may function in part to facilitate the survival of cells within an inflamed tissue environment. This alteration may occur early in cancer development—it has been reported that aurora kinase A and Bub1B are overexpressed in preneoplastic mucosa of ulcerative colitis patients [123]. Aberrant expression of proteins that promote mitosis may help ensure that cells do not arrest at prophase/prometaphase for a prolonged period of time when they may be more sensitive to ligand-induced apoptosis.

The mechanism linking death ligand sensitization and mitosis is not well understood. We found that mitotic arrest by AK3 showed enhanced cleavage of the initiator caspase-8 and -9. The enhancement of caspase-8 cleavage was, however, more dramatic; little cleavage, if any, was observed when cells were treated singly with TNF or AK3, whereas the combination

treatment lead to a near complete cleavage. Since TNFR1 is responsible for directing casapse-8 activation, its expression and cellular localization was analyzed. Although AK3 did not increase the overall expression of TNFR1, it did increase its appearance on the cell surface. These results suggest that AK3 works in part by increasing the level of TNFR1 on the cell surface, which would increase its ability to interact with TNF and form a death inducing complex (either on the cell surface or following endosome incorporation). Arresting cells in mitosis with BI2536, likewise, increased the expression of TNFR1 on the cell surface. It is somewhat counterintuitive that the increased surface expression of TNFR1 would induce caspase-8 cleavage, but not the activation of TNF/NF-κB target genes. Although there are a number of explanations for this observation, perhaps the most likely is that TNF also activates the expression of the NF-κB inhibitory proteins IκBα and p105, which establishes a negative feedback loop for TNF-induced gene activation [124]. In contrast, caspase-8 activation is characterized by positive feedback loops [125], such that repeated binding and stimulation of the receptor may lead to persistently increasing levels of caspase cleavage and death signaling.

Cell surface expression of TNFR1 on cancer cells was found to be highly variable, even under normal growth conditions. The reason for this high level of variability is not known, but presumably involves alterations in receptor trafficking through different membrane compartments. Relative to interphase cells, mitotic cells displayed elevated levels of TNFR1 surface expression, such that the overall frequency of surface expression was increased by AK3. We hypothesize that cells undergoing mitotic stress due to chromosome or spindle abnormalities display more TNFR1 on their surface to facilitate their elimination from the tissue. This may be an important checkpoint during cancer development. However, unlike other checkpoint pathways, such as those involving increased expression of $p16^{INK4A}$ or $p14^{ARF}$, this pathway

requires that presence of an extracellular death ligand [126]. The role of TNFR1 is colon cancer development is consistent with the finding that TNFR1 null mice are more sensitive to tumor formation than wild type animals (in the AOM/DSS model) [127]. Although the apoptosis rate in normal tissue is not changed in TNFR1 null animals, TNFR1 may reduce cancer risk by inducing apoptosis of rare, genetically damaged cells. The extent to which TNFR1 signaling eliminates damaged and mitotically arrested cells from the tissue remains to be determined. An interesting parallel, however, appears to exist in *Drosophila* where TNF and TNF receptor homologs Eiger and Wegen, respectively, serve to remove damaged cells from developing epithelial tissues [128].

The two most active compounds identified in our screen contain a piperazine core substituted at the nitrogens with a benzoyl group and a phenyl ring. The activity of this structure depends on the specific substituents present on the benzoyl and the phenyl rings, and it is possible that further elaboration of these domains could lead to higher potency compounds. The general structure of AK3 and AK10 does not appear to resemble any present mitotic inhibitor, suggesting that they are a new type of mitotic arresting agent. Although these compounds arrest mitosis at some point after survivin phosphorylation (at the Cdk1-cyclin B target site), the precise nature of this inhibition is not yet known. In vitro tubulin polymerization assays indicate that they do not directly target tubulin (data not shown). Whether these agents or their targets might be useful for the development of new pharmacological agents is not clear. However, understanding their mechanism of action may provide new insight into colon cancer etiology and suggest novel approaches to colon cancer treatment and prevention.

CHAPTER 3

Novel piperazine-based compounds inhibit microtubule dynamics and sensitize colon cancer cells to TNF-induced apoptosis

3.1. Abstract

We recently identified a series of mitotically acting piperazine-based compounds that potently increase the sensitivity of colon cancer cells to apoptotic ligands. Here we describe a structure-activity relationship study on this compound class and identify a highly active derivative 1-(3-chlorophenyl)-4-(2-ethoxybenzoyl)piperazine, referred to as AK301, the activity of which is governed by the positioning of functional groups on the phenyl and benzoyl rings. AK301 induced mitotic arrest in HT29 human colon cancer cells with an ED50 of ≈ 115 nM. Although AK301 inhibited growth of normal lung fibroblast cells, mitotic arrest was more pronounced in the colon cancer cells (50% vs. 10%). Cells arrested by AK301 showed the formation of multiple microtubule organizing centers with aurora kinase A and γ-tubulin. Employing *in vitro* and *in vivo* assays, tubulin polymerization was found to be slowed (but not abolished) by AK301. *In silico* molecular docking suggests that AK301 binds to the colchicine-binding domain on β-tubulin, but in a novel orientation. Cells arrested by AK301 expressed elevated levels of TNFR1 on their surface and more readily activated caspases-8, -9, and -3 in the presence of TNF. Relative to other microtubule destabilizers, AK301 was the most active TNF sensitizing agent, and also stimulated Fas- and TRAIL-induced apoptosis. In summary, we report a new class of mitosis-targeting agents that effectively sensitizes cancer cells to apoptotic ligands. These compounds should help illuminate the role of microtubules in regulating apoptotic

ligand sensitivity and may ultimately be useful for developing agents that augment the anti-cancer activities of the immune response.

3.2. Introduction

Eukaryotic cell division involves replication of DNA in S phase followed by equal segregation of mitotic chromosomes during anaphase [129]. Cell cycle checkpoints have evolved to ensure faithful DNA replication and chromosomal division. Cells that harbor defective cell cycle checkpoint regulators can result in genetic instability and aneuploidy, ultimately leading to tumor development [130]. Mitosis orchestrates multiple cellular changes and depends on many intricate signaling pathways, despite being the shortest phase of cell cycle [131]. Signaling pathways, including kinases and several checkpoint proteins, spacio-temporally regulate dynamic chromosomal rearrangements and reorganization. It is because of this intricacy that mitosis is considered the most sensitive phase of the cell cycle [132, 133]. Damage to cellular processes that affect mitosis can activate spindle assembly checkpoint (SAC), which delays progression into anaphase [134]. Prolonged arrest in mitosis makes the cells more sensitive to cellular insults, which has likely made mitosis a desirable target for chemotherapy [132, 135-137]. Aneuploidies and other genomic and chromosomal abnormalities can induce cellular stress on cancer cells and make them highly sensitive to agents that disrupt mitosis [138].

Microtubules form spindle fibers during mitosis that are critical for chromosomal alignment and segregation [139, 140]. Previous findings suggest that agents that target the mitotic spindle can make highly effective chemotherapeutic drugs. Successful use of several vinca alkaloids, taxanes, and other natural compounds for the treatment of human cancers has validated the effectiveness of microtubule-targeting drugs [141-143]. Several other mitotic

proteins have also emerged as potential targets of chemotherapy. These targets include kinases, motor proteins, proteasome inhibitors and inhibitors of chromatin reorganizing proteins. Some of these newly developed compounds may provide clinical benefits over some of the presently used drugs [132].

One of the primary challenges of cancer chemotherapeutics is the targeting of cancer cells, while sparing normal cells of the surrounding tissue [144]. The use of vaccines and immune stimulants to specifically target tumors has generated promising results. For colon cancer, complementing traditional chemotherapy with IL2 and GM-CSF was shown to significantly increase patient survival [77]. However, immune stimulants can sometimes result in modest cell killing activity. Cell killing by the activated immune response includes direct cell killing by cytotoxic T cells and NK cells, as well as cell killing apoptotic ligands, such as TNF.

We previously reported several novel synthetic small molecules that dramatically increase colon cancer cell death by TNF and other death ligands, while being unable to induce apoptosis on their own [145]. Interestingly, many of these compounds also induced mitotic arrest. To gain insight into the mechanisms of action of these compounds, we studied the structure-activity relationship of a particularly promising class of piperazine-based compounds. Here we report a structure-activity relationship study of this class of compounds and identify a highly active derivative, AK301. Furthermore, we show that AK301 hampers tubulin polymerization, triggers the formation of multiple microtubule organizing centers (MTOCs), and increases the surface expression of TNFR1. Molecular docking studies indicate that AK301 binds to β-tubulin near the colchicine-binding site, but in a novel orientation. Lastly, AK301 was found to be more effective in sensitizing cancer cells to TNF-induced apoptosis than other known microtubule destabilizing agents. We propose that AK301 and its derivatives represent a

novel class of microtubule-targeting compounds that will be useful for studying the relationship between microtubule dynamics and apoptosis sensitivity. This class of compounds may also have beneficial therapeutic properties due to their ability to sensitize cancer cells to ligand-induced apoptosis.

3.3. Materials and Methods

3.3.1. Cell culture

HT29 and HCT116 colon cancer and WI38 fibroblast cell lines were obtained from the American Type Culture Collection (Manassas, VA). HT29 and WI38 cell lines were cultured in McCoy's 5A medium and MEM medium, respectively, with 10% fetal bovine serum, non-essential amino acids and antibiotic/antimycotic (Life Technologies, Guilford, CT). The compounds tested were obtained from the ChemBridge DIVERSet^{TM} library (San Diego, CA). Drug treatments were performed approximately 24 h after passage for 18 h, unless otherwise indicated. TNF was obtained from Pierce Protein Research Products (Rockford, IL), TRAIL was obtained from R&D Systems (Minneapolis, MN), and α-Fas antibody (clone CH11) was obtained from Millipore (Billerica, MA).

3.3.2. Flow cytometry

HT29 and WI38 were analyzed for DNA content by ethanol fixation and staining with propidium iodide as previously described [89]. Floating and adherent cells were combined and analyzed by flow cytometry. Adherent cells were harvested using trypsin-EDTA, centrifuged together with the floating cells at 100 *X g* for 5 min and resuspended in 1 ml of cold saline GM. Cells were then fixed by adding 3 ml of cold 100% ethanol while gently vortexing and stored at -

20°C for at least 2 h. Cells were then pelleted and washed once with PBS containing 5 mM EDTA. Pelleted cells were stained with 30 μg/ml propidium iodide (Molecular Probes, Life Technologies Corp.) and 0.3 mg/ml RNase A (Sigma-Aldrich, St. Louis, MO) in 1 ml PBS solution for 40 min in dark at RT. The stained cells were filtered through 35 μm cell strainer tubes (BD Biosciences, San Jose, CA) prior to analysis on FACSCalibur flow cytometry (BD Biosciences) using Cell Quest software (BD Biosciences). The data were analyzed using FlowJo (version 9.6.2 for Mac, TreeStar Inc., Ashland, OR).

3.3.3. Cell viability assay

Cell viability was assessed using Trypan blue exclusion assay. After treatment, the cells were incubated with Trypan blue at room temperature. Viable/dye excluding cells were then counted using a hemocytometer.

3.3.4. Immunofluorescence microscopy

Cells cultured on coverslips were fixed with 4% paraformaldehyde or 100% ice cold methanol and then permeabilized with 0.5% Triton X-100 in PBS. Cells were blocked in 5% serum (in PBS) and then incubated for 1 h at room temperature on the shaker with the primary antibody (in 5% serum) against phosphohistone H3 Ser 28 (sc-12927, Santa Cruz Biotechnology, Santa Cruz, CA), β-tubulin (E7 monoclonal antibody, Developmental Studies Hybridoma Bank), or aurora kinase A (BD Biosciences). γ-tubulin antibody (Abcam, Cambridge, MA) incubation was performed overnight at 4°C. Appropriate secondary antibodies (Jackson ImmunoResearch, West Grove, PA) were used for 45 min incubation. Nuclei were visualized using DAPI (5 μg/ml in PBS; DI306, Life Technologies). Coverslips were mounted on slides using ProLong Gold

Antifade Reagent (Life Technologies). Images were acquired using Nikon A1R Confocal Microscope (version 2.11, Nikon Instruments Inc.) and NIS-Elements Advanced Research Software (version 4.13.01, build 916, Nikon Instruments Inc.). Quantification of immunostaining was performed using ImageJ image analysis software (http://rsb.info.nih.gov/ij) as previously described [88]. Following background subtraction and image stacking, both DAPI and immunofluorescence images were merged. Image brightness and contrast was modified with Adobe Photoshop software CS6 (Adobe Systems).

3.3.5. In vitro tubulin polymerization assay

The HTS-tubulin polymerization assay kit (BK004P, Cytoskeleton, Inc, Denver, CO) was used as per manufacturer instructions. The reaction assay contained 100 µl of 4 mg/ml tubulin in G-PEM buffer (80 mM PIPES pH 6.9, 0.5 mM EGTA, 2 mM MgCl2, and 1 mM GTP. 10 µl of 10X compounds were pre-warmed to 37°C in a half area 96-well plate (dH_2O was used as control). The polymerization was carried out at 37°C and light scattering was recorded at 340 nm every minute for 60 min using Spectramax M2 absorbance plate reader (Molecular Devices, Sunnyvale, CA).

3.3.6. Whole cell microtubule analysis

Microtubules in whole cells were analyzed by flow cytometry as described previously [146]. Cells were cultured in 24-well plates for 24-36 hrs and treated with the colchicine, AK301, or AK302 for 16 hrs. The medium was collected and the cells were harvested by trypsin EDTA treatment and pelleted by centrifugation at 600 *x g* for 5 min. Cell pellets were resuspended and fixed with 0.5% glutaraldehyde under permeabilizing conditions in microtubule

stabilizing buffer (MTSB; 80 mM PIPES (pH 6.8), 1 mM MgCl2, 5 mM EDTA, and 0.5% Triton X-100) for 10 min. Glutaraldehyde was quenched with 700 µl of 1 mg/ml $NaBH_4$ in PBS. Cells were pelleted by centrifugation at 1000 *x g* for 7 min. Cells were blocked with 5% donkey serum and immunostained with β-tubulin (E7 monoclonal) antibody for 1 hr at RT, followed by secondary staining with Alexa Fluor® 488 donkey anti-mouse antibody (Life Technologies) for 1 hr. Finally, cells were pelleted by centrifugation and treated with 0.3 mg/ml of RNase A and 50 µg/ml of propidium iodide solution in PBS. Cells were analyzed by flow cytometry. All steps in this protocol were carried out at room temperature.

3.3.7. In silico molecular docking

Structural representations of the ligand molecules (AK3, AK301, AK302, AK303, and AK304) were drawn using Accelrys Draw (version 4.1, Accelrys, Inc.) in MOL2 format and converted to PDB format using Accelrys Discovery Studio Client (version 3.5). Individual PDB files were modified in AutoDock using MGLTools 1.5.6 (Scripps Institute, La Jolla, CA). Crystal structures of tubulin complexed with colchicine, paclitaxel, and vinblastine (PDB IDs 1SA0 [147], 1TUB [148], and 4EB6 [149], respectively) were obtained from the Protein Data Bank. Water molecules, ligands and other heteroatoms were removed from the protein molecules using Accelrys Discovery studio client (version 3.5, Accelrys, Inc.). Addition of hydrogen atoms to the protein was performed using MGLTools (version 1.5.6) for AutoDock. For each known ligand type, grid maps were generated that corresponded to their respective known binding sites on tubulin.

AutoDock 4.2 and Vina 1.1.2 were used for initial docking studies [150]. Generally, the docking parameters were left to the default settings. However, the grid spacing was changed

from 0.375 to 1.0. The size of the grid was 30 Å X 30 Å X 30 Å. The internal scoring function was used to assess receptorligand interactions in five independent runs.

Additionally, Molegro Virtual Docker (MVD) software version 6.0 was used to perform computer simulated docking analysis in order to confirm the least-energy poses acquired using AutoDock Vina. Charges for both tubulin and the ligands were calculated by MVD and assigned to their respective models. Moreover, probable explicit hydrogens were added to tubulin as well as the ligands, possible missing bonds were assigned, and side chain minimization was performed. Finally, flexible torsions were manually applied to the ligands. Since tubulin is a relatively large protein, a molecular surface was created using MVD workspace grid points and top three cavities were identified using expanded van der Waals method for the molecular surface with volumes ranging from 5 to 10,000 cubic units and default settings. To perform docking, the cavity containing the colchicine-binding domain was used with a radius of 20 to cover the entire cavity. MolDock score with a grid resolution of 0.30 Å was used as a scoring function for the simulation [151]. Ten runs were performed for each of the ligands using MolDock simplex evolution (SE) algorithm for fast and accurate docking and scoring. 1500 iterations were performed for each of the runs to achieve least minimized energy poses for the ligands. During the virtual screening process, internal electrostatic interaction and hydrogen bond between ligand and protein were permitted. Energy minimization and H-bond optimization was applied to each of the poses post run.

3.3.8. Caspase-3 assay

Caspase-3 activity was determined as previously described [87, 145]. Cells were collected, centrifuged at full speed, and washed once with PBS. Pelleted cells were lysed by two

rounds of freeze-thaw in lysis buffer containing 10 mM Tris-HCl (pH 7.5), 0.1 M NaCl, 1 mM EDTA, and 0.01% Triton X-100 and centrifuged at 10,000 *X g* for 5 min. The assays were performed on 96-well plate by mixing 50 µl of lysis supernatant with 50 µl of 2X reaction mix (10 mM PIPES pH 7.4, 2 mM EDTA, 0.1% CHAPS, 10 mM DTT) containing 200 nM of the fluorogenic substrate Acetyl- Asp-Glu-Val-Asp-7-Amino-4-methylcoumarin (DEVD-AMC; Enzo Life Sciences). The fluorescence was quantified at the start of the reaction and after 30 min. Protein concentrations were determined using CBQCA Protein Quantitation Kit (Life Technologies). Caspase activity was determined by dividing the change in fluorescence by total protein content of the reaction mixture.

3.3.9. Western blot

RIPA buffer was used for total protein extraction and NP-40 buffer was used for membrane protein extraction [145]. 20 µg of protein was denatured under reducing conditions [90, 91] and separated on 4-20% gradient gels (Bio-Rad Hercules, CA) and transferred to nitrocellulose by voltage gradient transfer. The resulting blots were blocked with 5% (w/v) non-fat dry milk in PBS + 0.1% (v/v) Tween-20. Specific proteins were detected with appropriate antibodies using Signal- FireTM Elite ECL Reagent (Cell Signaling Technology, Inc., Danvers, MA). Immunoblotting antibodies were cleaved caspase-8 (18C8, Cell Signaling Technology), caspase-9 (human-specific, Cell Signaling Technology), TNFR1 (H-5, Santa Cruz Biotechnology), E-cadherin (G-10, Santa Cruz Biotechnology), and β-actin antibody (I-19, Santa Cruz Biotechnology).

3.3.10. Cell surface TNFR1 analysis

Cells were treated in a 24-well plate as described above. Treated live cells were transferred to ice, washed once with PBS and blocked with 5% donkey serum. Cells were immunostained with TNFR1 antibody overnight at 4°C, followed by staining with Alexa Fluor® 488 antibody for 1 hr at RT. Cells were fixed with 4% PFA, washed, and harvested by trypsin EDTA. Cells were pelleted by centrifugation and analyzed by flow cytometry.

3.3.11. Statistical analyses

All results are reported in triplicates as mean ± standard error of mean, unless specified otherwise. One-way analysis of variance (ANOVA) was used for comparing more than two groups. Tukey's post-hoc test was employed to determine the significance of differences between multiple groups, with $P < 0.05$ considered significant. Two-way ANOVA was used for more than two independent variables and Bonferroni correction was used for multiple comparisons ($P < 0.05$).

3.4. Results

3.4.1. Functional groups of AK3 mediate mitotic arrest in HT29 cells

In previous studies, we identified AK3 compound from the ChemBridge DIVERSet™ library that induced mitotic arrest in colon cancer cells at low micromolar concentrations (0.5-1 μM) [145]. To assess properties of the chlorophenyl and methoxybenzoyl functional groups of AK3, four different AK3 analogs were analyzed for their ability to induce mitotic arrest in HT29 colon cancer cells at 5 μM (Figure 3.1A). The analogs comprise positional isomers of chloride and methoxy groups on the phenyl (AK302) and benzoyl (AK303, AK304) rings, respectively,

as well as the substitution of an ethoxy (AK301) for methoxy on the benzoyl ring. Flow cytometric analysis of propidium iodide (PI)-stained HT29 colon cancer cells showed that a greater percentage of AK3-, AK301-, and AK303-treated cells arrested in G2/M phase of the cell cycle compared to untreated, AK302-, or AK304-treated cells ($P < 0.0001$) (Figure 3.1B). A titration of the most active compounds among the analogs (AK3, AK301 and AK303) and an assessment of the G2/M arrest by flow cytometry is shown in Figure 3.1C. AK301 induced a G2/M arrest more efficiently than AK3 or AK303 with a half maximal effective concentration (EC_{50}) value of approximately 115 nM. Further, HT29 cells showed decreased growth in the presence of AK3 or AK301, with dose response curves showing a higher potency of AK301 (Figure 3.1D). Together, these results indicate that the position of the functional groups on AK3 derivatives play an important role in determining their activity in inducing cell cycle arrest.

3.4.2. AK301 induces ad irreversible mitotic arrest in HT29 cells

To determine whether AK301-treated cells arrested in mitosis, HT29 cells were analyzed for presence of the mitosis marker phospho-histone H3 Ser 28 (p-HH3). Figure 3.2A and 3.2B show that both AK3 and AK301 increased phospho-histone H3 Ser 28 staining, consistent with mitotic arrest.

To further assess whether this state of mitotic arrest was reversible, AK301 was washed out of the growth medium after 18 hours of treatment and cell growth was observed at 24, 48, and 72 hours following drug washout. As shown in Figure 3.2B, AK301-treated cells did not recuperate after 72 hours post drug washout and showed significantly less growth compared to the untreated cells ($P < 0.0001$).

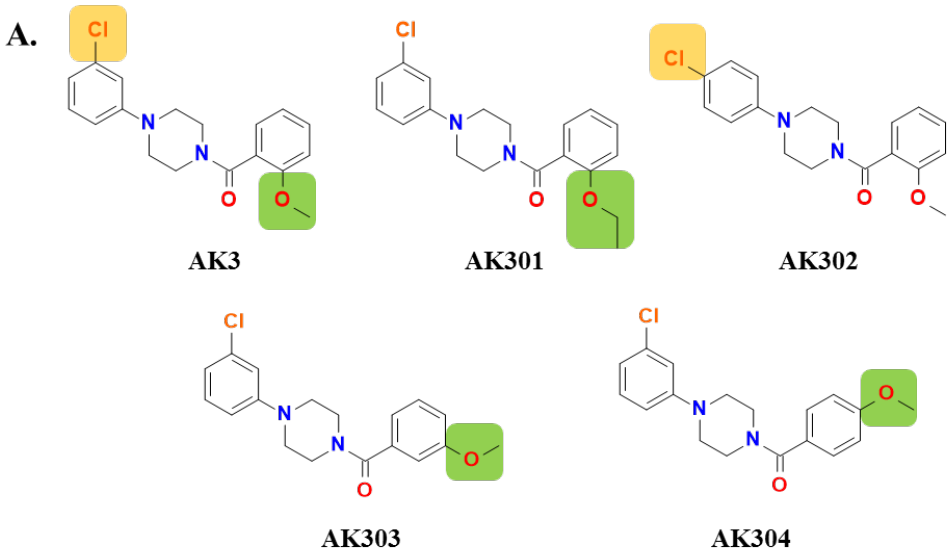
A.
AK3
AK301
AK302
AK303
AK304

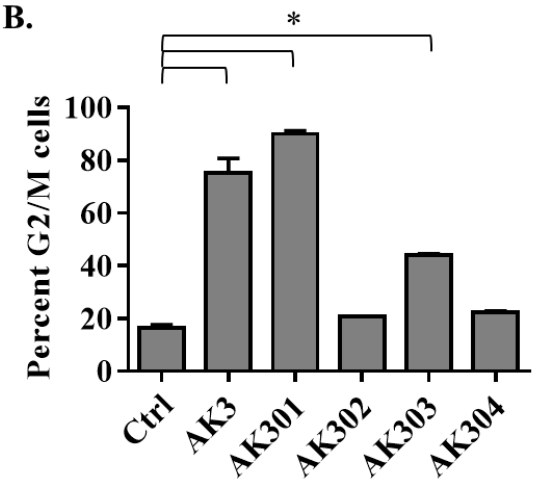
B.
*
Percent G2/M cells
100
80
60
40
20
0
Ctrl
AK3
AK301
AK302
AK303
AK304

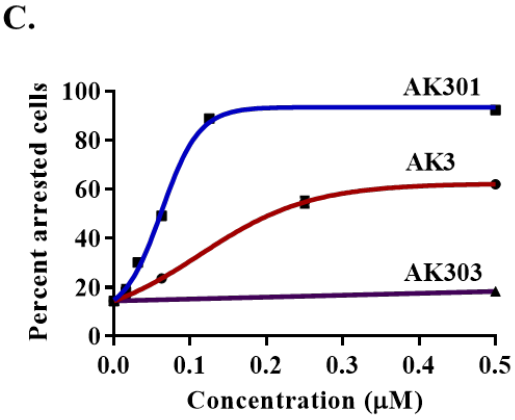
C.
Percent arrested cells
100
80
60
40
20
0
AK301
AK3
AK303
0.0
0.1
0.2
0.3
0.4
0.5
Concentration (μM)

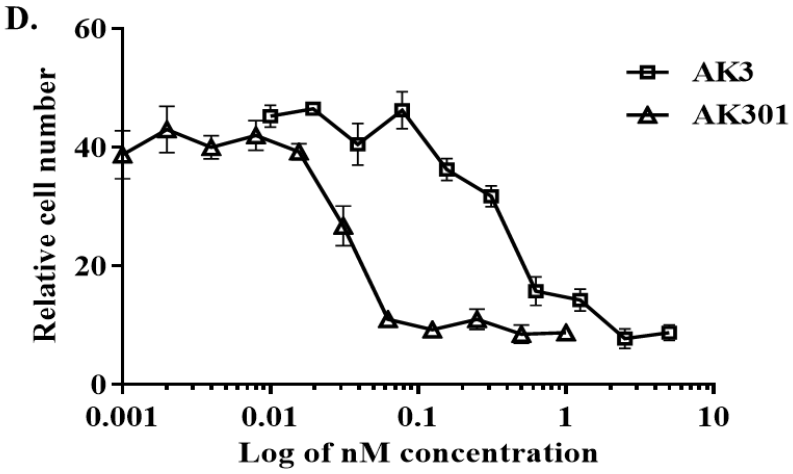
D.
Relative cell number
60
40
20
0
AK3
AK301
0.001
0.01
0.1
1
10
Log of nM concentration

Figure 3.1. Structural changes in the side groups of AK3 dictate its potency in inducing mitotic arrest.

(A) Structural analogs of AK3 [1-(3-chlorophenyl)-4-(2-methoxybenzoyl)piperazine] with modifications to the benzoyl group: AK301 [1-(3-chlorophenyl)-4-(2-ethoxybenzoyl)piperazine], AK303 [1-(3-chlorophenyl)-4-(3-methoxybenzoyl)piperazine], and AK304 [1-(3-chlorophenyl)-4-(4-methoxybenzoyl)piperazine], and the phenyl group [1-(4-chlorophenyl)-4-(2-methoxybenzoyl)piperazine]. (B) HT29 cells were treated with 5 μM of AK3 analogs for 18 h followed by an assessment of G2/M arrest by flow cytometry. Data suggest that AK3, AK301, and AK303 induce G2/M phase arrest, whereas AK302 and AK304 are inactive at this concentration (*$P < 0.0001$). (C) Dose-response analysis of AK3, AK301, and AK303-induced mitotic arrest by flow cytometry. AK3, AK301, and AK303 were titrated at different concentrations between 0 and 500 nM and G2/M was quantified by flow cytometry. AK303 induced significantly less mitotic arrest compared to AK3- or AK301-treated cells. AK301 was found to be the most potent compounds. (D) Dose-response curves showing reduced cell growth of AK3- and AK301-treated cells with increasing concentration. Cell viability of AK3- and AK301-treated cells were assessed by trypan blue exclusion assay.

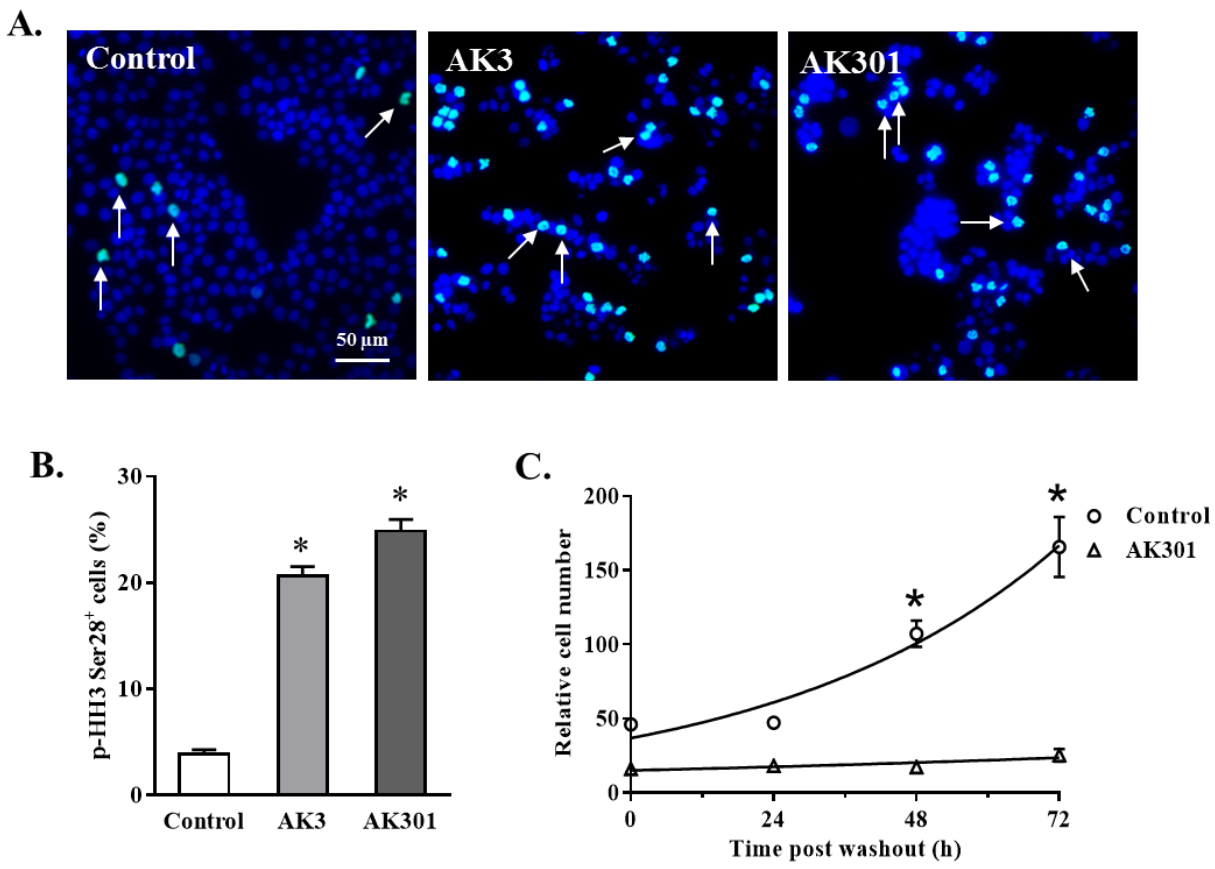

Figure 3.2. AK301 induces an irreversible mitotic arrest.

(A) AK3 and AK301 induce mitotic arrest in HT29 cells. Cells treated with 5 µM of AK3 or AK301 for 18 h were fixed, permeabilized, and stained with phospho-histone H3 (p-HH3) as a marker of chromosome condensation and mitosis. (B) Quantification of p-HH3 staining in Figure 3.2A shows a greater number of cells in mitosis. (C) Cells were treated with 500 nM of AK301 for 18 h. AK301 was then wash out and cell growth was observed at 24, 48, and 72 hours. AK301-treated cells showed no significant growth after AK301 withdrawal (*$P < 0.0001$).

3.4.3. AK301 affects microtubule function and results in multiple microtubule organizing centers (MTOCs)

To determine the effect of AK301 on spindle formation in the arrested cells, we performed immunostaining for β-tubulin. As shown in Figure 3.3A, AK301 induced the formation of multiple MTOCs, as is the case for AK3-treated HT29 cells. To further determine if the MTOC assemblies were stable or resulted from spontaneous microtubule assembly, HT29 cells were stained for aurora kinase A (AukA) and γ-tubulin. Aurora kinase A is responsible for recruitment of γ-tubulin to established centrosomes and γ-tubulin serves to nucleate and orient microtubules. As shown in Figure 3.3B, multiple aurora kinase A and γ-tubulin centers were observed following AK301 treatment of HT29 cells. These data suggest that AK301 leads to the formation of multiple MTOCs, including deposition of aurora kinase A and γ-tubulin at the spindle poles. We performed a dose-response analysis of β- tubulin immunostaining to assess the effects of AK301 on the formation of multiple MTOCs. As shown in Figure 3.4A, AK301 significantly induced spindle impairment or multipolarity compared to the inactive AK302 and AK304 at concentrations as low as 50 nM. We also quantified the number of aurora A kinase and γ-tubulin foci and found that AK301increased the number of these foci as well (Figures 3.4B and 3.4C).

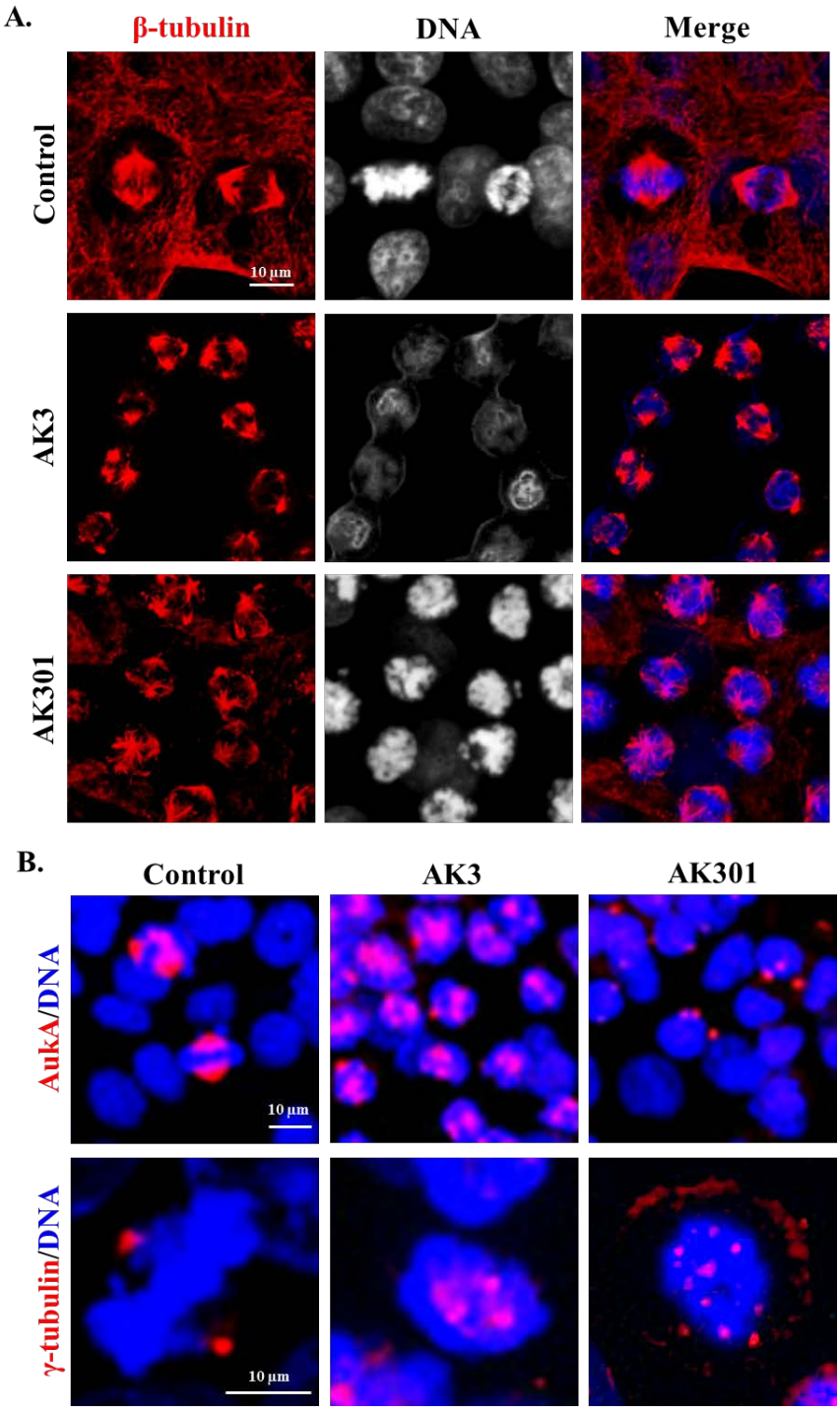
A.
β-tubulin
DNA
Merge
Control
AK3
AK301
10 μm
B.
Control
AK3
AK301
AukA/DNA
γ-tubulin/DNA
10 μm
10 μm

Figure 3.3. AK3 and AK301 induce the formation of multiple microtubule organizing centers (MTOCs).

HT29 cells treated with AK3 (1 μM) or AK301 (500 nM) were fixed and stained for (A) β-tubulin to visualize spindle assembly, (B) Aurora kinase A (AukA) (red; top panel) to understand the basis of multiple spindle organization, and γ-tubulin (red, bottom panel) to observe spindle nucleation. AK3- and AK301-arrested cells have multiple spindle nucleation sites, from which spindles arise.

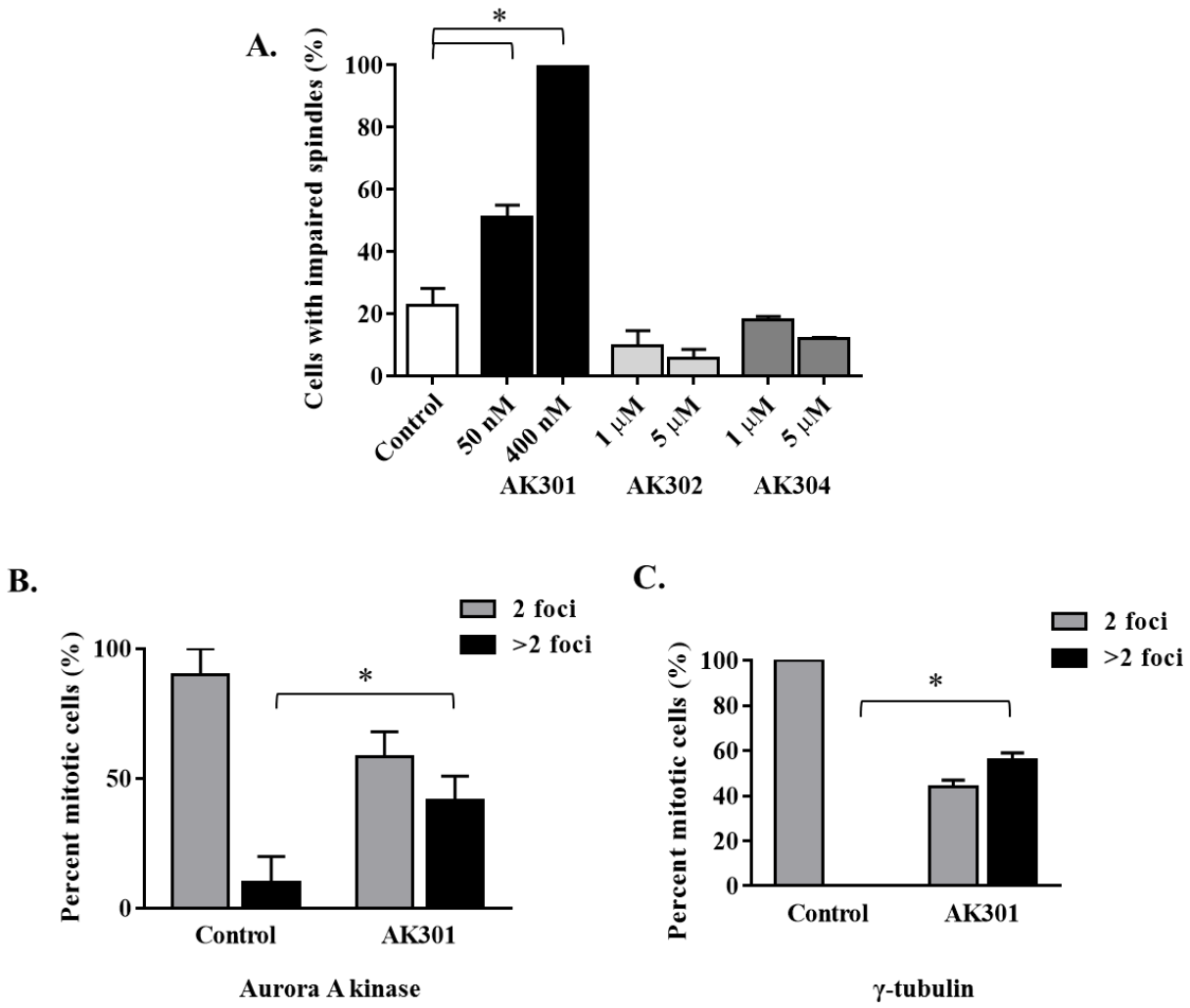

Figure 3.4. Quantification of MTOCs in AK301-treated cells.

(A) Quantification of cells with impaired spindles visualized by β-tubulin staining show multiple spindle poles. Quantification of (B) Aurora kinase A foci in HT29 cells, and (C) γ-tubulin foci in HT29 cells suggest the formation of multiple MTOCs in AK301-treated cells (*P < 0.0001).

3.4.4. AK301 induces G2 arrest in WI38 lung fibroblast cells

To assess the effects of AK301 on normal cells, we performed a dose response analysis for growth inhibition on WI38 lung fibroblast cells. As shown in Figure 3.5A, WI38 cells treated with AK3 or AK301 showed decrease in growth, similar to HT29 cells (Figure 1D). Comparison of the cell cycle data between AK301-treated HT29 and WI38 cells showed that AK301 induced a G2/M arrest in both cell lines (Figure .5B). However, quantification of mitosis using the mitosis-specific phospho-histone H3 staining revealed that AK301 induced significantly higher mitotic arrest in HT29 cells compared to WI38 cells (Figure 3.5C). Analysis of AK301-treated WI38 cells that were arrested in mitosis showed that they lacked multiple MTOCs and instead showed a more extensive microtubule breakdown (Figure 3.5D; arrowheads). AK301 altered microtubules of interphase cells; untreated WI38 cells showed elongated and spindle-shaped microtubules, whereas AK301-treated cells displayed a mesh-like network of microtubules. Together, these results suggest that AK301 can have cell-specific effects and that these effects may be mediated by changes in microtubule dynamics.

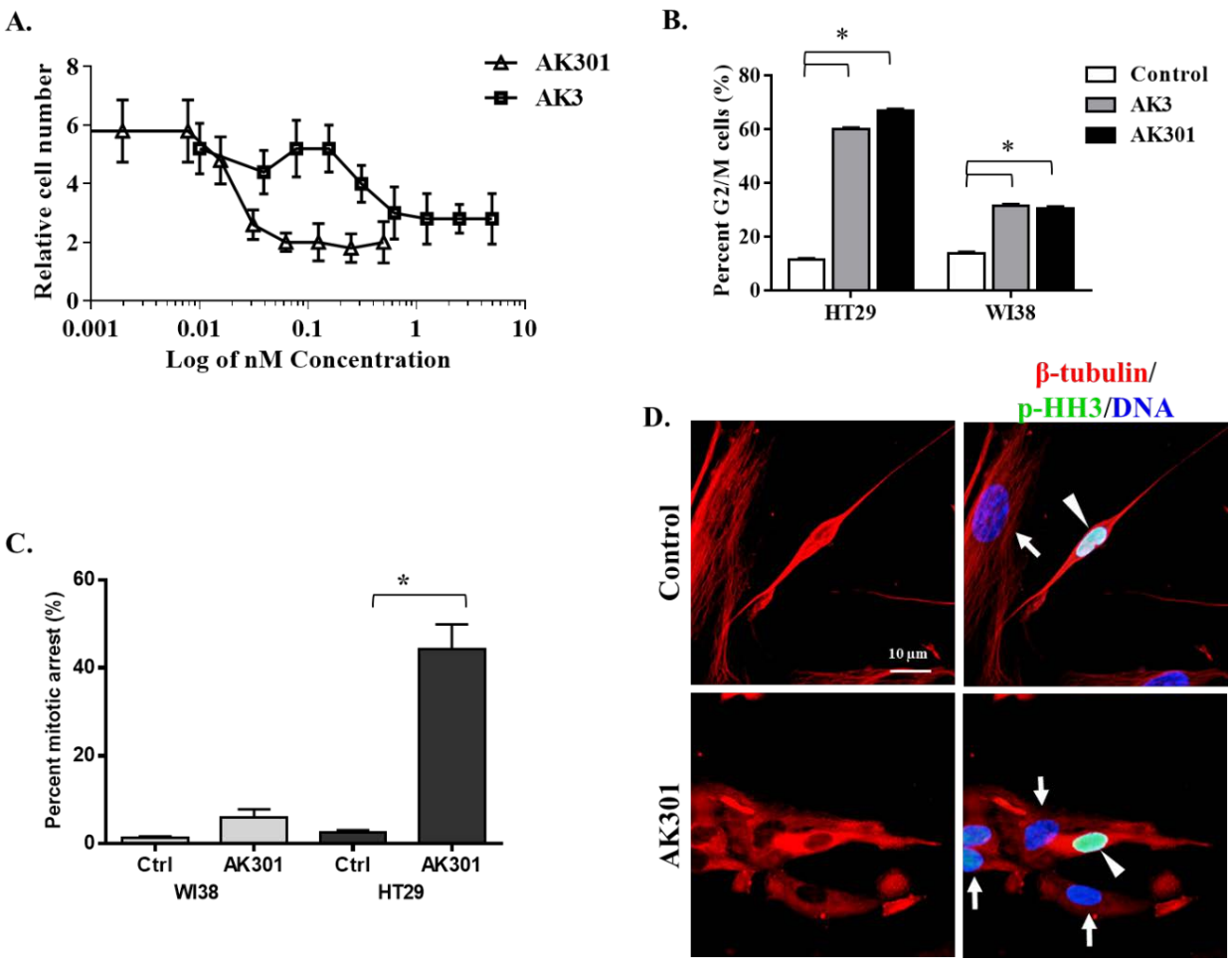

Figure 3.5. AK301 induces G2/M arrest in WI38 lung fibroblast cells.

(A) Dose-response analysis of WI38 cell growth inhibition by AK3 and AK301. Cells were treated with the indicated concentrations of the compounds followed by an assessment of viable cell number in the cultures (*P < 0.0001). (B) AK3 and AK301 induce G2/M arrest in HT29 and WI38 cells. Comparative cell cycle analysis of G2/M arrest in HT29 and WI38 cells was performed by flow cytometry (*P < 0.0001). (C) AK301 induces higher mitotic arrest in HT29 cells compared to that in WI38 cells. HT29 and WI38 treated with AK301 were immnostained for phospho-histone H3 and the mitotic index was determined in at least three microscopic fields.

Error bars indicate SEM (*P < 0.0001). (D) AK301-treated WI38 cells showed absence of spindle formation in mitotic cells. Treated cells were dual stained for phospho-histone H3 (green) and β-tubulin (red) to visualize spindle assembly in arrested cells. Arrows indicate interphase cells, whereas arrowheads indicate mitotic WI38 cells. AK30 disrupts spindle formation as well as cytoskeletal microtubules.

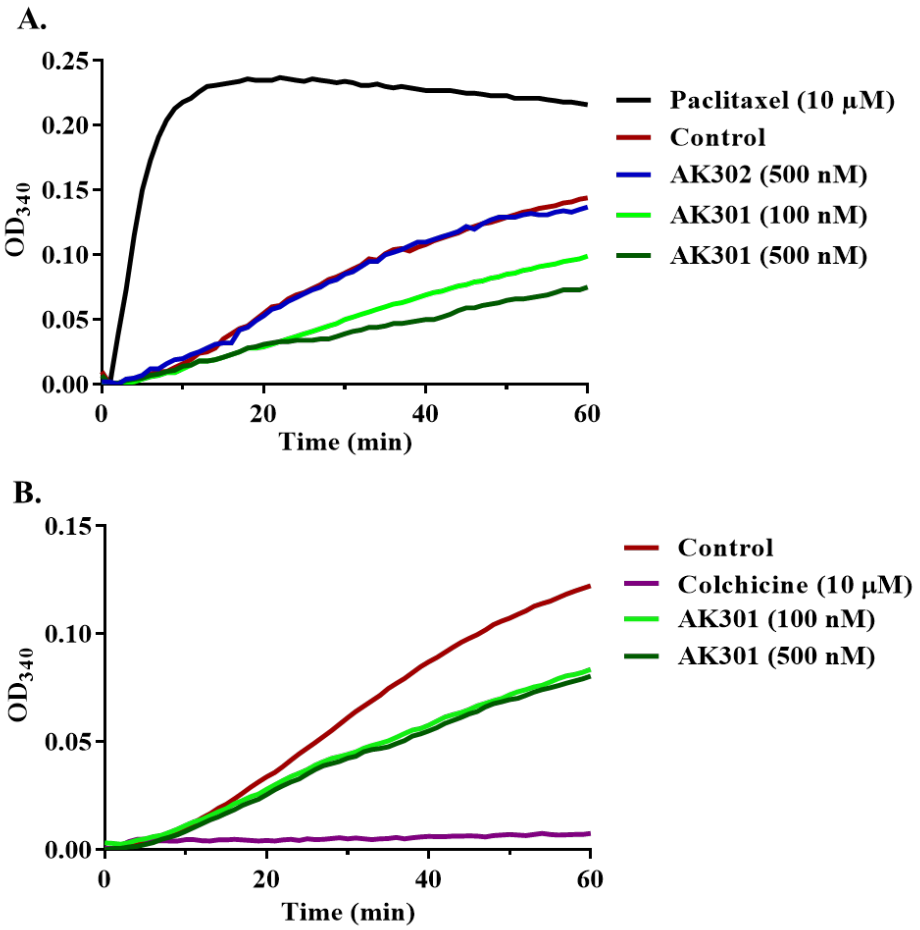

Figure 3.6. AK301 reduces the rate of tubulin polymerization.

(A) and (B) Tubulin subunits were allowed to polymerize in the presence of AK301, AK302, paclitaxel, or colchicine for 60 min. Tubulin polymerization (length of microtubules) was assayed in terms of absorbance at 340 nm. Assay indicates a decreased rate of tubulin polymerization in the presence of AK301, but not with AK302 (inactive compound), compared to control.

3.4.5. AK301 affects the rate of tubulin polymerization in vitro

Given the formation of multiple MTOCs in AK301-treated HT29 cells (Figures 3.3A and 3.3B) and the alteration of microtubule structures in WI38 cells, we assessed the effect of AK301 on the rate of tubulin polymerization, in an *in vitro* tubulin polymerization assay. As shown in Figure 3.6A, addition of AK301 slowed the rate of tubulin polymerization compared to the control sample. In contrast, AK302, identified as the inactive analog of AK3, did not alter the rate of polymerization. Colchicine, a known inhibitor of microtubule polymerization, acts by binding the β-subunit of tubulin dimer, and prevents their addition to the growing polymer. Microtubule formation was almost completely inhibited in the presence of colchicine, compared to AK301 (Figure 3.6B).

To assess the effect of AK301 on microtubule dynamics *in vivo*, we performed quantitative whole cell microtubule analysis as described previously. Figure 3.7A outlines this procedure that quantifies the degree of tubulin polymerization by flow cytometry. Figure 3.7B shows the mean fluorescence intensity (MFI) of mitotic cells treated with colchicine (500 nM), AK301 (250 nM), and its inactive analog, AK302 (1 μM). Colchicine shows the lowest microtubule fluorescence intensity, consistent with microtubule destabilization by colchicine. However, AK301-treatment shows a staining intensity intermediate to that of control and colchicine. AK302 did not induce significant reduction in staining. These data, along with the *in vitro* experiments, suggest that AK301 induces a partial breakdown of microtubules.

3.4.6. In silico molecular modeling

We performed molecular docking studies to assess tubulin as the potential target of AK301. We employed automated docking using AutoDock Vina with tubulin as the target receptor and

assessed SAR of the analogs to identify *in silico* conformations [150]. Colchicine, paclitaxel, and vinblastine were docked to their respective sites on tubulin to check for accuracy of molecular docking predictions (Figure A3; Figures A4A and A4B) [147-149]. AK3 and its analogs were docked to β-tubulin in the colchicine-, paclitaxel-, and vinblastine-binding sites. AutoDock Vina reported multiple conformations and corresponding binding affinities for each of the compounds in five independent trials. AK3 and its active analogs, AK301 and AK303, docked in same positions as indicated by superimposition of central piperazine core and the flanking functional groups of the small molecules (Figure A4C). The lowest energies for different compounds in known binding sites are shown in Table 1.1. Control binding affinities correspond to the energies obtained by docking colchicine, paclitaxel, vinblastine, and vincristine into their respective binding sites (vinblastine and vincristine were docked into the high affinity sites on tubulin). Active AK3 analogs showed compatibility for the colchicine site. In addition, the order of the predicted binding affinity matched the potency of AK3 analogs, as predicted by SAR studies.

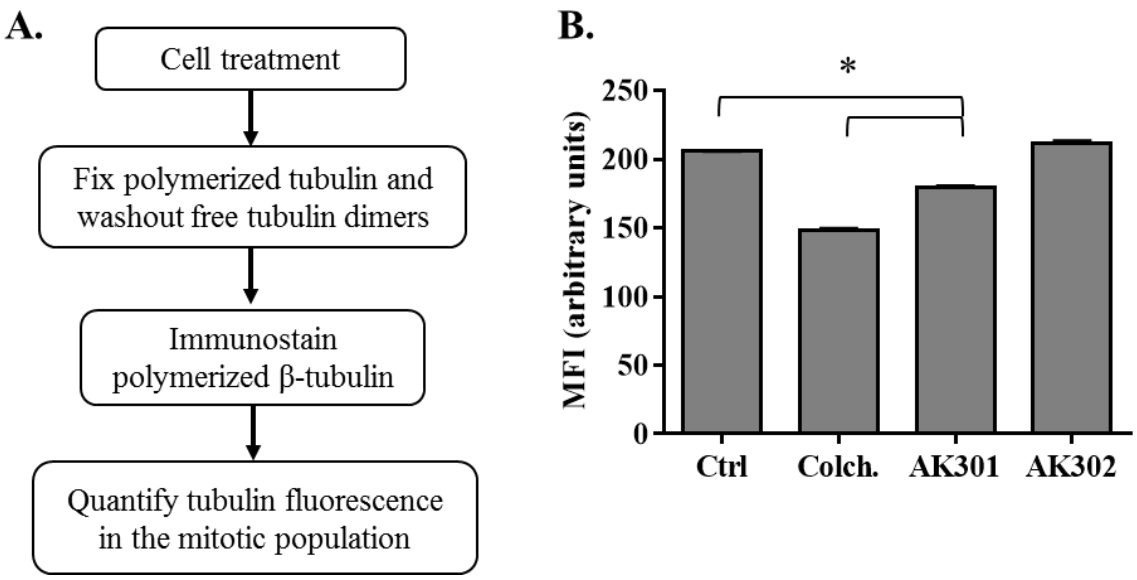

Figure 3.7. Disruption of *in vivo* microtubules in HT29 colon cancer cells.

(A) Schematic description of the methodology used for the assessment of *in vivo* microtubule stability in HT29 cells after AK301 treatment. (B) HT29 cells were treated with 500 nM colchicine, 250 nM AK301, or 1 µM AK302. Mean fluorescence intensity of mitotic cells was determined as described above. Data indicate decreased microtubule stability in AK301 and colchicine-treated cells, relative to AK302-treated and control cells (*P < 0.0001).

Figure 3.8A shows an *in silico* model of AK301 binding to tubulin in the colchicine-binding domain. Although AK301 docked into the colchicinebinding site, it assumed a different, novel orientation relative to colchicine. This orientation allows for hydrogen bond interactions between the oxygen atom of the ethoxy group or the carbonyl group and Asn 101 residue (3.0 Å and 2.9 Å, respectively). Further, this places the hydrophobic chloride proximal to hydrophobic tubulin residues—Leu 255 (3.9 Å) and Ile 378 (3.5 Å) (Figure 3.8B). In contrast, moving the chloride group from 3' C to 4' C of the halophenyl ring to generate the less-active AK302 compound changes the conformation of the molecule in the tubulin binding site. The changed conformation of AK302 decreased hydrophobic interactions with Leu 255 (6.7 Å) and Ile 378 (9.6 Å), and increased the distance for hydrogen bond interactions (6.6 Å for methoxy group and 5.8 Å for the carbonyl group) at the other end of the molecule (Figure 3.8C). Similar changes in conformation were also observed when the position of the methoxy group was moved from 2' C to 4' C, as is the case with AK304 compound. In general, the docking scores obtained correlated with the predicted *in vitro* activity and fit the SAR of AK3 analogs, with AK301 being the most potent among the analogs (Table 1). To confirm AK301 binding in the colchicine- binding domain of tubulin, we also performed molecular docking simulations in Molegro Virtual Docker [151]. We performed ten runs for AK301, targeting the largest cavity in tubulin, containing the colchicine-binding domain of tubulin. MolDock scoring function was used to assess the binding of the lowest energy poses. AK301, as predicted by AutoDock Vina, docked to the colchicine-binding domain of tubulin with the least energy poses superimposing each other (Figure 3.8D). The specific functional groups and their positions may, therefore, play an important role in determining the potency of AK3 analogs in inducing mitotic arrest in colon cancer cells.

Table 3.1. Predicted binding energies (in kcal/mol) of AK3 analogs docked in colchicine, paclitaxel, and high-affinity vinblastine site on β-tubulin.

Compound	Colchicine site	Paclitaxel site	Vinblastine site
Control	-8.8[#]	-9.7[†]	-10.7/-10.0[‡]
AK301	-8.7	-7.3	-7.5
AK3	-8.2	-7.3	-7.5
AK303	-8.3	-7.4	-7.6
AK302	-8.1	-7.3	-7.5

[#]colchicine, [†]paclitaxel, [‡]vinblastine/vincristine

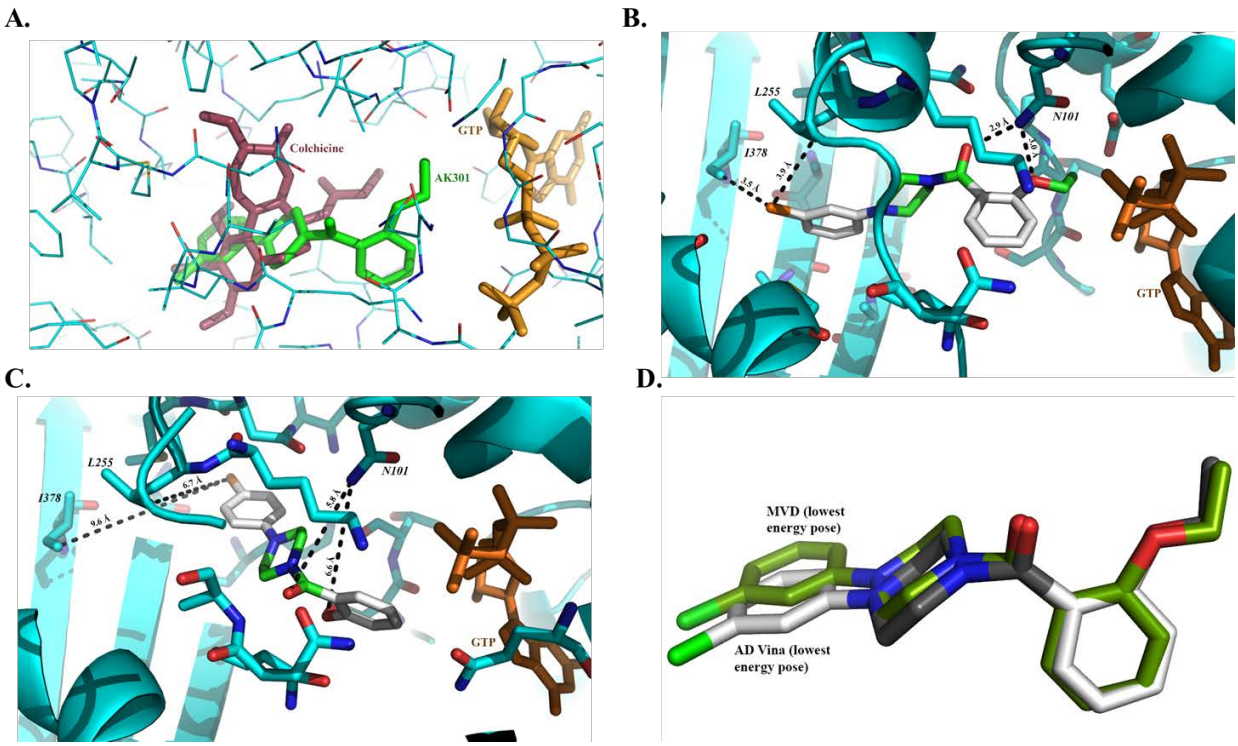

Figure 3.8. Predicted *in silico* novel binding orientation of AK301 to β-tubulin.

(A) Novel orientation of AK301 in the colchicine-binding site of β-tubulin as modeled by AutoDock. AK301 (shown in green) is predicted to bind to tubulin the colchicine-binding domain (colchicine is shown in red), but in a different orientation. (B) Residues surrounding AK301 allow for strong hydrogen bond interactions with Asn101 of β-tubulin. Consequently, the chloride group is positioned in tubulin surrounded by hydrophobic residues (Leu255 and Ile378). (C) Changing the position of the chloride in AK3 from 3' C to 4' C generates the inactive compound AK302. This change disrupts the hydrogen bond interactions of the methoxy and carbonyl groups on the methoxy-substituted benzoyl ring. Decreased hydrogen bond interactions result in lower binding affinity of AK302 to tubulin (Table 3.1). (D) Least energy poses of AK301, as predicted by AutoDock Vina (gray) and Molegro Virtual DOcker (green), docked to

β-tubulin. The least energy pose of AK302, predicted by MVD, had a similar orientation to that predicted by AD Vina.

3.4.7. TNF-dependent induction of apoptosis in AK301-treated cells

AK3 and other piperazinebased compounds were originally identified by their ability to acutely sensitize colon cancer cells to ligand-induced apoptosis [145]. To determine whether AK301 could also induce cell death in combination with TNF, we performed a dose-response analysis of AK301 in the presence and absence of TNF (Figure 3.9A). Analysis of the sub-diploid cell population indicated that AK301, on its own, did not induce apoptosis in HT29 colon cancer cells. However, in the presence of TNF, AK301- treated cells underwent significant apoptosis (EC_{50} of 172 nM) at concentrations approximately 5 times lower than those reported for AK3 [145].

To determine the association between mitotic arrest and TNF-induced apoptosis, the compounds shown in Figure 1A were tested for their ability to induce apoptosis in the presence of TNF. Figure 3.9B shows that only the compounds that induced a mitotic arrest could induce apoptosis in combination with TNF. This finding suggests an association between mitotic arrest and TNF sensitivity. To further assess the correlation between the two events, cell cycle analysis of HT29 cells was performed. As shown in Figure 3.9C, most of the cells in the control population are in the G1 phase of cell cycle. With TNF treatment alone, no significant shifts are observed. However, with the addition of AK301, cells shifted from G1 to G2/M. Finally, co-treatment of HT29 cells with AK301 and TNF resulted in a decrease in G2/M population and a subsequent appearance of sub-diploid population. These data suggest that the sub-diploid population is likely derived from the G2/M arrested cells.

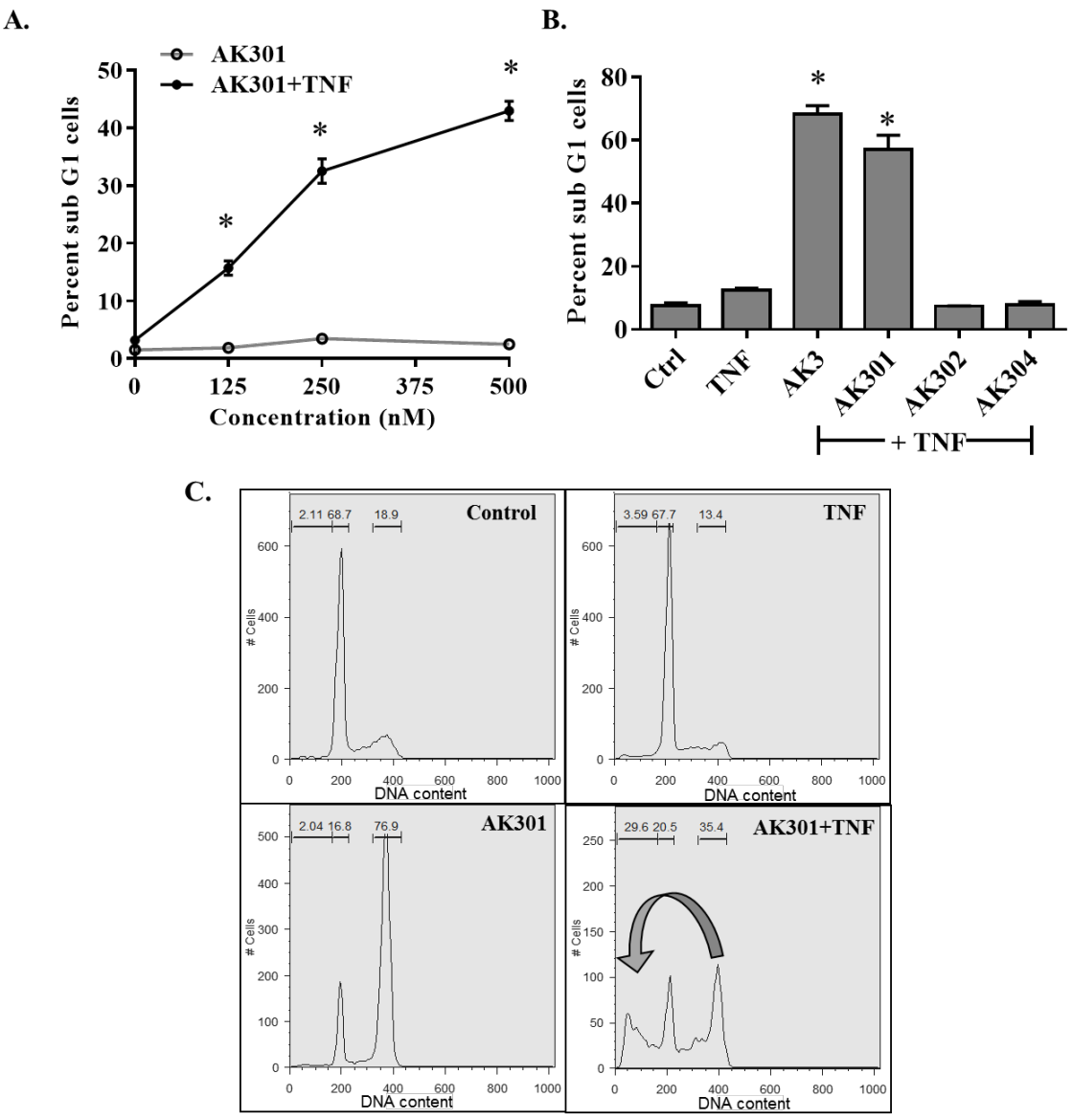

Figure 3.9. AK301-induced mitotically arrested cells undergo TNF-dependent apoptosis. (A) Dose-response analysis of AK301-treated cells in the presence and absence of TNF. HT29 cells were treated with AK301 (500 nM) or AK301 plus TNF (50 ng/ml) for 18 h, PI-stained and analyzed by flow cytometry. Significant apoptosis was observed only in the combination treatment (*P < 0.0001). (B) Induction of cell death following combination treatment with active AK3 analogs and TNF. Cells were treated with 5 μM of AK3, AK301, or AK303 and TNF (50

ng/ml) showed high percentage of sub-diploid population compared to TNF treatment alone (*P < 0.0001). Percentages of sub-diploid population with 5 μM of AK302 or AK304 and 50 ng/ml of TNF treatment were similar to those treated with TNF alone. (C) AK301 induces mitotic arrest and the appearance of sub-diploid cell fragments in the presence of TNF. In the presence of AK301 alone (500 nM), cells arrest in G2/M phase of mitosis (bottom, left panel). In the presence of TNF alone, there is no significant change in the cell cycle distribution (top, right panel). Following combination treatment with Ak301 and TNF (50 ng/ml), a decrease in the G2/M population was observed accompanied by the appearance of a sub-diploid population (*P < 0.0001).

3.4.8. Relationship between mitotic arrest and cancer cell apoptosis

To further examine the relationship between mitotic arrest induced by AK301 and its analogs and apoptosis, we performed a dose-response analysis of AK301, AK302, and AK304 on mitotic arrest and caspase-3 activation. As shown in Figure 3.10A, AK301 induced mitotic arrest in a dose-dependent manner, whereas AK302 and AK304 were inactive even at concentrations of 5 μM. Analysis of dose-dependent caspase-3 activity (using DEVD-AMC fluorogenic substrate) for these compounds in the presence of TNF is shown in Figure 3.10B. Data indicates similar trends in caspase-3 activation as those observed for mitotic arrest. These results demonstrate a close relationship between mitotic arrest by AK301 and TNF-induced apoptosis.

There are a number of known inhibitors of microtubules that are capable of inducing mitotic arrest [152-154]. To determine how these compounds compare to AK301 in sensitizing cells to TNF, HT29 cells were treated with two different concentrations each of AK301, colchicine, nocodazole, and a vinca alkaloid—vincristine in the absence or presence of TNF for 18 hours. Cell extracts were prepared for capase-3 enzymatic assay. As shown in Figure 3.10C, none of the compounds induced caspase-3 activation on their own. However, upon co-treatment of HT29 cells with the drugs and TNF, significant caspase-3 activation was observed (Figure 3.10D). Interestingly, AK301 induced the highest levels of caspase-3, even at 125 nM ($P < 0.0001$). Together with the results of previous experiments, this suggests that AK301 is a novel, potent inhibitor of microtubules capable of inducing arrest on its own and increasing cell sensitivity to TNF-induced apoptosis.

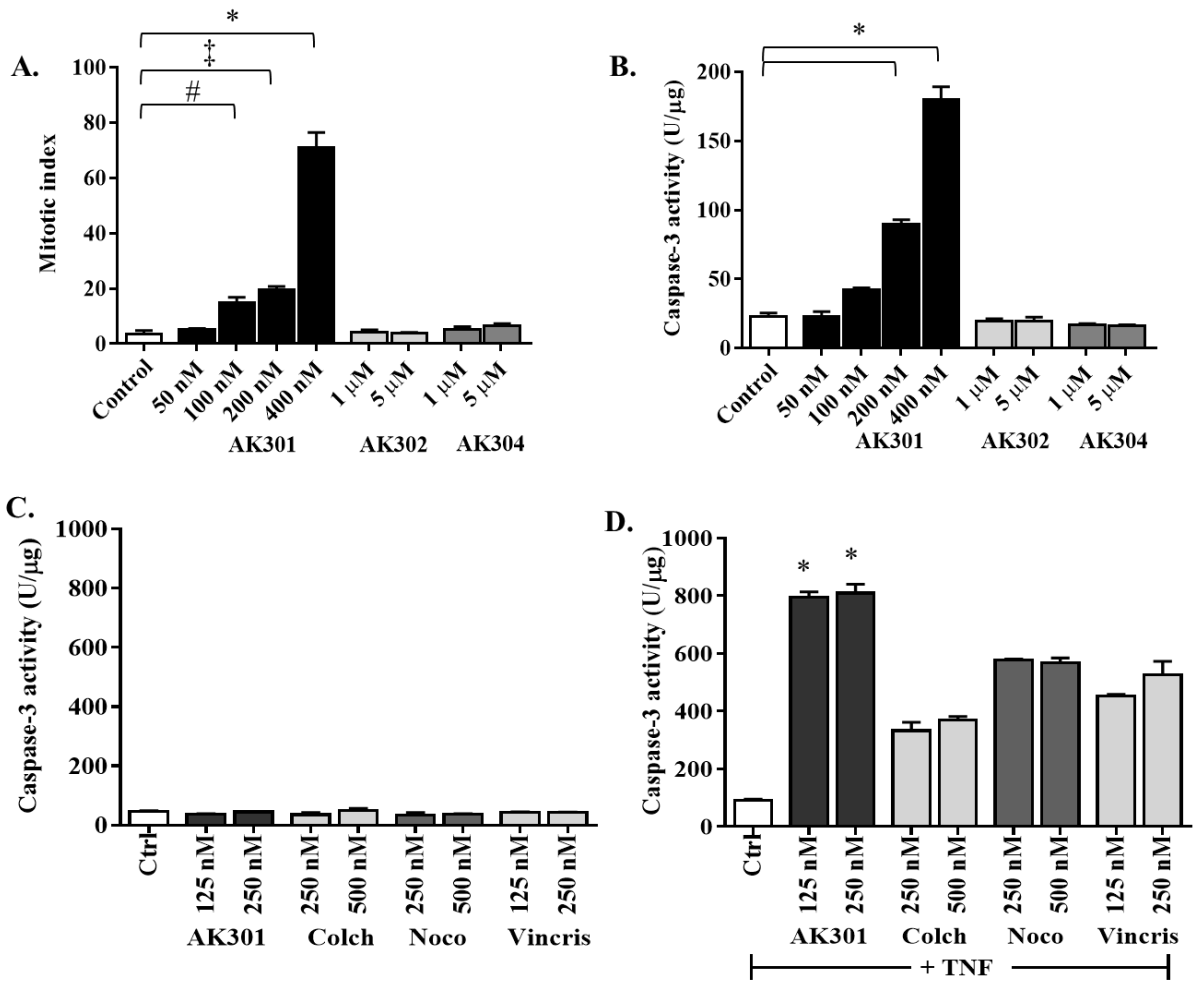

Figure 3.10. Effect of microtubule disruption on colon cancer cell apoptosis in the presence of TNF.

(A) Dose-response analysis of AK301, AK302, and AK302 mitotic arrest of HT29 cells. Cells were stained with p-HH3 post treatment and the mitotic index was determined. Data indicate a dose-response mitotic index in cells treated with AK302. (B) Dose-response analysis of AK301, AK302, and AK304 caspase activation in HT29 cells. Cell lysates were prepared and tested for caspase-3 activity using DEVD-AMC fluorogenic substrate. Data indicate dose-response of caspase-3 activation in cells treated with AK301, similar to mitotic index in Figure 3.10A ($^{\#}P < 0.05$, $^{\ddagger}P < 0.01$, $^{*}P < 0.0001$). HT29 cells were treated with microtubule inhibitors in the absence

(C) or presence (D) of TNF (50 ng/ml). AK301 and other known microtubule inhibitors (colchicine, nocodazole, and vincristine) did not induce significant levels of caspase-3 activity on their own (panel A). However, in combination with TNF, AK301 induced significantly higher levels of caspase-3 in HT29 cells, relative to the other microtubule destabilizers (panel B) (*P < 0.0001).

3.4.9. Generality of AK301 activity

To assess the general effects of AK301 sensitization, we determined the effect of AK301 on caspase-3 activation by TRAIL and Fas. As show in Figure 3.11A, AK301 enhanced TRAIL-induced caspase-3 activity. HT29 cells were more sensitive to Fas ligation, but AK301 further enhanced Fas-induced caspase-3 activity, as shown in Figure 3.11B. AK301 was also tested on HCT116 cells, another human colon cancer cell line (Figure 3.11C). HCT116 cells were more sensitive to TNF-induced apoptosis than HT29 cells. Despite their sensitivity, AK301 significantly enhanced TNF-induced caspase-3 activation over TNF background. ($^{\#}P < 0.01$). These data suggest that AK301 is broadly active on different cancer cell lines and with different death ligands, such as TRAIL and Fas.

3.4.10. Increased TNFR1 cell surface expression mediates enhanced caspase-8 and caspase-9 activation

TNF is coupled to caspase-8 through TNFR1, which in turn can activate procaspase-3 [155]. Moreover, activated caspase-8 can interact with the intrinsic death pathway by activating caspase-9 [156]. We analyzed the presence of caspase-8 and -9 in AK301 and AK301/TNF treated cells by immunoblotting. As shown in Figure 3.12A, AK301 or TNF treatment alone did not induce caspase-8 or caspase-9 activation. However, cells co-treated with AK301 and of both of these caspases.

To determine if caspase-8 was activated by an increased TNF-TNFR1 coupling at the cell surface, we assessed the levels of TNFR1 in the membrane fraction of HT29 cells (an NP40 extract) relative to a whole cell extract (RIPA). As shown in Figure 3.12B, cells treated with AK301 showed an increase in the appearance of TNFR1 in the membrane fraction. Moreover,

we observed an increase in TNFR1 in the RIPA extract after treatment with AK301 or TNF alone, which suggests that AK301 may act as a trigger for TNFR1 production. We quantitatively analyzed cell surface expression of TNFR1 in HT29 cells after treatment with AK301 analogs to determine if TNFR1 surface expression was specific to AK301. As shown in Figure 3.12C, HT29 cells treated with AK301 showed an increase in TNFR1 cell surface staining, whereas the other inactive analogs did not. Together, these data suggest that AK301 induces an increase in cell surface expression of TNFR1. This increase in surface expression may facilitate TNF binding and trigger an apoptotic cascade.

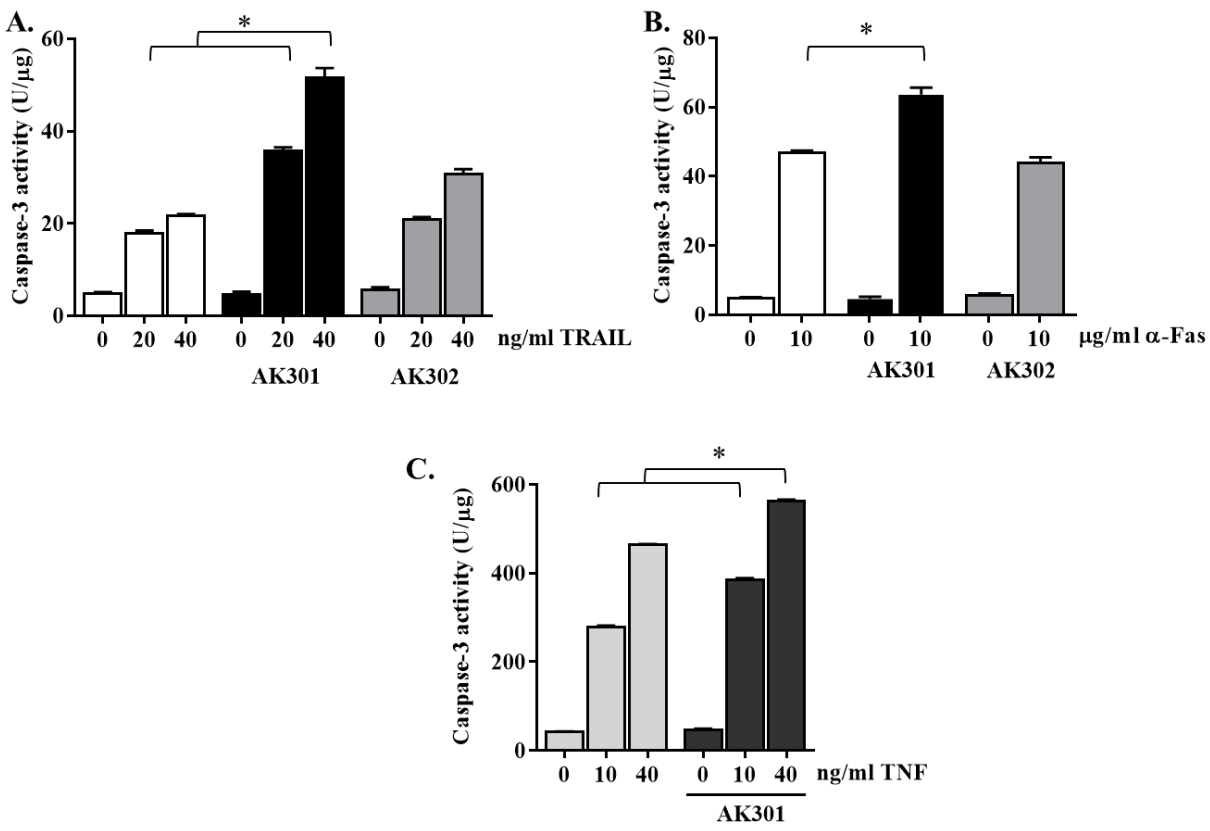

Figure 3.11. Effect of AK301 on other colon cancer cell lines and on TRAIL- and Fas-mediated cell death.

AK301 accentuated caspase-3 activation in the presence of (A) TRAIL, or (B) by Fas ligation. AK301-treated HT20 cells were co-treated with TRAIL (20 or 40 ng/ml) or anti-Fas antibody (10 µg/ml) and analyzed for caspase-3 activation. Both TRAIL and Fas ligation significantly enhanced caspae-3 activation, despite HT29 cells being more sensitive to Fas ligation (*P < 0.0001). (C) TNF was titrated on to HCT116 colon cancer cells in the presence or absence of 500 nM of AK301. AK301 significantly increased caspae-3 activity as observed by DEVD-AMC cleavage (*P < 0.0001), even though HCT116 cells are inherently more sensitive to TNF-induced cell death.

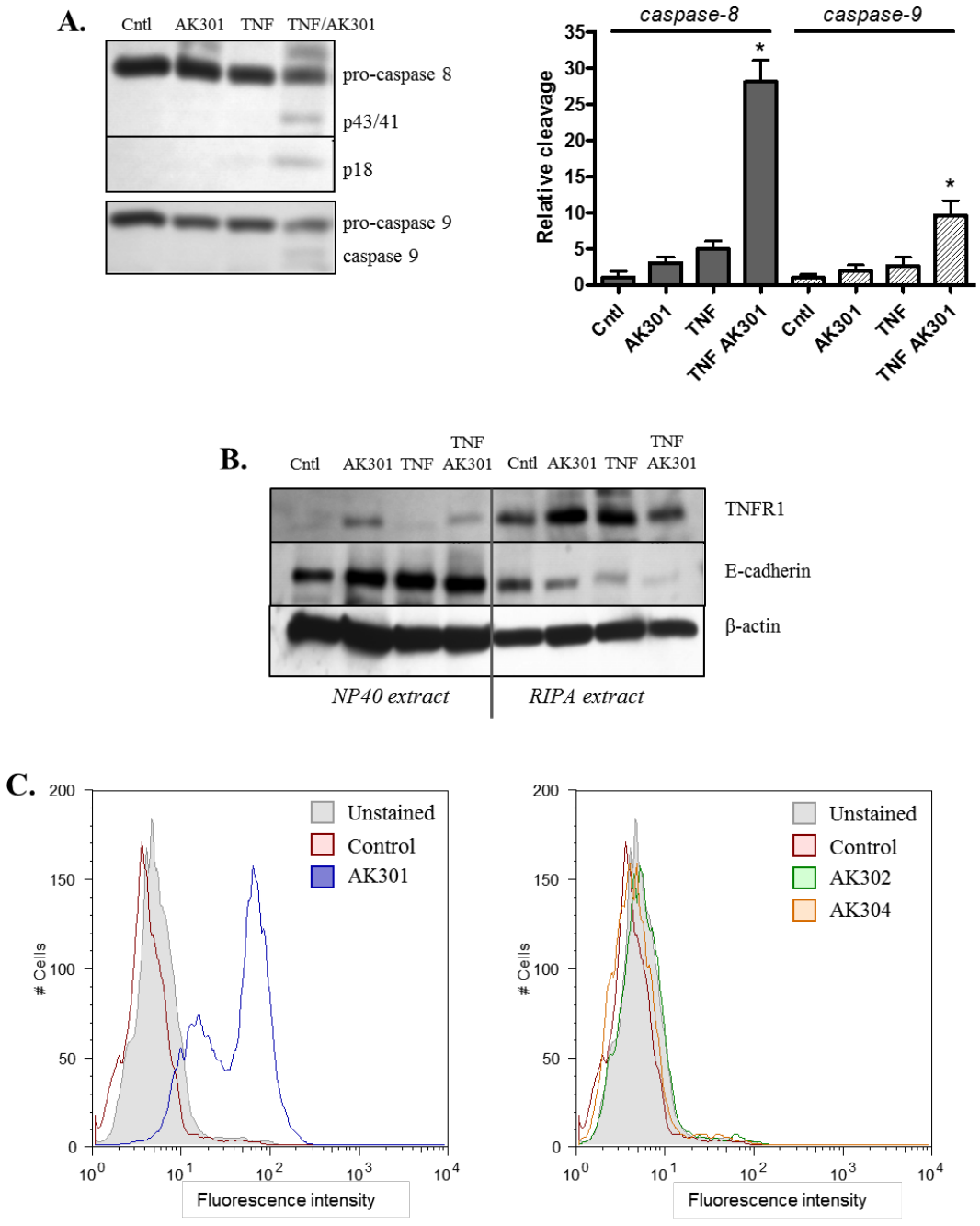

Figure 3.12. Increased TNFR1 cell surface expression and caspase-8 activation in AK301-treated cells.

(A) AK301 enhances TNF-induced activation of caspase-8 and caspase-9 (*P < 0.0001). Cells treated with AK301 for 16-18 h in the presence or absence of TNF. Immunoblot analysis of cell

lysates with antibodies against fill length and cleaved caspase-8 and caspase-9 showed cleaved caspase-8 and caspase-9 in cells co-treated with AK301 and TNF. (B) AK301 induces increased cell surface expression of TNFR1 on HT29 cells. Immunoblot analysis of an NP40 fraction (membrane proteins) and RIPA fraction (total protein/cell lysate) showed an increase in TNFR1 in the membrane fraction post AK301 treatment. (C) Increase in cell surface TNFR1 expression by flow cytometry. HT29 cells were treated with AK301 and its less active analogs were stained for TNFR1 and then fixed for flow cytometry. Data indicate increased cell surface expression of TNFR1 in AK301-treated cells, but not with the inactive analogs of AK301.

3.5. Discussion

We previously identified a class of small molecules that induced mitotic arrest in colon cancer cells and sensitized these cells to apoptosis in the presence of death ligands, such as TNF and FasL [145]. Here, we performed a detailed structure-activity relationship study on a piperazine-based compound (AK3) that was initially found to be highly effective at sensitizing colon cancer cells to apoptosis. Specifically, we identified 1-(3-chlorophenyl)-4-(2-ethoxybenzoyl)piperazine, referred to as AK301, that can induce mitotic arrest in colon cancer cells with an EC_{50} of ≈ 115 nM. This derivative is approximately five-fold more potent than the original AK3 compound identified in the initial screen. AK301 also increased the sensitivity of HT29 and HCT116 human colon cancer cell lines to TNF-induced apoptosis at relatively low concentrations. AK301 was also capable of inducing cell death in the presence of TRAIL and FasL. Our SAR studies also revealed a number of related compounds that were inactive for both mitotic arrest and TNF sensitization (AK302 and AK304). Together these compounds indicate a close relationship between mitotic arrest and sensitivity to TNF-induced apoptosis. In addition, these molecules were employed to determine a potential cellular target leading to mitotic arrest and apoptosis.

Characterization of the mitotic arrest state of AK301-treated cells indicated multipolar spindle assembly. The formation of the multipolar spindles was accompanied by appearance of multiple γ-tubulin and aurora kinase A staining loci, which is consistent with disruption of centrosome regulation and bipolar spindle formation. Most cancer cells have over-replicated centrosomes [157, 158], which are clustered at the poles during mitosis [159]; disruption of centrosome clustering by disruption of microtubule spindles by AK301 may prevent the concerted segregation of supernumerary centrosomes and lead to spindle multipolarity [160].

These complex, multipolar structures are apparently difficult to resolve as cell division is significantly inhibited even after the removal of AK301. The degree of AK301-induced mitotic arrest is cell-type dependent. Proliferation of the WI38 lung fibroblast cell line was reduced by AK301, but cells arrested more frequently in G2 than in mitotic phase. Although the reason for this difference in arrest phase is not known, it may be related to the presence of functional cell cycle checkpoints in non-transformed WI38 cells. Previous studies have shown that the checkpoint with forkhead and ring finger domains (CHFR) protein is a critical component in the cellular response to mitotic stress (including stress induced by microtubule disruption [161, 162]. Cells expressing a functional CHFR protein can delay entry into mitosis, thereby preventing catastrophic events during mitosis [163, 164]. On the other hand, studies have shown that HT29 cells and other cancer cells down-regulate CHFR expression (through promoter hyper-methylation) and are more likely to enter mitosis and not recover [165, 166]. The lack of functional mitotic checkpoints likely contributes to the effectiveness of mitosis-targeting chemotherapeutic agents and may explain to the different responses of HT29 and WI38 cells to AK301. However, microtubule disruption was observed in both arrested HT29 cells and WI38 interphase cells treated with AK301. This finding suggests that AK301 may target microtubules. This target is further supported by *in vitro* and *in vivo* tubulin polymerization studies and by *in silico* docking of AK301 to tubulin. It remains possible that AK301 interacts with other cellular proteins to achieve its effect of the cell cycle arrest and apoptosis, but all our dose-response and structure-activity studies point to microtubules as being an important target.

Microtubules are filamentous polymers of the cytoskeleton, composed of repeating α/β tubulin heterodimers, responsible for determining cell shape, motility, intracellular transport, and cell division [131]. Microtubules have long been known as the drivers of chromosome migration

and chromosome segregation [167]. Microtubules become highly dynamic during mitosis and generate bipolar spindles that capture the sister chromatids and align them at the equatorial plate [168, 169]. With proper chromosome alignment and cellular signaling, cells enter into anaphase and complete cell division [170]. The importance of microtubules in mitosis has made them a fruitful target for cancer therapies. However, it is clear that not all tubulin disruptors are equally useful as cancer therapies. This may be due in part to their influence on apoptosis pathways. Here we show that among microtubule disruptors, AK301 is particularly potent at sensitizing cancer cells to TNF and other apoptotic ligands. The interaction of microtubules with apoptosis is not limited to disrupting agents since paclitaxel can also sensitize cancer cells to TNF [171]. The mechanism by which apoptotic signaling is enhanced by microtubule targeting agents is not clear, but further study of this effect could improve our understanding of apoptosis regulation and may lead to the generation of more effective microtubule targeting agents. Our present data point to an increase in the expression of TNFR1 on the surface of cancer cells.

Molecular docking was employed to assess the potential of AK301 binding to tubulin dimers. For this analysis, we focused on the microtubule binding sites for colchicine, paclitaxel, and vinblastine. Molecular docking defines energy-optimized ligand orientations formed between the drug and its receptors [172]. Molecular docking predictions of AK301 and its derivatives showed relatively high affinity for the colchicine-binding region of tubulin, but docked in a different orientation than colchicine. Further analysis of these *in silico* complexes supported the significance of this binding position; we found that the longer chain ethoxy group of AK301 favored strong hydrogen bond interactions and positioned the chlorophenyl ring in a hydrophobic pocket. In summary, this theoretical structural analysis predicted the affinity of AK301 for tubulin.

We propose that AK301 represents a novel class of mitotic inhibitors, capable of inducing mitotic arrest on its own and inducing apoptosis in combination with TNF with high efficiency. How mitotic arrest leads to ligand-dependent cell death is not fully understood. We previously showed that mitotically arrested cells have increased cell surface expression of TNFR1 [145]. Increased TNF-TNFR1 interactions at the cell surface (or following TNF internalization) may increase the formation of death-inducing signaling complex (DISC) and caspase-8 activation [173, 174], which has been observed in arrested cells. Interestingly, AK301 was the most potent TNF-sensitizing agent tested in these studies, relative to other well-studied microtubule inhibitors (colchicine, nocodazole, and vincristine). How AK301 achieves such a high degree of TNF sensitization is not clear. Based on our tubulin polymerization assay, AK301 reduces the rate of tubulin polymerization, but does not prevent it completely (like colchicine). We speculate that AK301 interferes with tubulin polymerization, but just enough such that the cells can continue to deliver and present TNFR1 and/or Fas on the cell surface. However, it should be noted that AK301 might possibly interact with a microtubule-related target or an upstream target that affects tubulin polymerization. The activity of the AK301 class of compounds, both as effective mitotic inhibitors and as apoptotic ligand-sensitizing agents, suggests that they may be well-suited for cancer treatment, particularly when used on cancers with a high inflammatory cell infiltrate or following treatment with an immune stimulant. For basic research applications, this class of compounds should help illuminate how microtubules are employed to regulate apoptosis sensitivity.

CHAPTER 4

Novel microtubule inhibitor AK301 promotes the mitosis-to-apoptosis transition

4.1. Abstract

Precise genomic division during mitosis is a well-orchestrated process, mediated by microtubule spindles. Mistakes in the genomic division may result in cell cycle arrest or apoptosis, and if unchecked, can drive chromosome instability and tumorigenesis. Mitotic inhibitors are widely utilized chemotherapeutic agents, which take advantage of the high proliferative nature of cancer cells and defects in their m itotic checkpoints. We have identified a class of novel piperazine-based microtubule inhibitors, of which AK301 (1-(3-chlorophenyl)-4-(2-ethoxybenzoyl)piperazine), is the most potent derivative identified to date. Compared to other mitotic inhibitors, we show that AK301-arrested cells readily enter apoptosis following compound withdrawal or death ligand treatment ($IC_{50} \approx 150$ nM). This effect was more pronounced in p53-normal colon cancer cells. AK301-treated cells also exhibited higher levels of mitosis-associated ATM signaling and caspase-3 activation. Immunofluorescence confocal imaging of AK301-treated cells revealed the formation of characteristic multiple microtubule organizing centers and reduced microtubule growth. Upon AK301 withdrawal, microtubule networks and spindles reformed and readily entered apoptosis. In summary, our data show the development of a new class of mitotic targeting agents that may be useful for further drug development. This class of compounds can also serve as chemical probes for studying microtubule dynamics and cell signaling pathways regulating the mitosis-to-apoptosis transition.

4.2. Introduction

Mitosis is an intricate process in actively dividing cells, orchestrating a myriad of kinases and signaling pathways [129, 175]. Ascribing to this complexity, mitosis is considered to be the most sensitive phase of the cell cycle [132]. A number of mitotic checkpoints ensure the fidelity of chromosome segregation and cytokinesis; failure of mitotic checkpoints often results in chromosomal alterations, culminating in mitotic catastrophe or cancer-promoting chromosomal instability [130, 133]. Cancer cells often lack important checkpoint activities and will execute mitosis with improper spindle assembly [130]. Therefore, mitotic inhibitors are among the most widely utilized chemotherapeutic agents in the treatment of a number of malignancies [132]. However, the response of the cancer cells to mitotic inhibitors can be distinctly different–some cells remain arrested in mitotic phase, while others exit division and undergo apoptosis [176, 177]. In addition, different mitotic inhibitors result in varying levels of apoptosis [132]. How microtubule disrupting agents result in apoptosis and what cellular factors make the decision of mitotic arrest to apoptosis remain elusive. Previous studies indicate that the spindle assembly checkpoint (SAC) during mitosis is necessary for efficient induction of apoptosis; compromising SAC significantly reduces the sensitivity of anti-mitotic agents, including microtubule poisons [178, 179]. Thus, it is important to understand alterations in mitotic processes to effectively target cancer cells for apoptosis.

The SAC is enforced by a complex of proteins, including MAD2, BUB1, BUBR1, CHFR, and several others that are recruited to the kinetochores and centrosomes to ensure proper segregation of genetic material. MAD2, BUB1, and BUBR1 form the core of the SAC, while proteins, such as CHFR, act as modulators of spindle checkpoint by coordinating early mitotic progression and delaying chromosome condensation in cases of mitotic stress [180, 181].

Prolonged mitotic arrest due to activation of the SAC may result in senescence or apoptosis [177, 182]. Inactivation of checkpoint in cancer generally occurs through mutations in the core SAC proteins, suppressing the activity of mitotic checkpoint. In addition, studies also evidence inactivation of *CHFR* gene through hypermethylation [181]. Cancer cells, therefore, usually exhibit a dysfunctional mitotic checkpoint to continue to divide without restrictions imposed by the SAC.

One of the major hallmarks of cancers is the suppression of apoptotic responses [22]. The p53 protein is a tumor suppressor that acts as a guard against a variety of stress signals and mediates cellular arrest and/or apoptosis [183, 184]. Studies indicate that p53 may participate in the mitotic checkpoint as a protective measure against abnormal chromosomal ploidization due to mitotic failure [185]. BUBR1 directly interacts with and phosphorylates p53 at Ser15 and Ser46 residues [185]. Moreover, activation by phosphorylation of ATM at Ser1981 in response to spindle damage also stabilizes p53 during M phase, enforcing the SAC [186, 187]. Activated p53 in the arrested cells acts post-mitosis to eliminate cells with chromosome aberrations and polyploidy [185]. Missense mutations in *p53*, found in about 50 percent of human cancers, result in increased risk of DNA damage, errors in mitosis, and suppression of apoptosis [188, 189]. Moreover, mutations also occur in the p53 DNA binding domain, indicating that its activity as a transcription factor is pivotal for cancer suppression [190-192]. How this activity could function on condensed mitotic chromosomes is not clear, but it may determine the fate of cells following exit from mitosis.

We previously reported the identification of synthetic small molecule inhibitors that dramatically enhanced colon cancer cell death strictly in the presence TNF and other death ligands [145, 193]. The most potent of this piperazine-class of compounds, 1-(3-chlorophenyl)-4-

(2-ethoxybenzoyl)piperazine, referred to as AK301, was found to have activity in the low nanomolar range ($EC_{50} \approx 115$ nM) [193]. To gain insight into the mechanism of apoptosis in AK301-arrested cells, we studied the mitotic arrest state of AK301-treated cells in HCT116 cells. HCT116 cells differ from previously studies HT29 cells in a number of ways.. First, HCT116 cells are MLH1-deficient and exhibit weakened G2/M checkpoint [194]. Importantly, these cells have normal p53 tumor suppressor gene. Here, we show that apoptosis in HCT116 cells can be activated in a death ligand-independent manner, by removing AK301 from medium and releasing the cells from mitotic arrest. We also demonstrate that this mitosis-to-apoptosis transition requires a reversible mitotic arrest by AK301, unlike other mitotic arrest agents that induce a more permanent mitotic arrest. Finally, we show that cancer cells treated with AK301 arrest at a mitotic state that induced high levels of ATM activation and p53 stabilization relative to other mitotic arrest agents tested. The activation of p53 during mitosis culminates in an apoptotic response in cells following AK301 withdrawal. We propose that AK301 represents a novel class of compounds that will be beneficial for understanding how pro-apoptotic signaling via ATM-p53 pathway can be activated during mitosis for efficient apoptosis in cancer cells. The pathways targeted by AK301 may ultimately find therapeutic applications.

4.3. Materials and Methods

4.3.1. Cell Culture

HT29 and HCT116 colon cancer cell lines were obtained from the American Type Culture Collection (Manassas, VA). HT29 and HCT116 cell lines were cultured in McCoy's 5A medium, with 10% fetal bovine serum, non-essential amino acids and antibiotic/antimycotic (Life Technologies, Guilford, CT). Immortalized primary colon cell lines YAMC and IMCE

were a gift of Dr. R Whitehead (Vanderbilt University, Nashville, TN). YAMC and IMCE cells were cultured in RPMI medium containing 5% fetal bovine serum, non-essential amino acids, antibiotic/antimycotic, insulin-transferrin-selenium (Life Technologies), and 5 units of murine gamma interferons. The cells were grown at 33°C. AK301 was synthesized from compounds obtained from the ChemBridge DIVERSet^{TM} library (San Diego, CA). Colchicine and Vincristine, and BI 2536 were obtained from Sigma Aldrich (St. Louis, MO), Acros Organics (Pittsburgh, PA), and Selleck Chemicals (Houston, TX), respectively. Drug treatments were performed approximately 24 h after passage for 16 h, unless otherwise indicated. TNF was obtained from Pierce Protein Research Products (Rockford, IL).

4.3.2. Immunofluorescence microscopy

Cells cultured on coverslips were fixed with 4% paraformaldehyde at room temperature or 100% ice cold methanol at 4°C and then permeabilized with 0.5% Triton X-100 in PBS. Cells were blocked in 5% serum (in PBS) and then incubated with primary antibody (in 5% serum) on shaker for 1 h at room temperature against phosphohistone H3 Ser 28 (sc-12927, Santa Cruz Biotechnology, Santa Cruz, CA), β-tubulin (E7 monoclonal antibody, Developmental Studies Hybridoma Bank), or cleaved caspase-3 (Asp175, Cell Signaling). Appropriate secondary antibodies (Molecular Probes, Life Technologies or Jackson ImmunoResearch, West Grove, PA) were used for 45 min incubation. Nuclei were visualized using DAPI (5 μg/ml in PBS; DI306, Life Technologies). Coverslips were mounted on slides using ProLong Gold Antifade Reagent (Life Technologies). Images were acquired using Nikon A1R Confocal Microscope (version 2.11, Nikon Instruments Inc.) and NIS-Elements Advanced Research Software (version 4.13.01, build 916, Nikon Instruments Inc.). Quantification of immunostaining was performed using

ImageJ image analysis software (http://rsb.info.nih.gov/ij) as previously described [88]. Following background subtraction and image stacking, both DAPI and immunofluorescence images were merged. Image brightness and contrast was modified with Adobe Photoshop software CC 2014 (Adobe Systems).

4.3.3. Live cell imaging

Cells were plated into 8-well chamber plates (Nunc™ Lab-Tek®, Waltham, MA) and treated with compounds for 16 hrs. In the case of HT29 cells, drugs were replaced with SP600125 for 2 hrs, followed by fresh medium. The Andor iQ live cell imaging software (Oxford Instruments, Belfast, UK) with Clara Interline CCD or iXon EMCCD camera (Oxford Instruments) was used to image cells. Micro-Manager© (https://www.micro-manager.org) was used as acquisition controller. Images were processed and corrected using ImageJ image analysis software (http://rsb.info.nih.gov/ij).

4.3.4. Flow cytometry and cell cycle analysis

Cells were stained for γH2AX using the protocol described above for immunofluorescence staining. Briefly, cells were fixed with 4% PFA, permeabilized with 0.1% Triton X-100, and blocked with 5% donkey serum. Cells were then incubated with γH2AX antibody (sc-101696, Santa Cruz Biotechnology) followed by incubation with Alexa Fluor® 488 secondary antibody (Life Technologies). Cells were then harvested using trypsin-EDTA for 15 min at 37°C and washed once with PBS. Propidium iodide (30 µg/ml) was added to the cells prior to filtration through 35 µm cell strainer tubes. Cell were promptly analyzed by flow cytometry.

For cell cycle analyses, cells were analyzed for DNA content by ethanol fixation and staining with propidium iodide as previously described [89]. Cells were harvested using trypsin-EDTA, centrifuged at 1000 *X g* for 10 min and resuspended in 500 µl of cold saline GM. Cells were washed once with 1X PBS and then fixed for at least 2 hrs at -20°C in 3X volumes of cold 100% ethanol while vortexing. Cells were then pelleted and washed once with PBS containing 5 mM EDTA. Pelleted cells were stained with 30 µg/ml propidium iodide (Molecular Probes, Life Technologies Corp.) and 0.3 mg/ml RNase A (Sigma-Aldrich, St. Louis, MO) in 500 µl PBS solution for 40 min in dark at RT. The stained cells were filtered through 35 µm cell strainer tubes (BD Biosciences, San Jose, CA). All flow cytometric analyses were performed on FACSCalibur (BD Biosciences) using Cell Quest software (BD Biosciences). The data were analyzed using FlowJo (v10, TreeStar Inc., Ashland, OR).

4.3.5. Caspase-3 assay

Caspase-3 activity was determined as previously described [145]. Cells were collected, centrifuged at full speed, and washed once with PBS. Pelleted cells were lysed by two rounds of freeze-thaw in lysis buffer containing 10 mM Tris-HCl (pH 7.5), 0.1 M NaCl, 1 mM EDTA, and 0.01% Triton X-100 and centrifuged at 10,000 *X g* for 5 min. The assays were performed on 96 well plate by mixing 50 µl of lysis supernatant with 50 µl of 2X reaction mix (10 mM PIPES pH 7.4, 2 mM EDTA, 0.1% CHAPS, 10 mM DTT) containing 200 nM of the fluorogenic substrate Acetyl-Asp-Glu-Val-Asp-7-Amino-4-methylcoumarin (DEVD-AMC; Enzo Life Sciences). The fluorescence was quantified at the start of the reaction and after 30 min. Protein concentrations were determined using CBQCA Protein Quantitation Kit (Life Technologies). Caspase activity

was determined by dividing the change in fluorescence by total protein content of the reaction mixture.

4.3.6. Western blot

RIPA buffer was used for total protein extraction and NP-40 buffer was used for membrane protein extraction. 20 μg of protein was denatured under reducing conditions and separated on 10% polyacrylamide gels (Bio-Rad Laboratories, Hercules, CA) and transferred to nitrocellulose by voltage gradient transfer. The resulting blots were blocked with 5% (w/v) non-fat dry milk in PBS + 0.1% (v/v) Tween-20. Specific proteins were detected with appropriate antibodies using SignalFire™ Elite ECL Reagent (Cell Signaling Technology). Immunoblotting antibodies were cleaved caspase-8 (18C8, Cell Signaling Technology), p53 (OP03, Calbiochem, Germany), p-p53, ATM (2873, Cell Signaling Technology), and p-ATM Ser1981 (13050 Cell Signaling Technology)

5.3.6. Statistical analyses

One-way analysis of variance (ANOVA) was used when comparing two groups with Tukey's post hoc test. For more than two groups, two-way ANOVA was used with Bonferroni correct. Significance was calculated at an alpha of 0.05.

4.4. Results

4.4.1. AK301-arrested cells show increased caspase-3 activity

To compare the mitotic arrest-inducing ability of AK301, we tested various pharmacological agents, including microtubule inhibitors (colchicine and vincristine), and a

PLK1 inhibitor (BI2536) for their ability to induce mitotic arrest. HCT116 colon cancer cells were treated with either 250 nM or 500 nM of each of these agents. Flow cytometric analysis of propidium iodide (PI)-stained cells was performed to assess the DNA content of the cells. All of the agents tested were able to induce over 80% of mitotic arrest ($P < 0.0001$) (Figure 4.1A). To examine the relationship between induced mitotic arrest and sensitivity, we tested these agents for their ability to induce capase-3 activation in HCT116 cells, using a DEVD-AMC fluorogenic substrate. All agents were tested at 500 nM. As shown in Figure 4.1B, of the four mitosis-arresting agents, only AK301 ($P < 0.0001$) and BI2536 ($P < 0.05$) were able to induce significant levels of caspase-3 activity. These results demonstrate a close relationship between the phase of mitotic arrest and cell sensitivity.

4.4.2. AK301 withdrawal enhances apoptotic response in HCT116 cells

Mitotic inhibitors can bind reversibly or irreversibly to their target. To better understand the nature of AK301's interaction with its proposed target, β-tubulin, we withdrew AK301 from arrested HCT116 cell culture and monitored their progression through the cell cycle for 24 hours post release. Flow cytometric analysis performed at 3, 6, 12 and 24 hours post AK301 withdrawal showed the appearance of sub G1 population in the cells released from AK301 arrest as early as 3 hours after release (Figure 4.2B). However, cells arrested with AK301 showed little to no apoptosis during the 24 hour period (Figure 4.2A). These data demonstrate that AK301 may bind reversibly to microtubules and that withdrawal of the drug enhances the sensitivity of HCT116 cells to apoptosis.

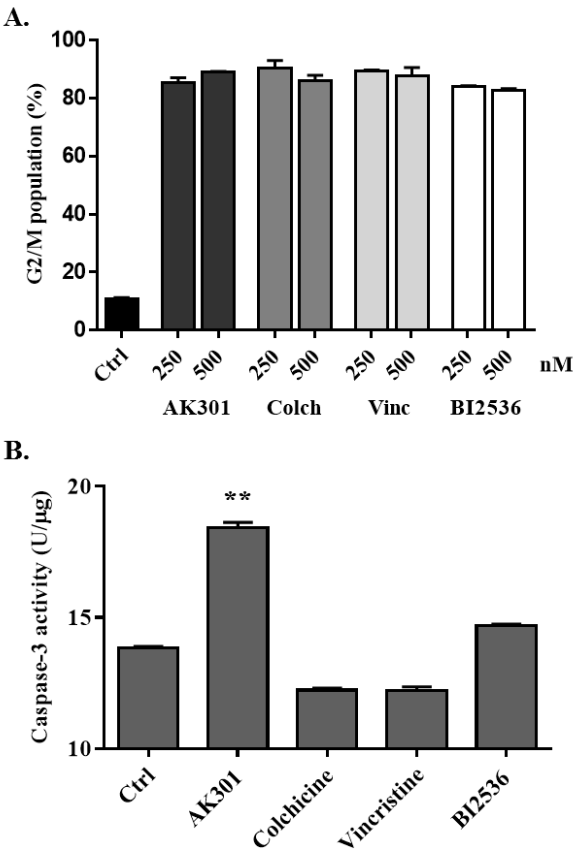

Figure 4.1. AK301 and BI2536 induce the highest levels of caspase-3 activation.

(A) HCT116 cells were treated with the indicated concentrations of AK301, colchicine, vincristine (microtubule inhibitors), and BI2536 (PLK1 inhibitor) for 16 h. Cells were fixed and stained with propidium iodide (PI) and analyzed by flow cytometry. All four drugs induced significantly high levels of G2/M arrest at both drug concentrations ($P < 0.0001$). (B) HCT116 cells were treated with 500 nM of each of the drug for 16 h. Cell lysates were prepared and tested for levels of caspase-3 activity using DEVD-AMC fluorogenic assay and protein concentration with CBQCA assay. AK301 (**$P < 0.0001$) and BI2536 (*$P < 0.05$) induced significantly higher levels of caspase-3 activation in HCT116 cells.

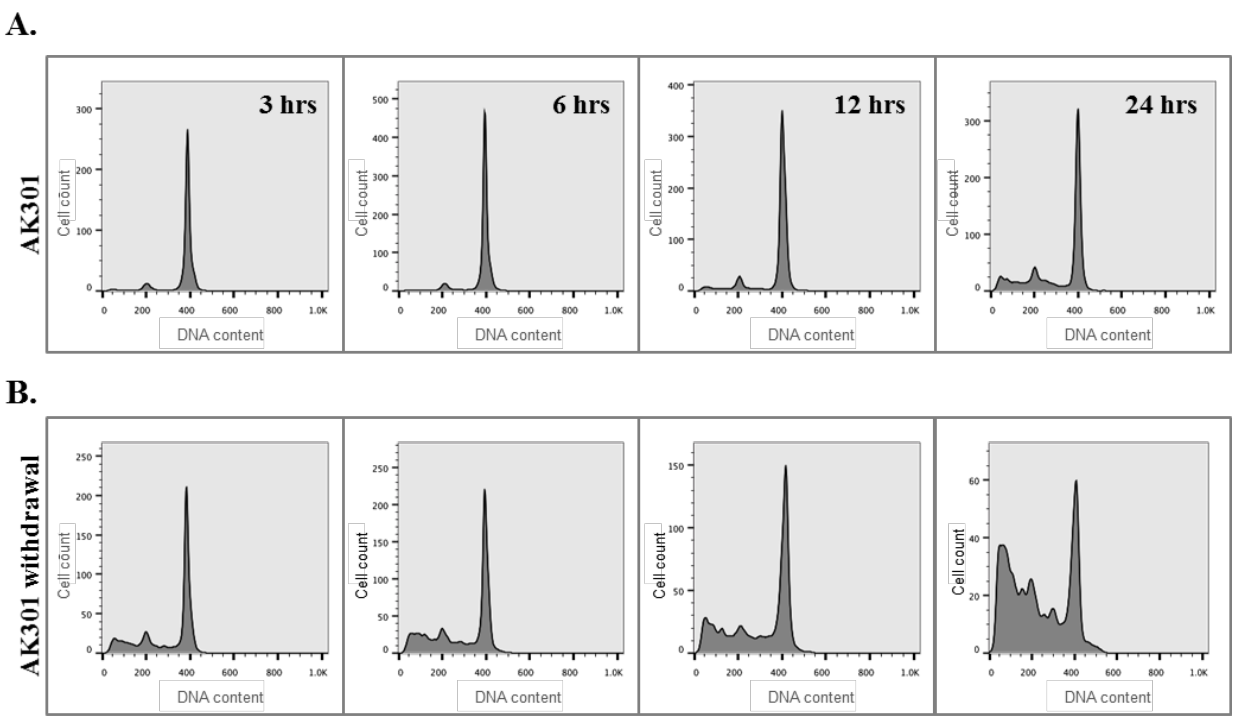

Figure 4.2. Release from AK301-induced mitotic arrest enhances apoptosis in HCT116 cells.

(A) HCT116 cells were treated with 500 nM of AK301 for 16 hrs. Subsequently, AK301 was (B) removed and the cells were allowed to grow in fresh medium for 3, 6, 12, and 24 hrs following AK301 withdrawal. For the arrested cells, AK301 was added to the medium. Cells were harvested at the indicated times post AK301 treatment. Consistent with Figure 1B, flow cytometric analysis of the DNA content of AK301-arrested cells showed significant increase in sub G1 population. However, removal of AK301 enhanced sub G1 population significantly at each of the indicated times post-withdrawal.

We compared the effect of AK301 withdrawal to that of colchicine, which forms a tight complex with β-tubulin. HCT116 cells treated with 500 nM of either AK301 or colchicine were analyzed at 6, 8, and 10 hours post drug withdrawal. As shown in Figure 4.3A, AK301-treated cells showed appreciably greater percentage of sub G1 population than cells treated with colchicine (Figure 4.3B). Colchicine-treated cells showed little to no sub G1 population. In addition, AK301-treated cells showed recovery from mitotic arrest into the interphase unlike colchicine-treated cells. These data suggest a reversibility of AK301 action in arresting cells in mitosis.

4.4.3. Arrested cells exiting mitosis are more prone to apoptosis

To determine the association between the reversibility of mitotic arrest and apoptosis, we analyzed colchicine, vincristine, and BI2536. HCT116 cells treated with these agents were subsequently allowed to exit mitosis for 8 hours prior to flow cytometric analysis of DNA content. Consistent with Figure 4.1A, all the agents tested induced high levels of mitotic arrest, as indicated by the G2/M population (Figure 4.4A). Cells released from AK301- and BI2536-induced arrest showed a significant decrease in the G2/M population ($P < 0.0001$) (Figure 4A). Moreover, subsequent analysis of sub G1 population indicated a significant increase in AK301-treated cells. BI2536, however, was not effective at sensitizing cells to apoptosis. Colchicine and vincristine did not show any significant increase in sub G1 population (Figure 4B). These data suggest that a reversible mitotic arrest of cancer cells may allow them to exit mitosis prematurely, resulting in apoptosis.

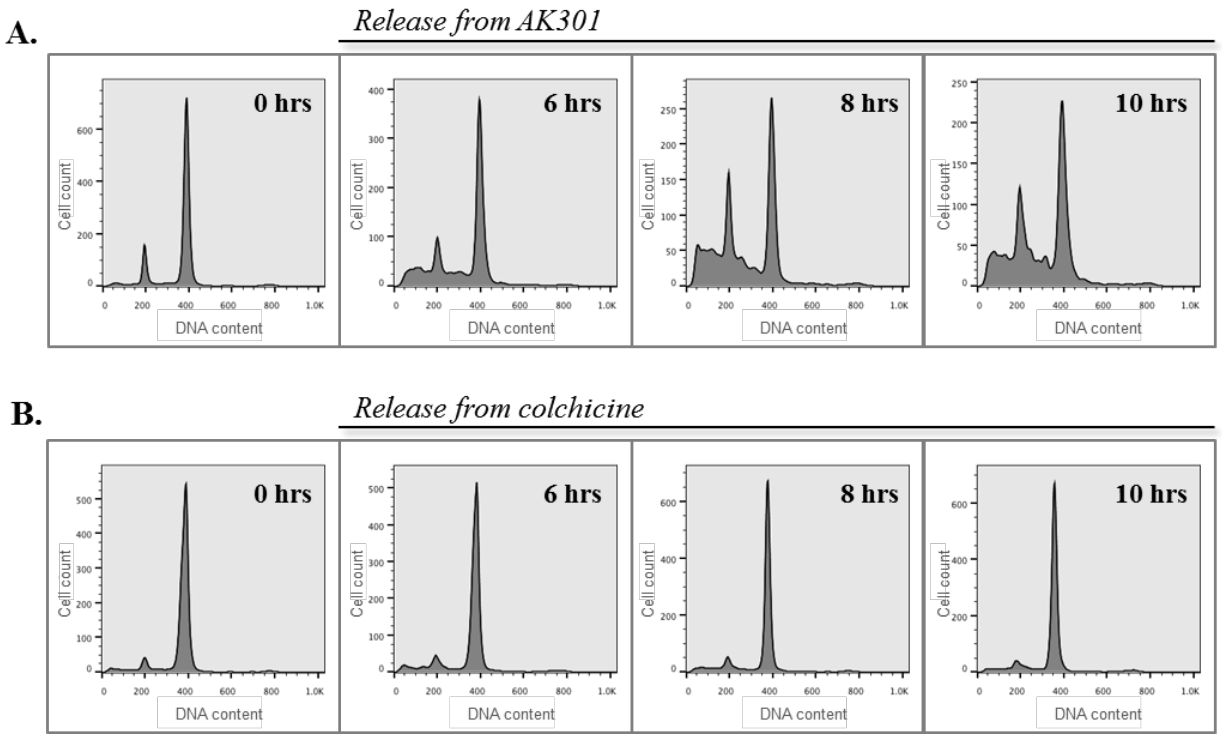

Figure 4.3. AK301 withdrawal induces significantly more apoptosis than that with colchicine withdrawal.

HCT116 cells were treated with 500nM of either (A) AK301 or (B) colchicine for 16 hrs. Cells were allowed to grow in fresh medium for indicated times. Flow cytometric analysis of DNA content showed that both AK301 and colchicine arrested HCT116 cells in G2/M phase of the cell cycle. However, upon drug withdrawal, AK301 resulted in a significantly greater increase in sub G1 population than those arrested with colchicine at each of the indicated times. Moreover, AK301-treated cells showed a time-dependent increase in sub G1 population following drug withdrawal.

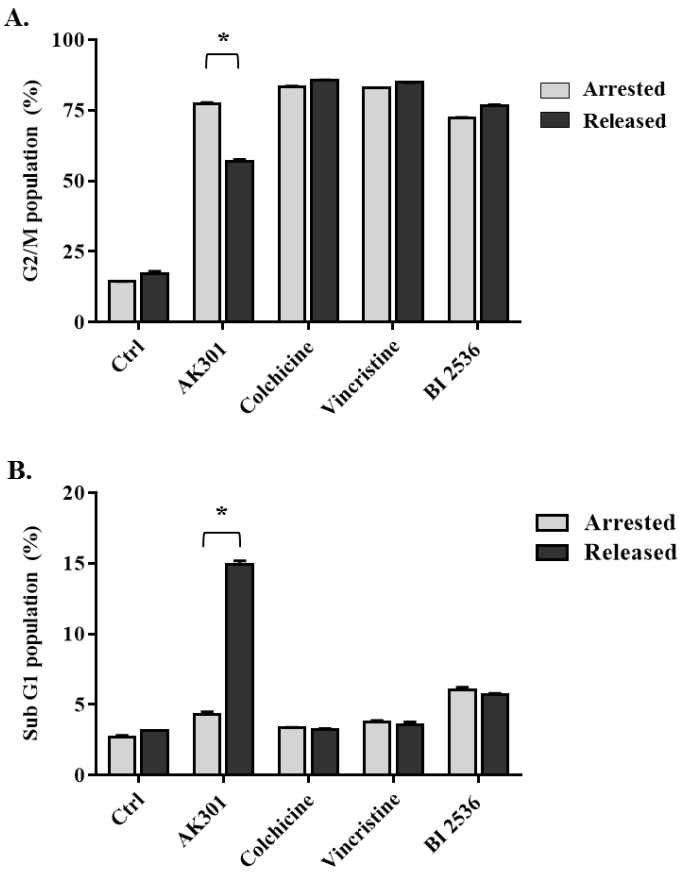

Figure 4.4. AK301-treated cells exiting mitosis following drug withdrawal undergo apoptosis.

HCT116 cells treated with 500 nM of each of the indicated drug for 16 h. Cells continued to grow in AK301-containing medium or drug-free medium for 8 h. (A) Flow cytometric analysis of the DNA content showed that all compounds induced a G2/M arrest, consistent with Figure 1B. Following release of the drugs, only AK301 treated cells showed a significant decrease in G2/M population (*$P < 0.0001$). (B) Analysis of the sub G1 population showed that only withdrawal of AK301 induced a significant increase in sub G1 population, but not other mitotic arrest compounds (*$P < 0.0001$).

4.4.4. AK301-treated cells show microtubule recovery after AK301 withdrawal

To gain insight into AK301's mechanism of action, we visualized differences in microtubule morphologies after treatment with AK301 and colchicine. HCT116 cells were allowed to exit mitosis after treatment with AK301 or colchicine. Arrested cells and post-drug withdrawal released cells were immunostained for β-tubulin and phospho-histone H3 (p-HH3), a chromosomal marker of mitosis. Consistent with the previous results, both AK301 and colchicine induced a mitotic arrest as indicated by an increase in the number of p-HH3 positive cells. Interestingly (data not shown), cells released from colchicine retained high mitotic index (condensed chromatin), in contrast to a low mitotic index in cells released from AK301-induced arrest (Figure 4.5B).

Both the agents induced disassembly of microtubule networks as anticipated (Figure 4.5A). Consistent with our previous findings, AK301 induced the least disruption of microtubule networks and exhibited the formation of multiple microtubule organizing centers (MTOCs). Colchicine-treated cells, however, showed a complete breakdown of microtubule networks. After drug withdrawal, AK301-treated cells showed recovery of microtubule networks, whereas colchicine-treated cells showed little to no recovery (Figure 4.5B). Together, these data indicate a more reversible mitotic arrest by AK301. We propose that this reversibility may play an important role in sensitizing colon cancer cells to apoptosis.

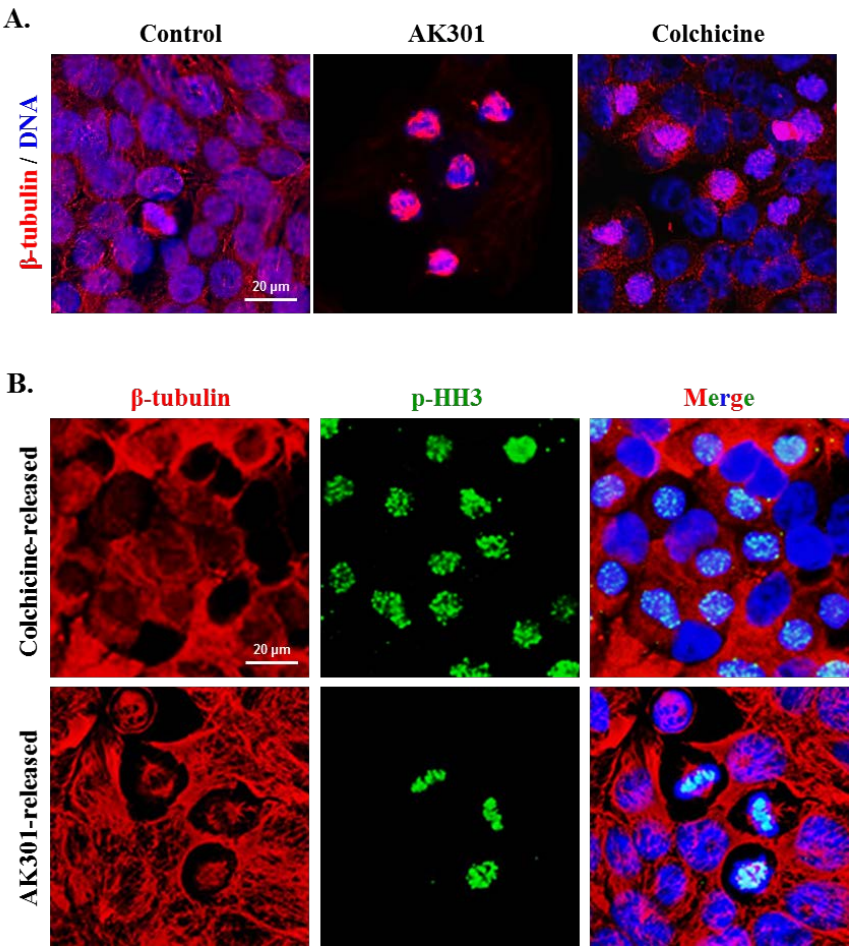

Figure 4.5. AK301 induces a more reversible mitotic arrest.

(A) HCT116 cells treated with AK301 or colchicine were fixed, permeabilized, and immunostained for β-tubulin. Both AK301- and colchicine-treated cells disrupted the formation of microtubules. AK301 treatment resulted in the formation of multiple MTOCs. (B) Cells released from mitotic arrest induced by AK301 or colchicine were immunostained for phospho-histone H3 Ser28 (green) and β-tubulin (red). Nuclei were counterstained with DAPI. Colchicine-treated cells show a higher proportion of cells stained with p-HH3 Ser28, whereas the proportion dropped after release from AK301-induced arrest. AK301-treated cells showed a normal bipolar assembly of microtubules after drug withdrawal, unlike colchicine.

4.4.5. Apc and p53 mutations enhance the sensitivity of HCT116 cells

Apc, a crucial protein in Wnt signaling and microtubule growth, is lost in most colon cancers, including HCT116 cancer cells [195, 196]. To assess the effect of *Apc* mutation on AK301-induced apoptosis, $Apc^{+/+}$ immortalized Young Adult Mouse Colonocytes (YAMCs) and *Apc* heterozygous ($Apc^{Min/+}$) Immorto-Mouse Colonic Epithelial cells (IMCEs) were treated with 500 nM of AK301 for 16 hours. Cells were allowed to exit mitosis in the absence of AK301 and cells were analyzed at 20, 30, and 40 hours post-release by flow cytometry as described above. As shown in Figure 4.6A, both cell lines showed an increase in sub G1 population, however, IMCEs showed a significantly higher sub G1 population over sub G1 in YAMCs at all sampling intervals. These data suggest that cells carrying microtubule-disruptive *Apc* mutations are more sensitive to the apoptotic inducing effects of AK301 compared to normal colon epithelial cells.

One of the most important proteins in the apoptotic pathway is p53, which is mutated in 50% of colon cancers [188]. To evaluate the role of p53 in AK301-induced apoptosis, we treated wild type ($p53^{+/+}$) and *p53* null ($p53^{-/-}$) HCT116 colon cancer cells with AK301 and assessed the level of capase-3 activation using a DEVD-AMC fluorogenic assay. As shown in Figure 4.6B, wild type HCT116 cells treated with AK301 showed a significant increase in active caspase-3, consistent with previous experiments. Conversely, *p53* null cells did not show a significant increase in caspase-3 activation after AK301 treatment. These data demonstrate that caspase-3 activation and apoptosis progression in AK301-treated HCT116 colon cancer cells is p53 dependent.

To further evaluate the role of p53, we performed cell cycle analysis on both p53 wild type ($p53^{+/+}$) and p53 null ($p53^{-/-}$) HCT116 cells. Cells were treated with AK301 and subsequently released as described above, followed by flow cytometric analysis. Consistent with

previous results, the wild type cells were more sensitive than their *p53* null counterparts. Moreover, wild type cells showed a significant increase in sub G1 population upon exit from AK301-induced arrest ($P < 0.0001$), in agreement with previous results. Conversely, no significant increase in sub G1 was observed between control *p53* null cells and *p53* null cells after AK301 withdrawal (Figure 4.6C).

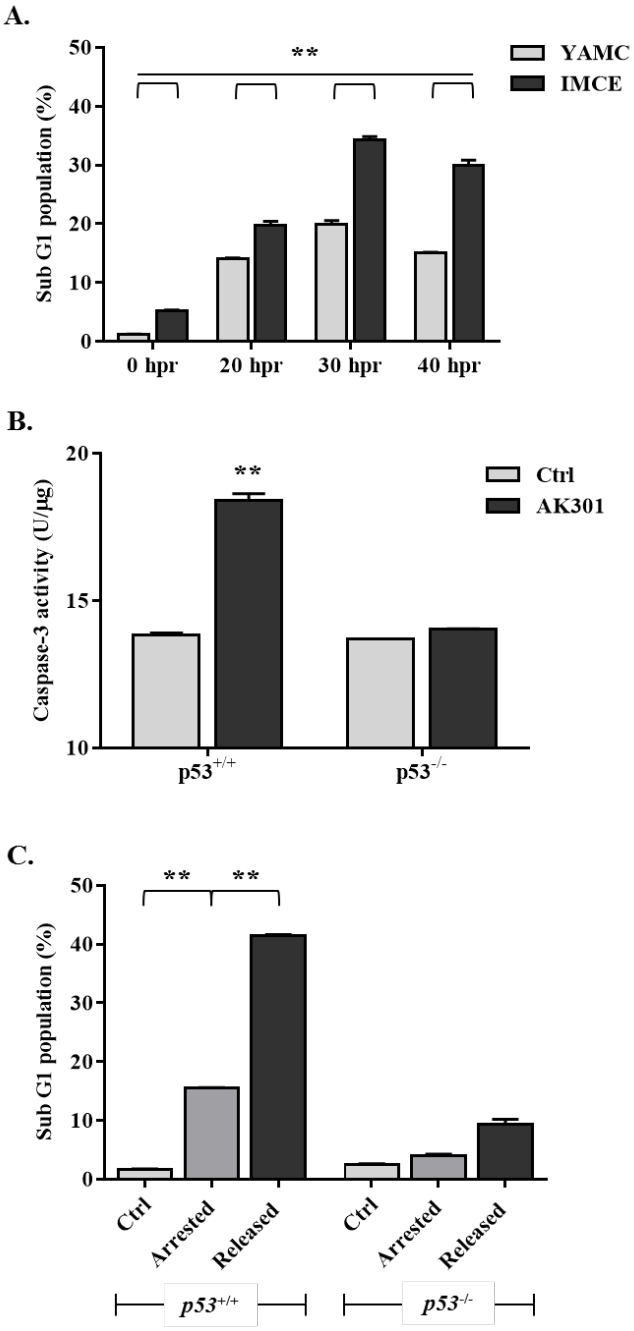

Figure 4.6. Apoptotic inducing ability of AK301 is p53-dependent and enhances the sensitivity of *Apc* mutant IMCE cells for apoptosis.

(A) *Apc*$^{+/+}$ YAMCs and *Apc*$^{Min/+}$ IMCE cells were treated with 500 nM of AK301 for 16 h, followed by a release from arrest for 40 h. Cells were harvested at the indicated times post-

release and their DNA content was analyzed by flow cytometry for the appearance of sub G1 population. AK301 induced significantly greater apoptosis in Apc mutant IMCE cells. The apoptosis effect was enhances in IMCE cells after AK301 withdrawal (**P < 0.0001). hpr: hours post release (B) *p53*$^{+/+}$ and *p53*$^{-/-}$ HCT116 colon cancer cells were treated with AK301 and caspase-3 activity was assessed using DEVD-AMC assay. AK301 induced significantly higher activation of caspase-3 in *p53*$^{+/+}$ cells compared to their p53$^{-/-}$ counterparts (**P < 0.0001). (C) *p53*$^{+/+}$ and *p53*$^{-/-}$ HCT116 cells were treated with AK301, followed by release from mitotic arrest. Cells were analyzed by flow cytometry for sub G1 population. AK301 induced a significantly greater arrest in *p53* wildtype cell compared to *p53* null cells. The sub G1 population of *p53*$^{+/+}$ cells was significantly enhanced when the cells were allowed to exit mitosis (**P < 0.0001).

4.4.6. ATM-dependent p53 activation is required for mitotic exit, but not for γH2AX activation

To determine whether γH2AX was activated in response to DNA damage in HCT116 cells, we immunostained for γH2AX phosphorylation at Ser139 in cells arrested with AK301, colchicine, vincristine, or BI2536. Flow cytometric analysis was performed to determine the association between mitotic arrest state and γH2AX phosphorylation. AK301-treated cells showed the highest percentage γH2AX positive cells ($P < 0.0001$) compared to other mitotic inhibitors tested ($P < 0.05$), indicated by cells in the second quadrant (Q2) of the dot matrix plot (Figure A5A). Quantification of γH2AX+ cells is shown in Figure A5B. Moreover, only the AK301 mitosis-arrested cells demonstrated phosphorylation of H2AX. To determine if the γH2AX activation was p53-dependent, we tested $p53^{+/+}$ and $p53^{-/-}$ HCT116 cells for activation of γH2AX in AK301-arrested cells and cells released from mitotic arrest. As shown in Figures 4.7A and 4.7B, both wild type and null cells exhibited γH2AX activation, suggesting a p53-independent mode of activation. However, upon AK301 withdrawal, $p53^{+/+}$ cells showed a significant decrease in γH2AX staining compared to their p53 null cell counterparts. Moreover, we compared γH2AX activation in cells treated with AK301 and other mitotic arrest inducing agents (colchicine, vincristine, and BI2536). As shown in Figures 4.7C and 4.7D, AK301-treatment induced γH2AX activation in a significantly greater proportion of cells compared to other mitotic arrest agents. Together, these data suggest that γH2AX activation in AK301-arrested cells is a p53-independent process, but induction of apoptosis following release from mitosis requires p53 activity.

Stabilization of p53 and γH2AX is an ATM-dependent process [187]. To investigate the possible role of ATM in the activation of p53 and γH2AX, we prepared lysates of HCT116 cells treated with AK301 for 18 hrs and those from which drug was withdrawn for 4 and 6 hrs and

immunoblotted for p-p53 Ser15, MDM2, and ATM phosphorylation at Ser1981. As shown in Figure 4.7C, AK301-treated cells showed phosphorylation of ATM Ser1981. This was accompanied by phosphorylation of p53 Ser15 and activation of MDM2. Release of HCT116 cells from AK301 enhanced the activity of ATM, p53, and MDM2. These data suggest that p53 activation is ATM-dependent. Activation of ATM increases after treatment with AK301, but is further enhanced after release of AK301.

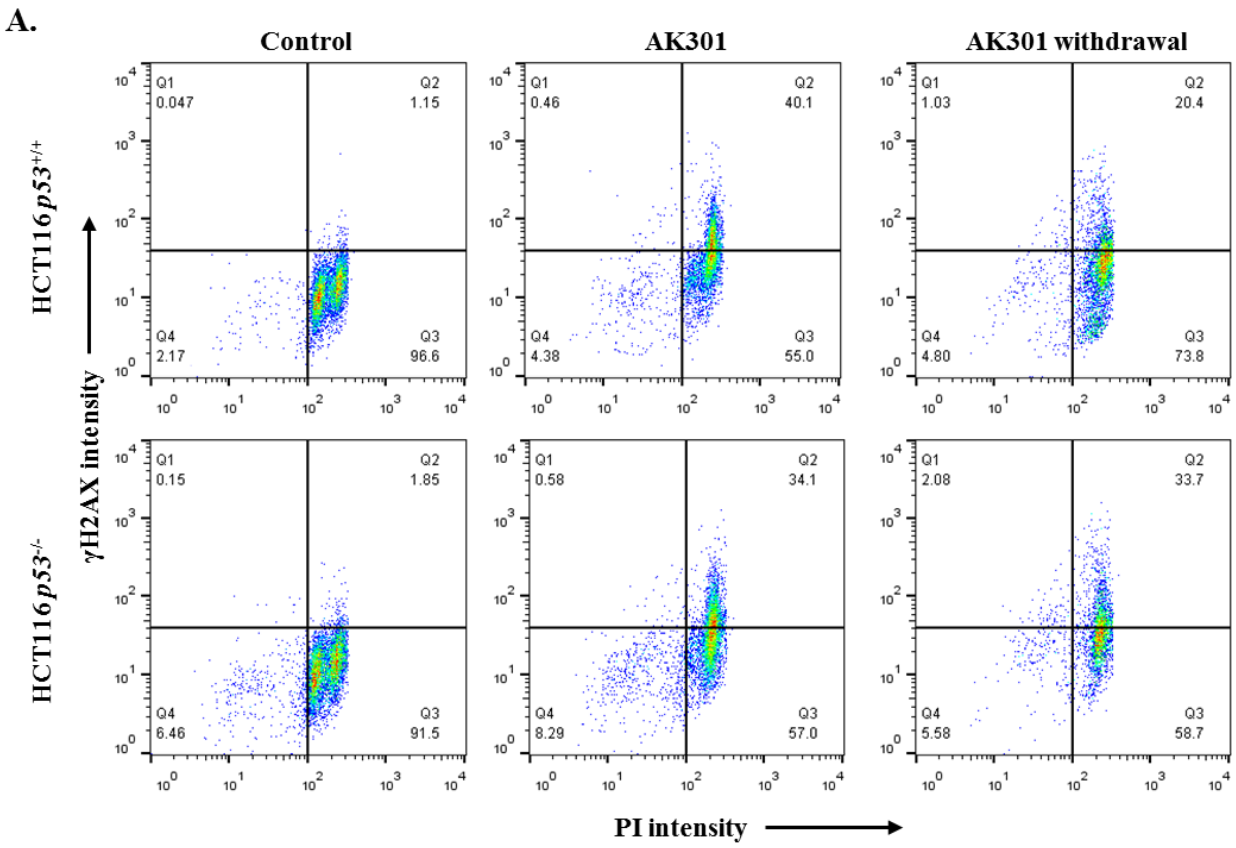
A.
Control
AK301
AK301 withdrawal
HCT116 p53+/+
HCT116 p53-/-
γH2AX intensity
PI intensity
Q1 0.047
Q2 1.15
Q4 2.17
Q3 96.6
Q1 0.46
Q2 40.1
Q4 4.38
Q3 55.0
Q1 1.03
Q2 20.4
Q4 4.80
Q3 73.8
Q1 0.15
Q2 1.85
Q4 6.46
Q3 91.5
Q1 0.58
Q2 34.1
Q4 8.29
Q3 57.0
Q1 2.08
Q2 33.7
Q4 5.58
Q3 58.7

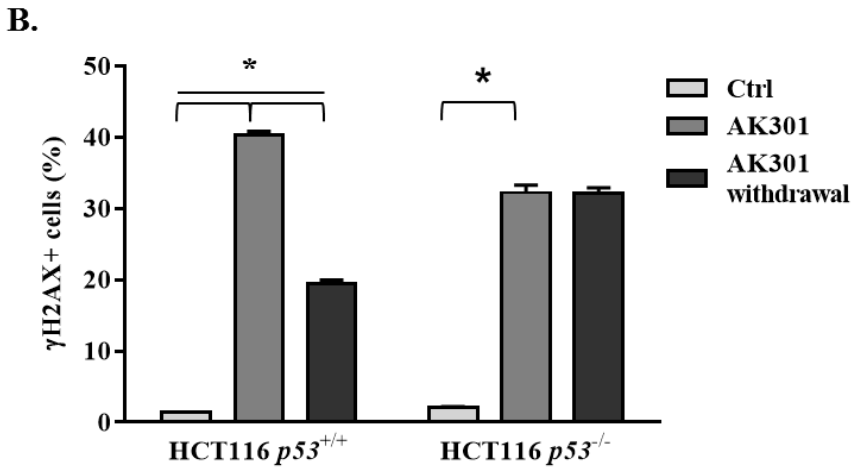
B.
γH2AX+ cells (%)
50
40
30
20
10
0
*
*
HCT116 p53+/+
HCT116 p53-/-
Ctrl
AK301
AK301 withdrawal

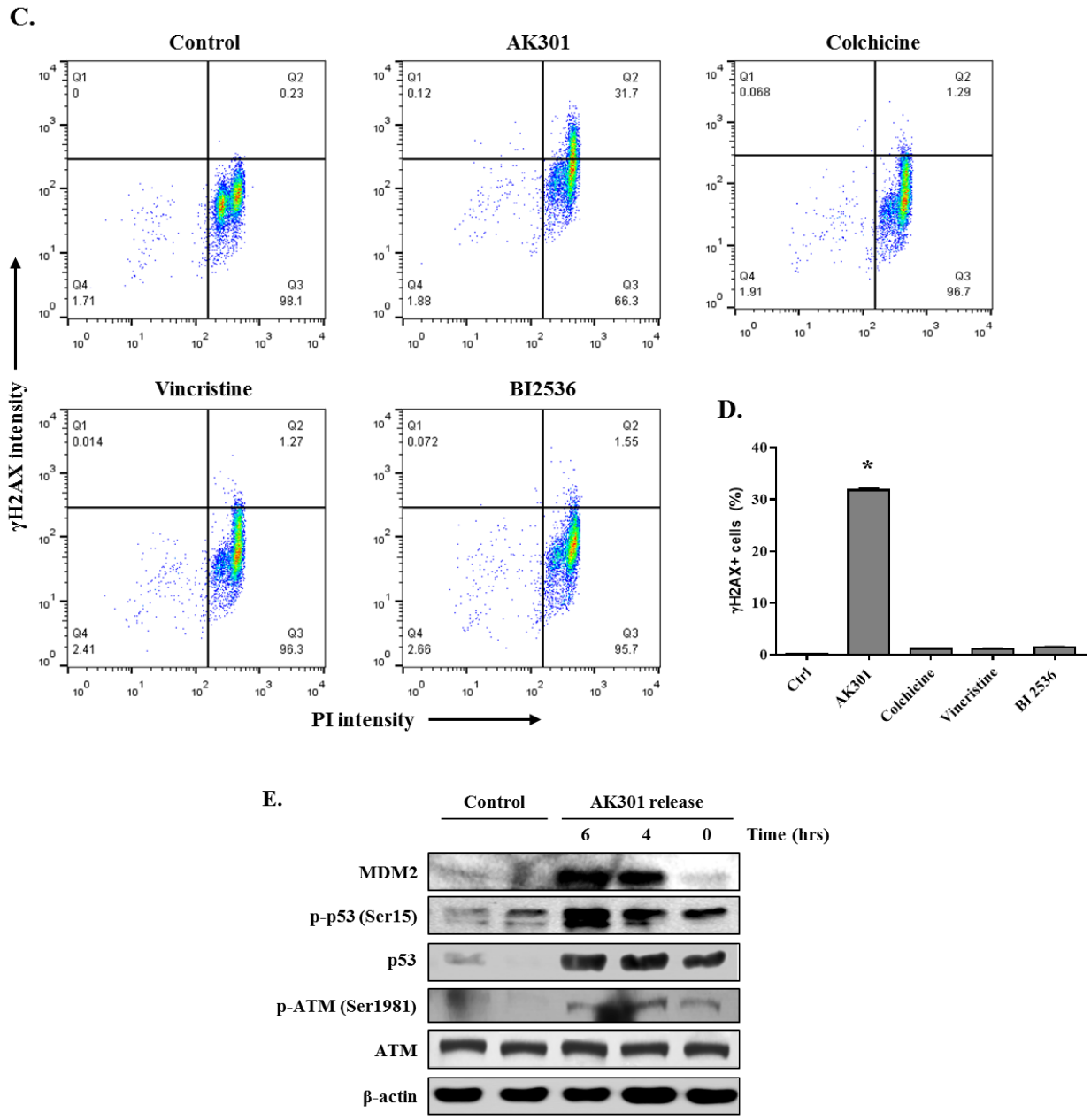

Figure 4.7. ATM-dependent stabilization of p53 in AK301-treated is enhanced after mitotic release.

(A) *p53*$^{+/+}$ and *p53*$^{-/-}$ HCT116 cells were treated with 500 nM of AK301 for 16 h followed by drug withdrawal. Cells were fixed with PFA and stained for γH2AX and PI counterstain was used to stain DNA. Dot matrix plots (quadrant 2, Q2) show that AK301 induced γH2AX

regardless of *p53* mutation status. Removal of AK301 significantly reduced γH2AX staining in *p53* wildtype, but not *p53* null cells. (B) Quantification of γH2AX staining in cells staining with PI (Q2) (*P < 0.0001). (C) γH2AX staining and flow cytometric analysis of $p53^{+/+}$ HCT116 cells treated with the indicated mitotic arrest agents – AK301, colchicine, vincristine, and BI2536. Treated cells were stained as described above (D) Quantification of γH2AX positive cells in response to each of the treatments in (D) above. AK301-treated HCT116 cells showed a significantly greater proportion of cells with γH2AX activation (*P < 0.0001). (E) $p53^{+/+}$ HCT116 cells were treated with AK301, followed by growth in fresh medium. Total protein was isolated by RIPA extraction after AK301 treatment and 4 and 6 hrs drug release from mitotic arrest. Immunoblot analysis shows phosphorylation of ATM at Ser1981, stabilization of p53 (p-p53 Ser15) and stabilization of MDM2 after AK301 treatment. The phosphorylation of ATM and p53 as well as activation of MDM2 was greatly enhanced, in a time-dependent manner, after releasing cells from mitotic arrest. β-actin was used as a loading control.

4.5. Discussion

We previously reported the identification of small molecule microtubule inhibitors that induced mitotic arrest in colon cancer cells and dramatically enhanced colon cancer cell death strictly in the presence of death ligands [145, 193]. Structure-activity relationship studies led to the identification of a more potent compound, AK301, with EC_{50} of 115 nM [193]. Moreover, we showed that these compounds reduced microtubule polymerization, unlike other microtubule inhibitors that completely abrogate microtubule polymerization [193]. The reduction in microtubule polymerization along with an increase in cell surface expression of TNFR1 led to apoptotic signaling in AK301-treated colon cancer cells. In this study, we show that AK301, in the absence of death ligands, is highly effective at inducing a mitosis-to-apoptosis transition following release from the mitotic arrest state. We also show that the activation of apoptosis is a p53-mediated process. Further, AK301 is able to induce the activation of ATM, which is necessary for p53 activation, ultimately resulting in a robust apoptotic response in cancer cells exiting mitosis (Figure 4.8).

Mitotic checkpoints safeguard entry into and exit from mitosis [130]. Mutations in checkpoint kinases, such as those involved in the spindle assembly checkpoint (SAC) and DNA repair pathways, have been implicated in development of colon cancer [28, 40, 197-199]. Based on the *in vitro* microtubule disruptive activity of AK301, we anticipated that removal of AK301 would restore bipolar spindle formation in arrested cells and that the cells would complete mitosis. Consistent with our previous studies [193], we showed that AK301 effectively arrested cells in mitosis at low nanomolar concentrations. Surprisingly, however, cells exiting mitosis after AK301 withdrawal were susceptible to apoptosis. Notably, release from AK301-induced mitotic arrest, but not from other mitotic inhibitors, resulted in apoptosis. These results suggest

that limited disruption of microtubules by AK301 allows the arrested cancer cells to reassemble microtubules and aberrantly exit mitosis. In addition, other labs have also shown that weakening of SAC and aberrant exit from mitosis results in effective apoptosis [179, 200-202]. Taken together, our findings suggest that cancer cells are vulnerable to mitotic slippage following AK301 withdrawal, which induces apoptosis in these cells. It would be of interest to determine whether these arrested cells complete mitosis and arrest at a post-mitotic checkpoint following drug withdrawal or they simply slip out of mitosis and undergo cell death pending activation of apoptotic signaling. Moreover, how these cells transition from an aberrant mitosis to apoptosis needs to be further investigated.

APC mutations are frequently found in colon cancers and aid in tumor progression [195, 203, 204]. It is thought to be one of the first genes mutated in colon carcinogenesis [205, 206], and its mutation leads to an increase in Wnt signaling [207, 208]. APC is also known to regulate spindle assembly during mitosis by stabilizing microtubule plus (growth) ends [195, 208]. Further, APC binds to and recruits end-binding protein 1 (EB1) to microtubule plus ends for stability [208], and is also involved in the activation of SAC by direct interaction with BUB1 and BUBR1 [209]. C-terminal truncating mutations of APC, most commonly found in colon cancers act in a dominant negative fashion to inhibit the function of wildtype APC protein [195, 204, 210]. Since AK301 acts to reduce the polymerization of microtubules, we anticipated that AK301 withdrawal would selectively induce apoptosis in an *Apc* mutant mouse colonocyte cell line (IMCE). We found that $Apc^{Min/+}$ IMCEs were more sensitive to AK301 treatment. This is likely due to the additive effect of microtubule disruption by AK301 in an *Apc* mutant cell line. In addition, exit from mitosis after AK301 withdrawal triggered apoptosis in *Apc* heterozygous IMCE cells, higher than that in *Apc* wildtype YAMCs. Note that unlike HCT116 cells, *Apc*

mutant IMCE cells lack a robust SAC, thus making it easier for arrested cells to aberrantly exit mitosis upon drug withdrawal. These data not only reinforce the requirement of mitotic slippage for an effective apoptotic response, but also demonstrate the specificity of AK301 in targeting *APC* mutant cells.

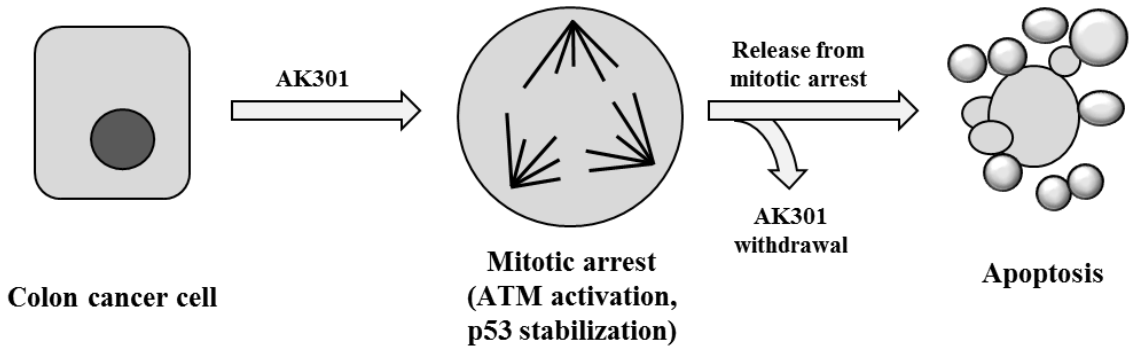

Figure 4.8. Proposed model for AK301's mechanism of action.

Treatment of cancer cells with AK301 results in a mitotic arrest with multiple MTOCs. AK301 induces high levels of activated ATM, which stabilizes p53. Releasing cells from mitotic arrest by removal of AK301 induces apoptosis in cells via the p53 pathway.

Although our results and other studies have shown that p53 is not required for the activation of SAC and mitotic arrest [185, 211], it is required for activation of apoptosis in cells exiting mitosis [182, 212]. However, p53 localizes to the centrosomes during mitosis and displaced upon spindle damage [213, 214]. Considering the localization of p53 during mitosis and its role as a tumor suppressor, it is conceivable that p53 is activated in response to mitotic damage. In fact, the activity of p53 might act as a secondary fail safe mechanism to SAC during mitosis. In turn, the activation of p53 can result in apoptosis or a more permanent exit from cell division post-mitosis. p53 can be activated by several different kinases during mitosis [186, 215]. In contrast to a recent study that showed the requirement of both γH2AX and p53 activation for cell cycle arrest [216], our results suggested otherwise; AK301-induction of mitotic arrest was observed to be p53- and γH2AX-independent. However, our results indicated that p53 activation is required for an effective mitosis-to-apoptosis transition after releasing cells from mitosis. γH2AX activation, in this case, may be induced by the activation of a kinase, ataxia telangiectasia mutated (ATM), in a DNA damage-independent manner. The role γH2AX activation, if any, during or after mitotic arrest, however, is unclear.

To address the DNA damage-independent activation of p53 during mitosis, we investigated the possible involvement of ATM. Immunoblot analysis showed the phosphorylation of ATM at Ser1981, suggesting a DNA damage-independent mode of ATM activation, resulting in the activation of p53. ATM activation, in turn, can be attributed to defects in microtubule function. Studies have shown that ATM is activated by default (by phosphorylation at Ser1981) in cells undergoing mitosis and localizes to the centrosomes [217]. Activation of SAC displaces ATM, which localizes throughout the cytoplasm and activates p53 [187]. We propose that defects in mitotic spindle assembly, induced by AK301, result in high

levels of ATM-dependent p53 activation, which ultimately leads to apoptosis in cells that exiting mitosis [218, 219].

Microtubule disruptors have been used for decades as the clinical treatment of some cancers [220]. Vincristine and its derivatives are used in the treatment of cancers, such as B-cell lymphoma [221]. These drugs are successful at diminishing tumor size but their general toxicity results in undesirable side effects for patients. Therefore, there is an urgent need to identify therapeutic compounds that specifically target cancer cells. In this study, we illuminated the mechanism of action of AK301 and provide a paradigm for the activation of apoptosis in both cancer cells as well as non-transformed *APC* mutant colon cancer cells. However, further investigation is required to identify targets of AK301 and explore in detail the ability of AK301 in inducing mitotic arrest and efficient apoptosis following release from mitosis. Unlike other microtubule inhibitors, AK301 may target the microtubule defects associated with an APC mutation more directly. Understanding the vulnerabilities of cancer cells may ultimately help in the development of therapeutics that effectively and specifically target these cells for elimination.

CHAPTER 5

Targeting *APC*$^{-/-}$ mutant cells for apoptosis via microtubule disruption by AK301

5.1. Abstract

Adenomatous polyposis coli (*APC*) is a tumor suppressor which is mutated in a majority of colorectal cancers. The role of APC in Wnt signaling is well understood. However, the effect of *APC* mutations on microtubule polymerization and stability are less well studied. Using *Apc*$^{+/+}$ and *Apc*$^{Min/+}$ mouse colonocyte cell lines, we show that *APC* heterozygous mutant cells exhibit microtubule defects, especially during mitosis. In addition, we show that *Apc* mutant cells are sensitive to a small molecule microtubule disrupting agent, AK301, we previously identified. In the presence of AK301, *Apc* mutant colonocytes display microtubule defects and form multiple microtubule organizing centers (MTOCs). Further, we show that *Apc* mutant colonocytes undergo apoptosis upon AK301 treatment. Expression of APC C-terminus truncated protein (APC$^{\Delta C}$) in human HEK293 cells showed similar defects in microtubule networks and bipolar spindle formation, which were aggravated by AK301 treatment. Understanding the mechanisms by which cells cope with *APC*-associated microtubule defects may help identify novel targets and aid in the development of specific and potent chemotherapeutic and chemopreventive agents.

5.2. Introduction

Colon cancer begins in a single cell with a genetic mutation that gives that cell a growth advantage [206]. From there, a series of mutations in tumor suppressor genes and oncogenes cause a colon cancer to develop and progress [222, 223]. Genes in the Wnt signaling pathway are critical for the initiation and progression of colon cancer [224-226]. According to Vogelstein's

model for the development of colorectal cancer, the initial genetic alteration in most colon cancers is the loss of function of the tumor suppressor gene, adenomatous polyposis coli (APC) [206]; APC mutations are found in 80-90 percent of colon cancers [40, 203]. APC is involved in normal intestinal development and influences a variety of cellular processes [226, 227]. Loss of APC function results in intestinal neoplasia in both mice and humans [228]. Mutations in *APC* deregulate Wnt signaling and lead to stabilization and nuclear translocation of β-catenin, which results in aberrant transcriptional activation of TCF/LEF target genes [207, 229]. However, APC also plays a role in microtubule polymerization and stabilization, and microtubule anchoring to cellular attachment sites to establish cell polarity [195, 230-232]. The effect of *APC* mutations on microtubule dynamics and assembly has been proposed to participate in cell transformation, including the acquisition of the chromosomal instability (CIN) phenotype that can drive cancer progression [233-235]. Although the cancer promoting effects of an *APC* mutation are well established, there is some evidence that this defect can render mutant cells sensitive to specific treatments [236]. Here, we focus on the potential effectiveness of targeting the microtubule and mitotic defects associated with an *APC* mutation.

Proper spindle formation during mitosis is crucial to ensure proper alignment and segregation of chromosomes [168]. Microtubules are highly dynamic at their plus ends; their stability at the plus ends is largely regulated by EB1 and APC [169, 237, 238]. Binding of APC to the carboxy-terminus of EB1 enhances the ability of EB1 to bind polymerized microtubules, suggesting that APC may help to stabilize microtubules, and therefore, cell polarity establishment, and chromosome capture and segregation during mitosis [230, 239, 240]. Moreover, APC also binds directly to the plus ends of growing microtubules and has been found to be localized at the kinetochore-microtubule complexes [230, 241]. Recent studies indicate that

expression of truncated forms of APC dominantly compromises microtubule dynamics [242] and kinetochore-microtubule attachments [208, 243], indicating that the influence of *APC* mutation on cancer progression occurs even before both alleles are mutated. Aberrant mitosis and failed cytokinesis have been observed in normal tissue of $Apc^{Min/+}$ mice [244-246]. Although colon cancer cells cope with the loss of APC function, it is unclear how they compensate for this loss. However, loss of APC function may be an "Achilles heel" of a mutated cell; we will explore this possibility in this chapter.

In this study, we demonstrate that $Apc^{Min/+}$ heterozygous cells with truncated APC have defects in their microtubule networks. Moreover, $Apc^{Min/+}$ cells were found to be sensitive to microtubule disruption by a piperazine-based agent, 1-(3-chlorophenyl)-4-(2-ethoxybenzoyl)piperazine, referred to as AK301, previously identified for its ability to induce mitotic arrest and apoptosis in colon cancer cells. Expression of the C-terminus truncated APC ($APC^{\Delta C}$) in HEK293 cells showed effects on microtubule formation similar to those observed with $Apc^{Min/+}$ IMCE cells. Further, aurora kinase A was found to be mislocalized in *APC* mutant cells was observed to be particularly sensitive to AK301 treatment, consistent with a more severe disruption in the structure and/or composition of the spindle assembly apparatus. Understanding how APC mutations affect colonic epithelial cells could provide insight into early cellular changes in colon cancer develop, which may prove useful in colon cancer prevention.

5.3. Materials and Methods

5.3.1. Cell culture, transfections, and preparation of stable cell lines

YAMC and IMCE cell lines were a gift from Dr. Robert Whitehead (Vanderbilt University, Nashville, TN) [247]. YAMC and IMCE cells were cultured in RPMI medium

containing 5% fetal bovine serum, non-essential amino acids, antibiotic/antimycotic, insulin-transferrin-selenium (Life Technologies), and 5 units of murine gamma interferons. The cells were grown at 33°C in 5% CO_2. HEK293 cells were a gift from Dr. Antonio Garmendia (University of Connecticut, Storrs, CT). HEK cells were cultured in DMEM, containing 10% fetal bovine serum, non-essential amino acids, and antibiotic/antimycotic. The cells were grown at 37°C in 5% CO_2. Cells were transfected with either pEGFP-C1 or APC-containing pEGFP-C1 plasmid using Lipofectamine® 3000 reagent (Life Technologies) following manufacturer's instructions [248]. Briefly, cells were placed in reduced serum OptiMEM. 1 µl Lipofectamine 3000 reagent was diluted in 25 µl of OptiMEM per well for a 24-well plate. 1 µg of plasmid per well was diluted in 25 µl of OptiMEM and 1 µl of P3000 reagent per well was added. Diluted Lipofectamine and plasmids were mixed and allowed to sit for 20 min before adding to cells. Cells were incubated overnight at 37°C. For preparation of stable cell lines, transfected cells were grown in the presence 400 µg/ml of geneticin for two weeks. Remaining cells were plated in a 100 mm dish at low density and colonies were allowed to form. Single colonies expressing GFP were transferred to each well of a 24-well plate in the absence of geneticin. Extracts from these cells were tested for the presence of $APC^{\Delta C}$-GFP by western blot. AK301 was obtained from ChemBridge DIVERSet™ library (San Diego, CA). Drug treatments were performed approximately 24 h after passage for 16 h, unless indicated otherwise. TNF was obtained from Pierce Protein Research Products (Rockford, NJ).

5.3.2. Generation of constructs expressing GFP-$APC^{\Delta C}$

End-sequenced human *APC* cDNA clones were obtained from TransOmic (TCHS1003, Huntsville, AL). A pair of primers were designed with a mutant base (T to A) in the reverse

primer. Primers 5'-GGGG CTCGAGATGGCTGCAGCTTCATATGAT-3' (forward) and 5'-GGGGGTCGACCTAACTTCTGTC TTTCTCAGA-3' (reverse), which contain non-homologous sequences at each 5' end that were used to add SalI and XhoI sites of pEFGP-C1 plasmid. The primers were used to amplify the short *APC* fragment using a high fidelity *Pfu* polymerase. Amplification was confirmed by agarose gel electrophoresis, and PCR products were purified with a QIAquick® PCR Purification Kit (28104, Qiagen, Valencia, CA). Purified samples were sequenced using ABI Prism Big Dye Terminator Cycle Sequencing (Perking-Elmer Applied Biosystems, Carlsbad, CA). The resulting *APC* fragment was ligated to pEGFP-C1 plasmid by Gibson Assembly Kit (New England Biolabs, Ipswich, MA). The plasmid DNA was amplified in the *E. coli* strain DH5α (Life Techologies) and extracted using QIAGEN® Plasmid Midi Kit (12143, Qiagen) following manufacturer's instructions. Purified plasmid was resuspended in nuclease-free water and checked by agarose gel electrophoresis and OD readings at 260 and 280 nm. The final plasmid was sequenced as described above to ensure no mutations were introduced by PCR amplification.

5.3.3. Immunoflorescence microscopy

Cells cultured on coverslips were fixed with 4% paraformaldehyde at room temperature or 100% ice cold methanol at 4°C and then permeabilized with 0.5% Triton X-100 in PBS. Cells were blocked in 5% serum (in PBS) and then incubated with primary antibody (in 5% serum) on shaker for 1 h at room temperature against β-tubulin (E7 monoclonal antibody, Developmental Studies Hybridoma Bank) or aurora kinase A (610938, BD Biosciences, San Jose, CA). Appropriate secondary antibodies (Molecular Probes, Life Technologies, Guilford, CT or Jackson ImmunoResearch, West Grove, PA) were used for 45 min incubation. Nuclei were

visualized using DAPI (5 µg/ml in PBS; DI306, Life Technologies). Coverslips were mounted on slides using ProLong Gold Antifade Reagent (Life Technologies). Images were acquired using Nikon A1R Confocal Microscope (version 2.11, Nikon Instruments Inc.) and NIS-Elements Advanced Research Software (version 4.13.01, build 916, Nikon Instruments Inc.). Quantification of immunostaining was performed using ImageJ image analysis software (http://rsb.info.nih.gov/ij) as previously described [88]. Following background subtraction and image stacking, both DAPI and immunofluorescence images were merged. Image brightness and contrast was modified with Adobe Photoshop software CC 2014 (Adobe Systems).

5.3.4. Flow cytometry and cell cycle analysis

Cells were stained for γH2AX using the protocol described above for immunofluorescence staining. Briefly, cells were fixed with 4% PFA, permeabilized with 0.1% Triton X-100, and blocked with 5% donkey serum. Cells were then incubated with γH2AX antibody (sc-101696, Santa Cruz Biotechnology) followed by incubation with Alexa Fluor® 488 secondary antibody (Life Technologies). Cells were then harvested using trypsin-EDTA for 15 min at 37°C and washed once with PBS. Propidium iodide (30 µg/ml) was added to the cells prior to filtration through 35 µm cell strainer tubes. Cell were promptly analyzed by flow cytometry.

For cell cycle analyses, cells were analyzed for DNA content by ethanol fixation and staining with propidium iodide as previously described. Cells were harvested using trypsin-EDTA, centrifuged at 1000 *X g* for 10 min and resuspended in 500 µl of cold saline GM. Cells were washed once with 1X PBS and then fixed for at least 2 hrs at -20°C in 3X volumes of cold 100% ethanol while vortexing. Cells were then pelleted and washed once with PBS containing 5

mM EDTA. Pelleted cells were stained with 30 μg/ml propidium iodide (Molecular Probes, Life Technologies Corp.) and 0.3 mg/ml RNase A (Sigma-Aldrich, St. Louis, MO) in 500 μl PBS solution for 40 min in dark at RT [89]. The stained cells were filtered through 35 μm cell strainer tubes (BD Biosciences, San Jose, CA). All flow cytometric analyses were performed on FACSCalibur (BD Biosciences) using Cell Quest software (BD Biosciences). The data were analyzed using FlowJo (v 10, TreeStar Inc., Ashland, OR).

5.3.5. Caspase-3 assay

Caspase-3 activity was determined as previously described [145]. Cells were collected, centrifuged at full speed, and washed once with PBS. Pelleted cells were lysed by two rounds of freeze-thaw in lysis buffer containing 10 mM Tris-HCl (pH 7.5), 0.1 M NaCl, 1 mM EDTA, and 0.01% Triton X-100 and centrifuged at 10,000 *X g* for 5 min. The assays were performed on 96 well plate by mixing 50 μl of lysis supernatant with 50 μl of 2X reaction mix (10 mM PIPES pH 7.4, 2 mM EDTA, 0.1% CHAPS, 10 mM DTT) containing 200 nM of the fluorogenic substrate Acetyl- Asp-Glu-Val-Asp-7-Amino-4-methylcoumarin (DEVD-AMC; Enzo Life Sciences). The fluorescence was quantified at the start of the reaction and after 30 min. Protein concentrations were determined using CBQCA Protein Quantitation Kit (Life Technologies). Caspase activity was determined by dividing the change in fluorescence by total protein content of the reaction mixture.

5.3.6. Statistical analyses

One-way analysis of variance (ANOVA) was used when comparing two groups with Tukey's post hoc test. For more than two groups, two-way ANOVA was used with Bonferroni correct. Significance was calculated at an alpha of 0.05.

5.4. Results

5.4.1. $Apc^{Min/+}$ IMCE cells exhibit microtubule defects

Previous studies have shown localization of APC at the growing (plus) ends of microtubules and that APC mutations reduce the rate of microtubule polymerization *in vitro* [208, 242, 244]. We sought to characterize overall defects in microtubule morphology of $Apc^{Min/+}$ heterozygous cells. We used a set of conditionally immortal cell lines derived from C57/BL6 mice, $Apc^{+/+}$ Young Adult Mouse Colonocytes (YAMCs) and $Apc^{Min/+}$ Immorto-Mouse Colonic Epithelial cells (IMCEs), developed by Dr. Robert Whitehead (Vanderbilt University, Nashville, TN). We immunostained YAMCs and IMCEs for β-tubulin to identify changes in microtubule structures. As shown in Figure 5.1A, *Apc* heterozygote IMCE cells show overall aberrations in microtubule networks. Generally, cells are more elongated and display microtubules network that are concentrated towards the periphery of the cell. Additionally, some cells lack partial or complete microtubule networks. Microtubules are highly dynamic during mitosis and require precise spindle assembly for proper chromosomal division. Interestingly, no gross microtubule abnormalities were observed in mitotic cells with regards to their mitotic spindles.

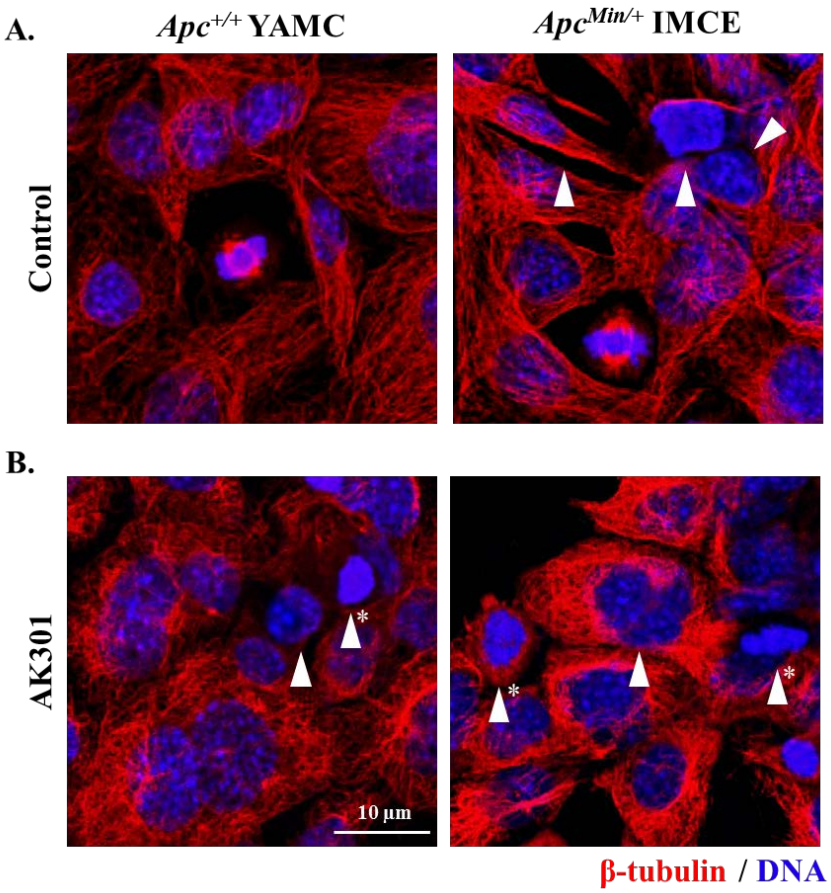

Figure 5.1. AK301 disrupts microtubule networks in both *Apc*$^{+/+}$ YAMCs and *Apc*$^{Min/+}$ IMCE cells.

(A) Mouse colonocyte cell lines YAMCs and IMCEs were fixed, permeabilized, and immunostained for β-tubulin (red). Nuclei were counterstained with DAPI (blue). In general, *Apc* mutant IMCE cells exhibited spindle shape compared to a more rounded cell shape in *Apc* wildtype YAMCs (arrowheads). Moreover, IMCE cells showed disruption or lack or microtubule networks. (B) β-tubulin of AK301-treated YAMC and IMCE cells showed increased disruption of microtubule networks; cells exhibited peripheral staining for β-tubulin and mitotic cells lacked microtubule spindle assembly (arrowheads).

5.4.2. Apc mutant IMCE cells show multiple microtubule organizing centers (MTOCs) following AK301 treatment

To determine if AK301would alter microtubule networks in YAMCs and IMCE cells, we stained treated cells with AK301 and immunostained them for β-tubulin. As shown in Figure 5.1B, AK301 disrupted microtubule networks in both YAMCs and IMCE cells. Non-mitotic cells showed microtubule networks clustered at the periphery of the cells; mitotic cells showed peripheral microtubule networks, but no spindle assembly. Moreover, spindle-shaped IMCE cells appeared more circular in shape with peripheral microtubule staining.

Previously, we showed that AK301-treated colon cancer cells showed multiple MTOCs. To determine if there were difference in microtubule organizing centers between *Apc* normal and *Apc* mutant cells, we treated YAMCs and IMCE cells with 100 nM of AK301 and stained with a centrosomal marker, aurora kinase A. Untreated cell mitotic YAMCs and IMCEs showed normal bipolar localization of aurora kinase A (Figure 5.2A). Treatment of *Apc* normal YAMCs showed aurora kinase A deposition at two foci. This localization is consistent with aurora kinase A association at the centrosome, where it is normally localized in mitotic cells. (Figure 5.2B, left panel). However, AK301 treatment of *Apc* mutant IMCE cells showed the formation of multiple diffuse foci for aurora kinase A (Figure 5.2B, right panel). The emergence of multipolar aurora kinase A centers in IMCE cells suggests that *Apc* mutant cells are more sensitive to the centrosome disruption or centrosome assembly.

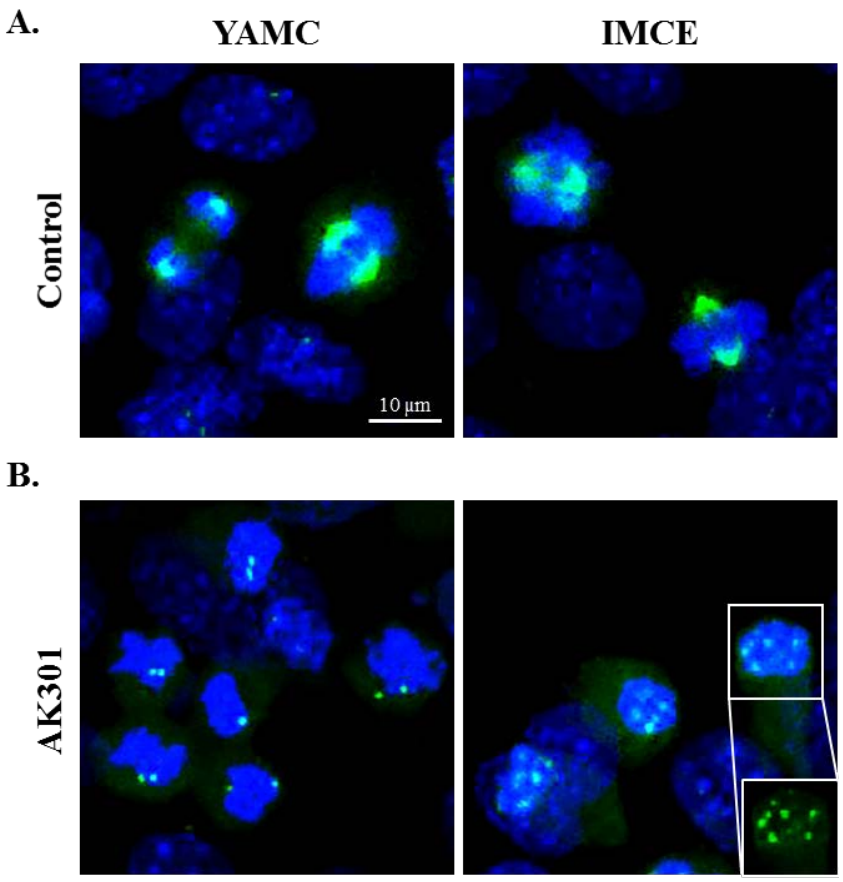

Figure 5.2. AK301 induces the formation of multiple aurora kinase A foci in *Apc* mutant IMCE cells.

(A) YAMCs and IMCE cells were immunostained for aurora kinase A (green). Nuclei were counterstained with DAPI (blue). Untreated YAMCs and IMCE cells show a bipolar localization of aurora kinase A in mitotic cells (cells with condensed chromosome morphology). (B) Aurora kinase A immunostaining of AK301-treated YAMCs and IMCE cells shows diffused and unsegregated localization of aurora kinase A in mitotic cells of both YAMCs and IMCE cells. Moreover, AK301 treatment of IMCE cells induced the formation of multiple diffused aurora kinase A foci. Inset shows a higher magnification of one representative IMCE cell treated with AK301.

5.4.3. *Apc$^{Min/+}$ IMCE cells are sensitive to AK301 treatment and undergo apoptosis in the presence of TNF*

To assess the sensitivity of *Apc*-mutant cells to a microtubule disrupting agent, we treated YAMC and IMCE cells with 200 nM and 400 nM of a novel and potent microtubule inhibitor, AK301, previously identified in our laboratory. Although AK301 induced caspase-3 activation in both *Apc* normal and *Apc* mutant cells, active caspase-3 was found to be about four times higher in *Apc* mutant IMCE cells compared to YAMCs (Figure 5.3A). To confirm that the cells were undergoing apoptosis, we perfomed Annexin V staining of YAMCs and IMCEs treated with AK301. As shown in Figure 5.3B, IMCE cells treated with AK301 showed increased Annexin V staining, suggesting that *Apc* mutant cells treated with AK301 are more susceptible to apoptosis, but not Apc normal cells. Previously, we provided evidence for the reversibility of AK301-induced mitotic arrest and showed that cells exiting mitosis aberrantly underwent apoptosis more effectively. We hypothesized that AK301 would induce similar increase in apoptosis in IMCE cells compared to YAMC cells following AK301 removal. We treated the cells with AK301 and followed sub G1 population at 20, 30, and 40 hrs post mitotic release. Consistent with our results above, AK301 induced significantly greater apoptosis in IMCE cells compared to YAMCs (Figure 5.3C). More importantly, release from AK301 enhanced apoptosis in both YAMCs and IMCE cells, but the increase was significantly greater in IMCE cells at each time interval post mitotic release.

Studies from our laboratory have demonstrated that pharmacological disruption of the rate of microtubule polymerization can result in enhanced death receptor trafficking, primarily TNFR1, to the cell surface [145, 193]. To determine the sensitivity of *Apc$^{Min/+}$* IMCE cells to TNF, we treated YAMC and IMCE cells with 50 ng/ml of TNF for 10 hrs and 20 hrs and

determined the levels of active caspase-3. As shown in Figure 5.3D, *Apc*-mutant IMCE showed significant activation of caspase-3 after 10 h and 20 h of treatment compared to YAMCs, suggesting the enhanced sensitivity of *Apc*-mutant cells to TNF. Interestingly, *Apc* wildtype YAMC cells showed a significant decline in active caspase-3 levels, suggesting a protective effect of TNF on these cells. Consistent with the role of TNF in inducing cell survival and cell death, these data suggest cell-specific dual function of TNF signaling – a protective function for normal cells and as an inducer of apoptosis for mutant cells. Together, these data indicate that *Apc* mutant cells exhibit morphological differences at the cellular level that can be targeted for elimination of mutant cells.

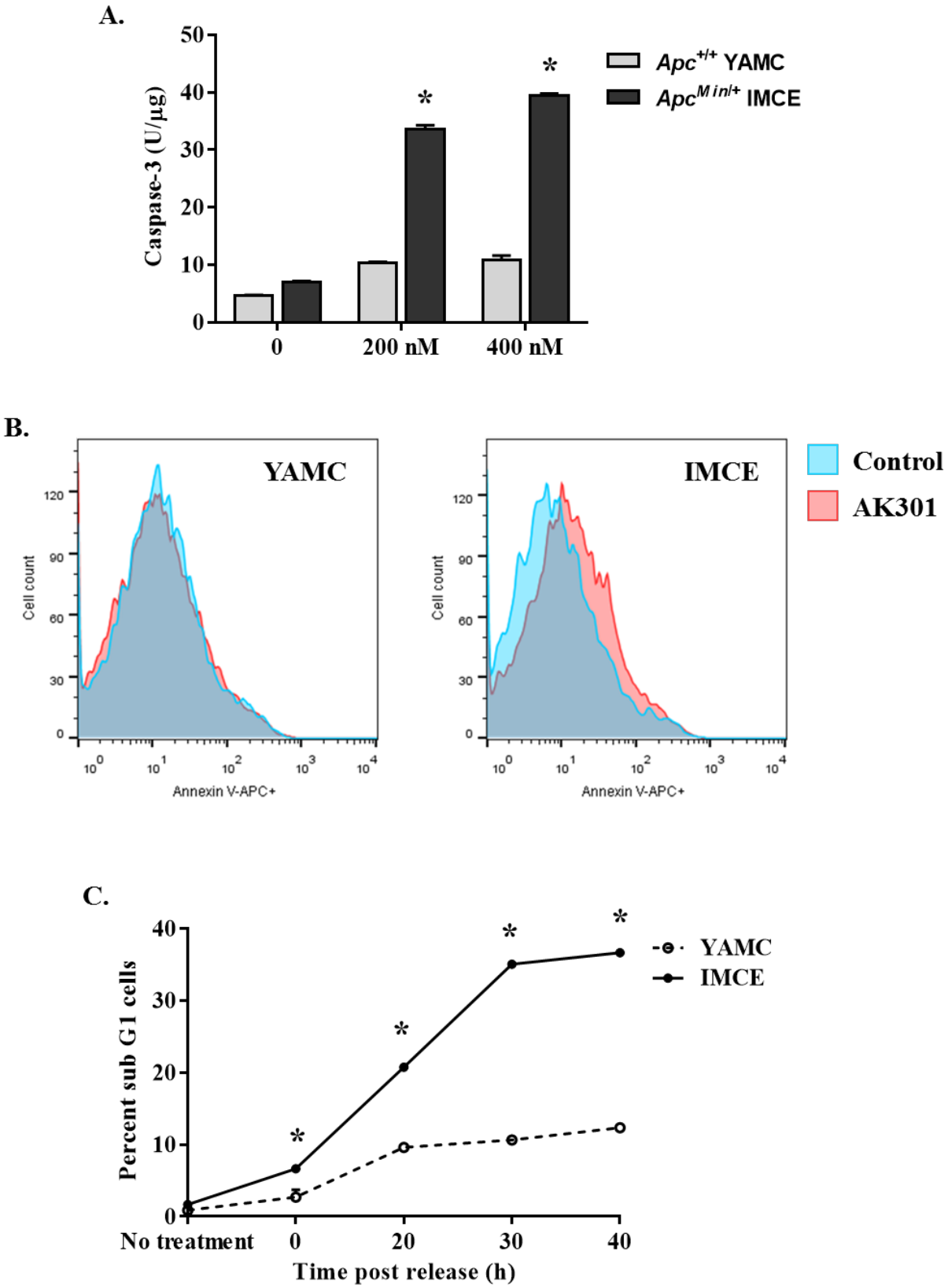
A.
Caspase-3 (U/µg)
50
40
30
20
10
0
*
*
0
200 nM
400 nM
Apc+/+ YAMC
ApcMin/+ IMCE
B.
YAMC
IMCE
Cell count
120
90
60
30
0
10^0
10^1
10^2
10^3
10^4
Annexin V-APC+
Control
AK301
C.
Percent sub G1 cells
40
30
20
10
0
*
*
*
*
No treatment
0
20
30
40
Time post release (h)
YAMC
IMCE

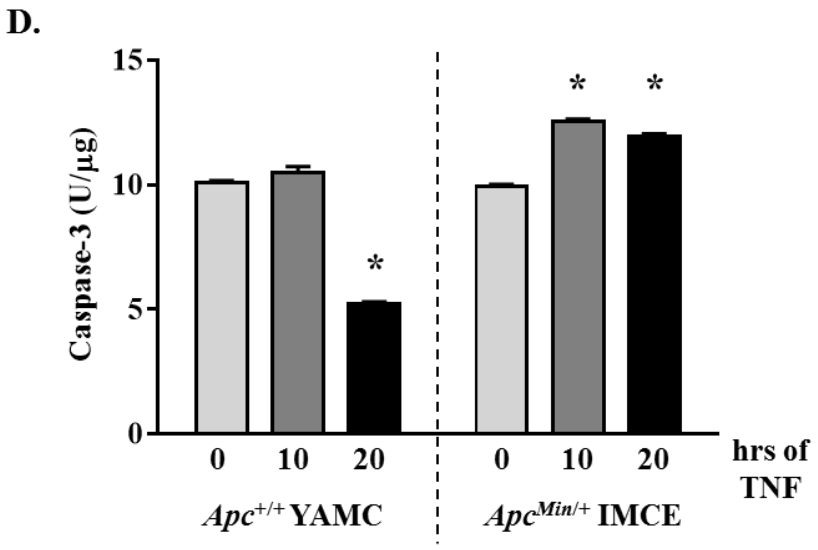

Figure 5.3. AK301 enhances the sensitivity of *Apc* mutant IMCE cells during mitosis and following mitotic release.

(A) YAMCs and IMCE cells were treated with 200 and 400 nM of AK301 for 16 h. Cell lysates were prepared and tested for active caspase-3 by DEVD-AMC fluorogenic assay. AK301 induced significantly high levels of caspase-3 activation in IMCE cells at both concentrations (*P < 0.0001). (B) Annexin V staining of YAMCs and IMCE cells showed a higher proportion of AK301-treated IMCE cells staining positive for Annexin V on the cell surface, indicating that IMCE cells are undergoing apoptosis in response to AK301 treatment. (C) YAMCs and IMCE cells were treated with AK301. Following treatment, AK301 was removed and cells were released from mitotic arrest. Cells were harvested at the indicated times and their DNA content was analyzed by flow cytometry. Analysis of the sub G1 population showed that release from AK301-induced mitotic arrest resulted in significantly greater sub G1 population in IMCE cells compared to their YAMC counterparts (*P < 0.0001). (D) Apc wildtype YAMCs and Apc mutant IMCE cells were treated with 50 ng/ml of TNF for 10 or 20 hrs. Cell lysates were prepared and analyzed for caspase-3 activation by DEVD-AMC assay. TNF induced

significantly higher caspase-3 activation in IMCE cells compared to untreated control cells (*P < 0.0001). Interestingly, 20 hrs of TNF treatment showed a reduction in caspase-3 activation in YAMCs (*P < 0.0001), suggesting a protective role of TNF in wildtype cells.

5.4.4. Overexpression of C-terminus truncated APC and treatment with AK301 induces multiple MTOCs in HEK293 cells

To assess if overexpression of the truncated APC would have similar effects on MTOCs to that in IMCE cells, we transiently transfected HEK293 cells with a truncated human *APC* gene (truncated at the same site as the *Min* mutant). This *APC* was fused to the 3' end of *Gfp* in a pEFGP-C1 vector, under the control of CMV promoter. The resulting $APC^{\Delta C}$ protein was fused to GFP, which was used as a marker for screening cells with $APC^{\Delta C}$. Figure 5.4 shows a schematic of the methodology used to generate $APC^{\Delta C}$-GFP fusion protein. Using our transfection protocol (See Section 5.3.1), we obtained a transfection efficiency greater than 85 percent (Figure A6A). We prepared whole protein extract from both GFP and $APC^{\Delta C}$-GPF expressing cells and immunoblotted for the N-terminus of APC to confirm the expression of APC-GFP in HEK293 cells (Figure A6B). Immunostaining for aurora kinase A showed results similar to those obtained with YAMC and IMCE cells (Figure 5.4B). Untreated $APC^{\Delta C}$-GFP cells showed diffused, bipolar localization of aurora kinase A; treatment with AK301 resulted in the formation of multiple, diffused aurora kinase A foci. Further, consistent with the YAMC/IMCE data, $APC^{\Delta C}$-GFP expressing HEK293 cells are elongated with spindle-shaped microtubule networks. AK301 treatment disrupts the microtubule networks in both GFP and $APC^{\Delta C}$-GFP cells (Figure 5.4C). These data, together with YAMC/IMCE data, suggest that C-terminus truncating mutation of APC can affect aurora kinase A deposition and that treatment of APC mutant cells with AK301 results in aberrations in spindle assembly during mitosis.

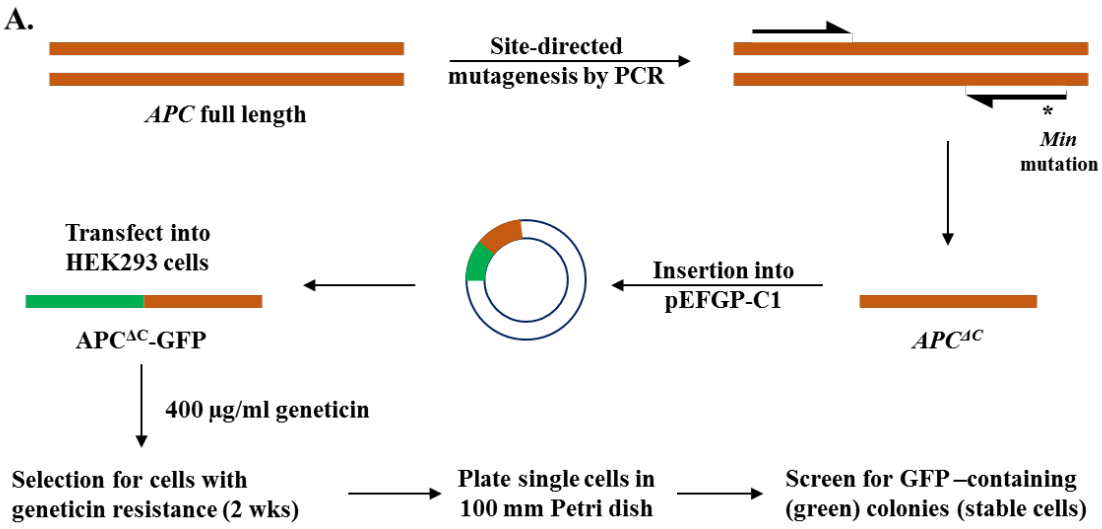
A.
Site-directed
mutagenesis by PCR
APC full length
*
Min
mutation
Transfect into
HEK293 cells
Insertion into
pEFGP-C1
APCΔC-GFP
400 µg/ml geneticin
Selection for cells with
geneticin resistance (2 wks)
Plate single cells in
100 mm Petri dish
Screen for GFP –containing
(green) colonies (stable cells)

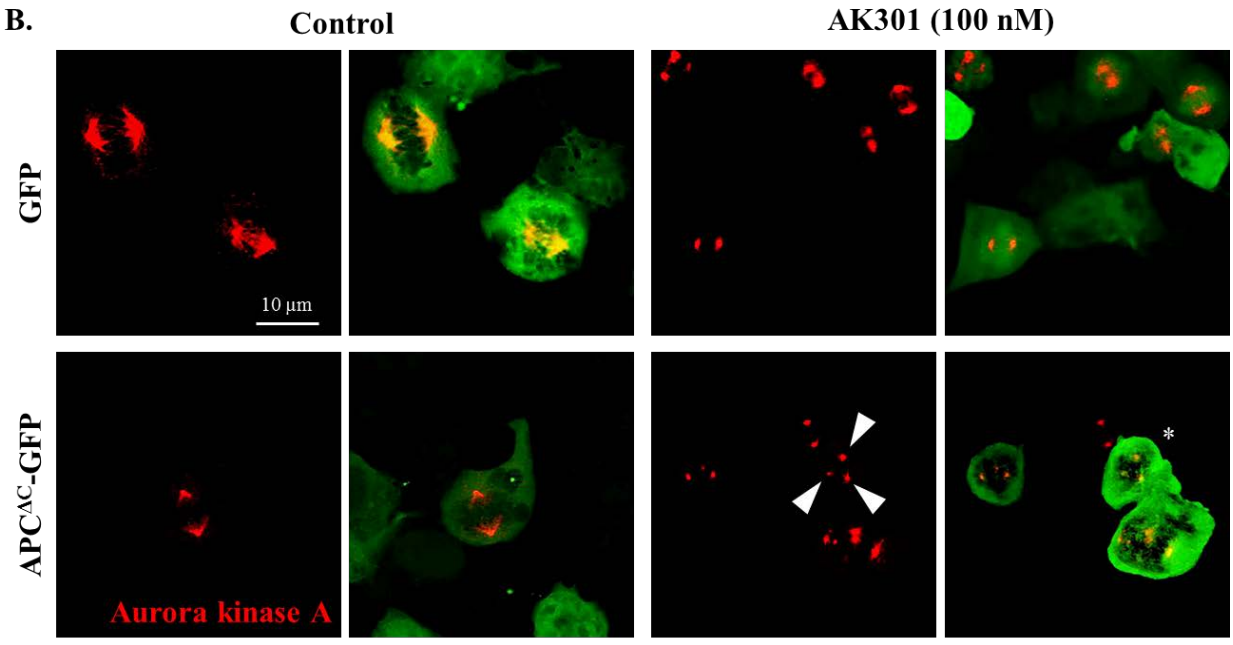
B.
Control
AK301 (100 nM)
GFP
APCΔC-GFP
10 µm
Aurora kinase A
*

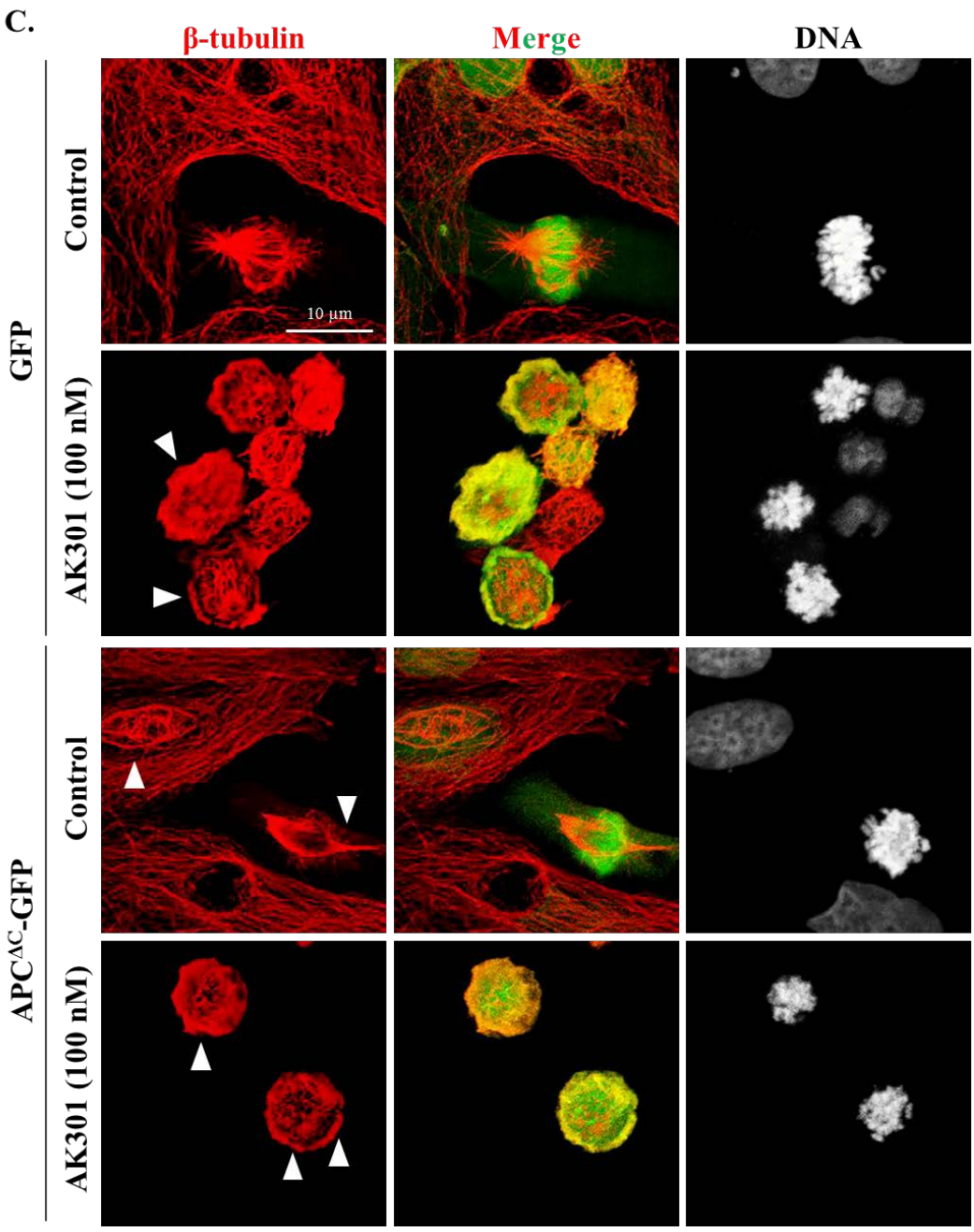

Figure 5.4. AK301 induces the formation of multiple aurora kinase A foci in HEK293 cells overexpressing C-terminus truncated APC (APC$^{\Delta C}$)

(A) Schematic of the generation of GFP-tagged C-terminus truncated APC and generation of stable cell lines. Mutations were introduced in full length human *APC* gene by PCR and

confirmed by agarose gel electrophoresis and capillary electrophoresis. The truncated APC fragment was ligated into pEGFP-C1 vector at the 5'-end of *Gfp*. Cells were transfected using Lipofectamine 3000® reagent and selected for geneticin resistance. Cells were screened based on the GFP expression. GFP and $APC^{\Delta C}$-GFP expressing HEK293 cells were treated with 100 nM of AK301 and immunostained for (B) aurora kinase A and (C) β-tubulin. (B) Untreated cells show bipolar localization of aurora kinase A. However, treatment with AK301 resulted in diffused multiple aurora kinase A foci (arrowheads). (C) Similar to Apc mutant IMCE cells, $APC^{\Delta C}$-GFP expressing HEK293 cells exhibited spindle cell shape compared to GFP expressing HEK293 cells. Treatment with AK301 resulted in disruption of microtubule networks with a more peripheral tubulin staining. Moreover, microtubule disruption in $APC^{\Delta C}$-GFP resulted in a more round shape, consistent with AK301-treatmetn of IMCE cells.

5.4.5. AK301 enhances apoptosis in cells with truncated APC

To determine if overexpression of truncated APC conferred growth advantage in HEK293 cells, we followed the growth of transiently transfected HEK293 cells over 72 h. Cells were harvested and analyzed by flow cytometry. As shown in Figure 5.5A, $APC^{\Delta C}$-GFP cells were significantly more sensitive to apoptosis after transfection, which was enhanced by up to 3-fold by 24 hours post transfection. However, the apoptosis in truncated APC-expressing cells decreased over time with about 5 percent apoptotic events by 72 h.

To assess the effect of AK301 treatment on truncated APC-expressing HEK293 cells, we treated transiently transfected HEK293 GFP and $APC^{\Delta C}$-GFP cells with increasing concentrations of AK301 and analyzed the appearance of sub-diploid population by flow cytometry. AK301 induced a mitotic arrest in both cells, and a modest, but significantly greater arrest in $APC^{\Delta C}$-GFP cells (data not shown). More importantly, AK301 significantly enhanced apoptosis in $APC^{\Delta C}$-GFP, but not GFP expressing cells (Figure 5.5B). Moreover, the apoptotic response of $APC^{\Delta C}$-GPF cells followed a dose response with an EC_{50} of about 45.2 nM with a 95% confidence interval of 37.9 nM and 53.9 nM. Together with YAMC/IMCE data, these results indicate the *APC* mutant cells are sensitive to AK301-induced microtubule disruption readily undergo apoptosis.

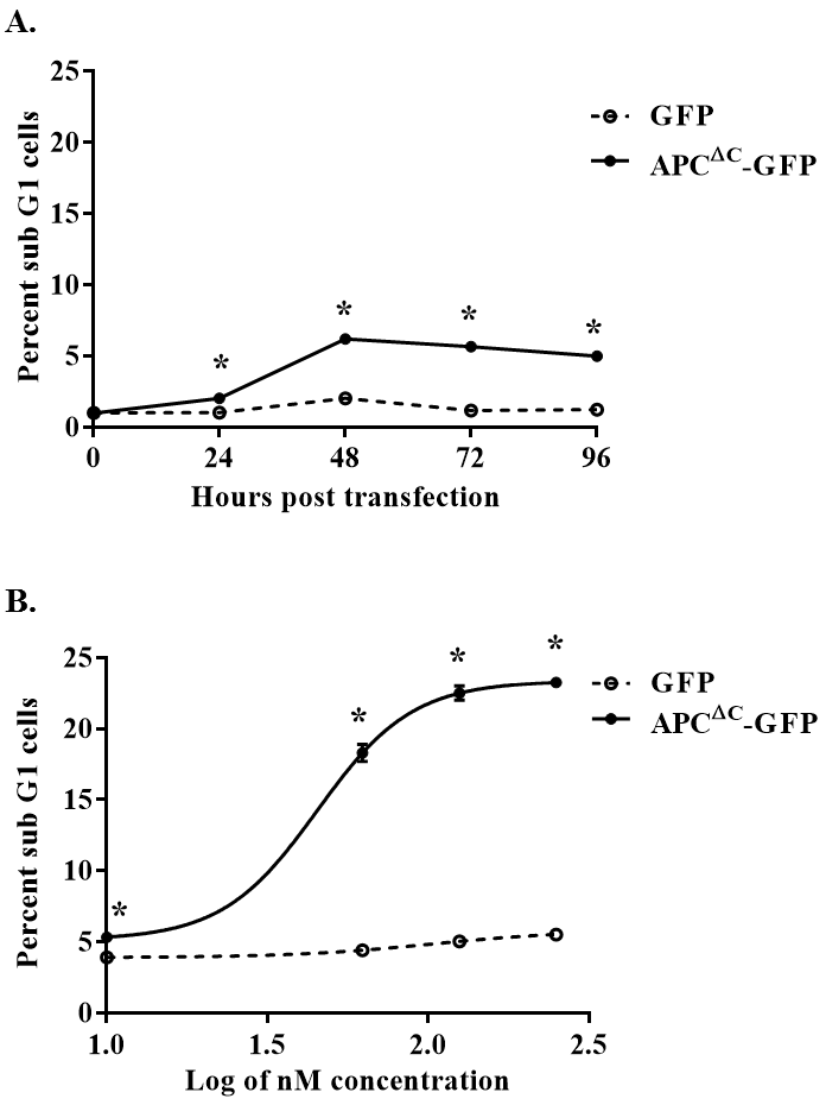

Figure 5.5. AK301 enhances apoptosis in APC$^{\Delta C}$-GFP expressing HEK293 cells in a dose-dependent manner.

(A) HEK293 cells were transiently transfected with APC$^{\Delta C}$-GFP and GFP containing plasmids for 24 hrs. Cell were transferred to fresh medium and cell growth was followed for 72 hrs. Cells were harvested and stained with PI. Flow cytometric analysis of the sub G1 population showed significantly greater apoptosis in AK301-treated APC$^{\Delta C}$-GFP cells (*P < 0.0001). (B) Representative dose-response curves of sub G1 population with increasing concentrations of

AK301. Significant sub G1 proportions were observed in $APC^{\Delta C}$-GFP expressing HEK293 cells at all concentrations of AK301 (*$P < 0.0001$). EC_{50} of $APC^{\Delta C}$-GFP expressing HEK293 cells was determined to ≈ 45 nM.

5.5. Discussion

Mutations in *APC* are found in a majority of colon cancers and are considered to be the first mutations in colon tumorigenesis [203, 206]. Loss-of-function mutations in *APC* trigger a chain of molecular alterations that lead to colon tumorigenesis. We previously identified a class of small molecules that induced mitotic arrest in colon cancer cells and sensitized these cells to apoptosis by increasing the cell surface expression of death receptors [145, 193]. AK301 was the most potent compound identified in this class. In this study, we report that AK301 sensitizes untransformed *APC* mutant cells to apoptosis. Our data demonstrate that *APC* mutations, leading to reduced microtubule polymerization, renders a cell sensitive to spontaneous apoptosis or to death ligands, such as TNF. We further show that APC mutant cells are also sensitive to AK301-induced microtubule disruption with an EC_{50} of ≈ 45 nM. Consistent with our previous studies, our results indicate that declustering of centrosomes may lead to an enhanced apoptotic response in mutant cells. To the best of our knowledge, our study is the first to describe an association between *APC* mutation status and cell sensitivity to a microtubule disrupting agent.

APC plays an important role in microtubule polymerization at the plus ends and recruits end binding protein 1 (EB1) for stabilization of microtubule fibers [238, 239, 249]. The C-terminus of APC contains domains for both microtubule and EB1 binding [250]. Consistent with the role of APC in microtubule polymerization, both $Apc^{Min/+}$ and $APC^{\Delta C}$-expressing HEK293 cells showed aberrant microtubule shape (spindle-shaped microtubule fibers). Additionally, *Apc*-mutant cells, occasionally, lacked microtubule networks, while exhibiting more peripheral localization of microtubules. This may be attributed to the role of microtubules in cortical anchoring and cell-cell adhesion, which is necessary for cell survival [251, 252]. Furthermore, mutations in APC have also been shown to upregulate EB1 during colorectal cancer (CRC)

progression to enhance the stability of microtubules during mitosis [253, 254]. A number of microtubule disrupting agents tested (*e.g.*, vinca alkaloids and nocodazole), *in vitro*, target cells independent of *APC* mutation [255-257]. Therefore, targeting pathways that results in reduced microtubule stability and enhanced cell death signaling may lead to the development of specific and effective chemopreventive agents.

Previously, we demonstrated that disruption of microtubule polymerization can enhance the cell surface expression of death receptors, such as TNFR1 [145]. This is consistent with our finding that *Apc* mutant IMCE cells were sensitive to cell death by TNF. We also showed that AK301 and other active derivatives induced the formation of multiple microtubule organizing centers (MTOCs) in colon cancer cells. In this study, we show that supernumerary centrosomes are an early step in colon carcinogenesis, following *APC* mutation. Centrosomes are the primary sites for microtubule organization, regulating cell shape, polarity, motility, and cell division [258, 259]; centrosome amplification is a common characteristic of various human cancers [157, 159, 260, 261]. We propose that *APC* mutations result in over-duplication of centrosomes during synthesis phase of cell cycle. These centrosomes are then clustered into two foci to ensure proper segregation of the genome. Disruption of microtubules polymerization (*e.g.*, AK301 and derivatives), without their complete abrogation (as in the case of vinca alkaloids), or centrosome declustering (*e.g.*, bromo-noscapine, EM011 [262]) may be an effective way of targeting mutant cells for elimination. How *APC* mutations result in centrosome amplification and how declustering of centrosomes sensitizes cells to apoptosis requires further investigation. This may have implications in preventing colon cancer in patients at high risk for developing the disease.

Akin to the role of APC in microtubule polymerization, APC is required for regulation of microtubule-kinetochore attachments, and thus, mitotic checkpoint [209]. Moreover, APC

interacts directly with mitotic checkpoint proteins, BUB1 and BUBR1, providing stable microtubule-kinetochore attachments [263]. Therefore, mutations in *APC* lead to dysfunctional mitotic checkpoint and may result in cells slipping from mitosis. This gives rise to chromosomal instability and results in tetraploidy *in vivo*. Tetraploidy has been correlated with poor cancer prognosis [235]. Genetic instability (or chromosomal instability) is not only cancer-promoting, but also tumorigenic [235, 264]. Consistent with our previous results with colon cancer cells, analysis of AK301-treated cells showed that AK301 arrested cells in mitosis. However, it should be noted that only *APC* mutant cells (both IMCE and $APC^{\Delta C}$-GFP HEK293 cells) were prone to apoptosis, albeit mitotic arrest similar to APC normal cells. We propose that microtubule disruption by AK301 induces the formation of multiple MTOCs, activating mitotic checkpoint in an APC-independent manner. In light of our previous results, it is possible that disruption of microtubules by AK301 enhances death receptor signaling and aggregation of death receptors may activate caspase cascade, resulting in apoptosis.

In summary, *APC* mutations result in genetic alterations and molecular aberrations that promote colon carcinogenesis. Our results shed light on the early molecular changes in colon cells following *APC* mutations. It is important to understand the mechanisms that undermine apoptosis and promote aberrant cell division. This could lead to development of novel, targeted therapies and chemopreventive agents for elimination of mutated cells from colon crypts.

CHAPTER 6

CONCLUSIONS

Our initial work was focused on understanding how colon cancer cells survive their inflammatory micro-environment with high levels of death ligands, such as TNF. We identified a novel class of piperazine-based compounds that sensitized colon cancer cells to death ligands. Further studies on these compounds generated a more potent AK301 with EC_{50} of 115 nM and elucidated their role in mitotic arrest through disruption of microtubule polymerization and ligand-dependent apoptosis by increasing the surface expression of death receptors. Additional studies to understand the vulnerability of AK301-arrested cells indicated that activation of ATM and stabilization of p53 in the mitotically arrested cells were responsible for inducing apoptosis in mitotically arrested following their exit from the arrest. Furthermore, we showed that AK301 was able to target *APC* mutant cells *in vitro* effectively in the absence of death ligands. Table 6.1 summarizes the apoptotic inducing effects of AK301 treatment on different cell lines analyzed in this dissertation, both in the presence of TNF or following release from mitotic arrest. Table 6.2 describes how patients with different types of colonic lesions would be predicted to respond to treatment with AK301. As shown in the table, mutations in *APC* and/or *p53* are predicted to respond differently to AK301 and TNF. Over 80 percent of colorectal cancers have mutations in the *APC* tumor suppressor gene, most of which result in a truncated protein. Since *APC* mutant cells are more sensitive to AK301 treatment, we envision administration of AK301 would selectively target mutant cells for elimination. This targeting would be observed in initiated colon tissue that is still heterozygote for *APC* and would be accentuated in tissue environments with high levels of TNF, which is typically found in colon cancers. The activation of p53 would

play an important role in elevating apoptosis, particularly after AK301 levels have dropped following excretion. Approximately 50 percent of all colorectal cancers express wildtype p53 and AK301-induced apoptosis would be high in these tumors after Ak301 levels drop and cells are released from arrest. In general, our data suggest that colon cancers with a mutated *APC* gene and a wildtype p53 gene would be most sensitive to AK301 treatment due to a combined effect of p53-induced apoptosis and by extrinsic apoptosis by TNF in the tumor microenvironment.

There are two general classes of colon cancers—those showing chromosomal instability and those with a hypermutator phenotype. Hypermutated cancers, which represent ~20% of colon cancers, are usually p53-normal, but about half of the hypermutated cancers have *APC* mutant [40]. Based on these statistics, we predict that AK301 could potentially provide a significant therapeutic benefit to ~10% of colon cancer patients.

Overall, mutations in colorectal cancers result in molecular alterations that may be targeted with specificity and more effectively. Moreover, understanding the ways in which cancer cells take advantage of *APC* mutations will provide insight into pathways that promote tumorigenesis. In these studies, we explore the critical regulation of microtubule spindle formation and mitotic checkpoints by APC, identify small molecule agents that target *APC* mutant and colon cancer cells with more specificity.

Table 6.1. AK301-induced apoptosis in different cell lines in the absence or presence of TNF

Cell type	Mutation status		Apoptosis with AK301	
	APC	*TP53*	- TNF	+ TNF
YAMC or GFP HEK293 (normal)	+/+	+/+	Low	Low
HT29	-/-	-/-	Low	High
HCT116	+/+	+/+	High	High
HCT116 $p53^{-/-}$	+/+	-/-	Low	-
IMCE	-/+	+/+	High	High
$APC^{\Delta C}$-GFP HEK293	-/+	+/+	High	-

Table 6.2. Predicted effects of AK301-induced mitotic arrest and release from mitotic arrest on different colon tumor types

Tissue type	Mutation status	AK301 treatment	AK301 excretion
Cancer (hypermutated)	*APC*$^{-/-}$ *TP53*$^{+/+}$	Mitotic arrest, High TNF, High apoptosis	Highest apoptosis
Cancer (hypermutated)	*APC*$^{+/+}$ *TP53*$^{+/+}$	Mitotic arrest, High TNF, High apoptosis	High apoptosis
Cancer (chromosomal instability)	*APC*$^{-/-}$ *TP53*$^{-/-}$	Mitotic arrest, High TNF, High apoptosis	Continuing mitotic arrest, Residual apoptosis
Initiated	*APC*$^{-/+}$ *TP53*$^{+/+}$	Mitotic arrest, Low TNF, Moderate apoptosis	Completion of mitosis, Moderate apoptosis
Normal	*APC*$^{+/+}$ *TP53*$^{+/+}$	Mitotic arrest, Low TNF, low apoptosis	Completion of mitosis, Low apoptosis

6.1. Enhancing apoptosis in colon cancer cells

Immune and inflammatory cells frequently infiltrate colon cancer cells and early colonic lesions [75, 265, 266]. Even though inflammatory cytokines have anti-tumor activity, chronic inflammation can promote cancer progression through the production of growth stimulating factors and DNA-reactive metabolites [267, 268]. We identified AK301 and its analogs that sensitized colon cancer cells to death ligands without significantly affecting cell survival. These compounds induced mitotic arrest in cancer cells and apoptosis in the presence of the death ligands. We showed that cellular sensitivity to the death ligands was primarily due to increased death receptor expression on the cell surface. These compounds (especially our most potent compound, AK301), are therefore, particularly useful in activating apoptotic signaling and sensitizing colon cancer with high levels of inflammatory signaling.

Structure-activity relationship studies revealed that AK301 and its analogs reduced the rate of microtubule polymerization in contrast to agents that induced greater disruption of microtubules. This reduced polymerization (over abrogation) may play a role in death signal trafficking on microtubule networks. One possible explanation is that AK301 alters microtubule networks in a way that the death receptors can be delivered to the cell surface more efficiently, but their removal is hindered.

Furthermore, studies to understand the mechanism of AK301 showed that mitosis-to-apoptosis transition requires exit from mitosis. Interestingly, we found that AK301 treatment and withdrawal was sufficient to induce apoptosis in p53-normal colon cancer cells. AK301 arrest induced high levels of activated ATM, which stabilizes p53, resulting in apoptosis. Some studies suggest that ATM activation, by itself, may target the activation of death receptors and caspase-8 [269, 270]. Activation of ATM signaling was not observed with other agents that abrogated

microtubule polymerization. How AK301-induced mitotic arrest results in ATM signaling is unclear.

Overall, our studies suggest that cancer cells can be sensitized to undergo apoptosis and understanding the mechanisms that reactivate apoptotic processes in cancer cells can lead to the development of targeted chemotherapeutic agents.

6.2. Targeting mutant, non-transformed colon cells with AK301

The five-year survival rate for stage I colon tumors is 90 percent [2, 5]. Unfortunately, less than 40 percent of colon tumors are detected at an early stage; the five-year survival rate drops rapidly with each subsequent stage of colon cancer [1, 2]. Moreover, 30-50 percent of the patients undergoing curative resection for colon cancer have recurrent disease [5]. Besides early diagnosis and accurate staging of colon cancer patients, there is a need to identify new chemopreventive agents to reduce the risk of colon cancer in at-risk patients. Studies indicate that mutated cells of the colonic crypt as well as early lesions exhibit molecular differences due to *APC* and other mutations [203, 229, 239, 250]. These differences may be exploited, such as with AK301, to target mutated cells, making them vulnerable to cell death, thereby reducing the risk of developing colon tumors. We envision AK301 interfering with microtubule polymerization in a manner similar to mutated APC. This disruption may accentuate mitotic arrest at a state that activates ATM signaling. Whether these compounds can be used for this application remains to be determined.

6.3. Future directions

Our studies identified novel compounds that sensitize *APC* mutant (non-transformed) cells and colon cancer cells to apoptosis through a mitotic-to-apoptotic transition of the exiting arrested cells. In our previous studies, we showed that the positioning of chloride group on phenyl and ethoxy group on benzoyl groups on the piperazine core were required for the activity of these compounds. Currently, further structure-activity relationship studies are underway to modify these side groups develop more potent compounds that can robustly and specifically transition cancer cells into apoptosis. Moreover, new generation of compounds will feature probes that will aid in target identification and the mechanism of action in more detail.
All of the studies have been carried out in *in vitro* systems using either cancer cell lines or non-transformed cells. Although these systems provide a cost and time effective method for screening and development of new agents, it is challenging to extrapolate *in vitro* results *in vivo*. Our near-future goals are to determine the effect of these agents in *Apc* mutant and xenograft mouse model, assessing the effect of AK301 on survival and tumor volumes in mice.

In summary, current clinical diagnosis and treatment of colon cancer demands new approaches for prevention and treatment of colon cancer. A move towards individualized approach to treatment could yield better outcomes. Our studies provide evidence that *APC* mutations could result in cytoskeletal aberrations in the colonic cells that can be targeted effectively, reducing the risk of disease progression. Moreover, our studies provide a paradigm for targeting mitotic spindle defects and mitotic checkpoint with small molecule agents. Further development of pharmacological agents for specific targets will help in detailed understanding of

the processes at play in mutated cells and aid in the identification of novel chemopreventive and chemotherapeutic agents.

References

1. American Cancer Society. What are the key statistics about colorectal cancer? *Colorectal Cancer* 2014. Accessed 2014. http://www.cancer.org/cancer/colonandrectumcancer/detailedguide/colorectal-cancer-key-statistics.
2. Centers for Disease Control and Prevention. Colorectal Cancer Statistics. *Colorectal Cancer* 2014. Accessed 2014. http://www.cdc.gov/cancer/colorectal/statistics/.
3. American Cancer Society Colorectal Cancer Screening. *Colorectal Cancer: Facts & Figures, 2014-2016*, 2014.
4. National Cancer Institute. Summary of Evidence. *Colorectal Cancer Screening (PDQ®)* 2014. Accessed 2014. http://www.cancer.gov/cancertopics/pdq/screening/colorectal/HealthProfessional/page1.
5. American Cancer Society. Survival rates for colorectal cancer. *Colorectal Cancer* 2014. Accessed 2014. http://www.cancer.org/cancer/colonandrectumcancer/overviewguide/colorectal-cancer-overview-survival-rates.
6. American Cancer Society. Chemotherapy for colorectal cancer. *Colorectal cancer* 2014. Accessed 2014. http://www.cancer.org/cancer/colonandrectumcancer/detailedguide/colorectal-cancer-treating-chemotherapy.
7. U.S. Preventive Services Task Force. Screening for Colorectal Cancer: U.S. Preventive Services Task Force Recommendation Statement. 2008. http://www.uspreventiveservicestaskforce.org/uspstf08/colocancer/colors.htm.
8. Centers for Disease Control and Prevention. What Should I Know About Screening? *Colorectal (Colon) Cancer* 2014. Accessed 2014. http://www.cdc.gov/cancer/colorectal/basic_info/screening/.
9. National Cancer Institute. Tests to Detect Colorectal Cancer and Polyps. 2013. Accessed 2014. http://www.cancer.gov/cancertopics/factsheet/detection/colorectal-screening.
10. Amonkar, M.M., Hunt, T.L., Zhou, Z., et al., Surveillance patterns and polyp recurrence following diagnosis and excision of colorectal polyps in a medicare population. *Cancer Epidemiol Biomarkers Prev*, 2005. **14**(2): p. 417-21.
11. Boone, C.W., Kelloff, G.J., and Malone, W.E., Identification of candidate cancer chemopreventive agents and their evaluation in animal models and human clinical trials: a review. *Cancer Res*, 1990. **50**(1): p. 2-9.
12. Lipkin, M., Yang, K., Edelmann, W., et al., Preclinical mouse models for cancer chemoprevention studies. *Ann N Y Acad Sci*, 1999. **889**: p. 14-9.
13. Steele, V.E. and Lubet, R.A., The use of animal models for cancer chemoprevention drug development. *Semin Oncol*, 2010. **37**(4): p. 327-38.
14. Funkhouser, E.M. and Sharp, G.B., Aspirin and reduced risk of esophageal carcinoma. *Cancer*, 1995. **76**(7): p. 1116-9.
15. Wakabayashi, K., NSAIDs as Cancer Preventive Agents. *Asian Pac J Cancer Prev*, 2000. **1**(2): p. 97-113.
16. American Cancer Society. What are the survival rates for colorectal cancer by stage? *Colorectal cancer* 2015. Accessed 2015.

http://www.cancer.org/cancer/colonandrectumcancer/detailedguide/colorectal-cancer-survival-rates.
17. Chai, J., Du, C., Wu, J.W., et al., Structural and biochemical basis of apoptotic activation by Smac/DIABLO. *Nature*, 2000. **406**(6798): p. 855-62.
18. Portt, L., Norman, G., Clapp, C., et al., Anti-apoptosis and cell survival: a review. *Biochim Biophys Acta*, 2011. **1813**(1): p. 238-59.
19. Elmore, S., Apoptosis: a review of programmed cell death. *Toxicol Pathol*, 2007. **35**(4): p. 495-516.
20. Coleman, M.L., Sahai, E.A., Yeo, M., et al., Membrane blebbing during apoptosis results from caspase-mediated activation of ROCK I. *Nat Cell Biol*, 2001. **3**(4): p. 339-45.
21. Edinger, A.L. and Thompson, C.B., Death by design: apoptosis, necrosis and autophagy. *Curr Opin Cell Biol*, 2004. **16**(6): p. 663-9.
22. Hanahan, D. and Weinberg, R.A., The hallmarks of cancer. *Cell*, 2000. **100**(1): p. 57-70.
23. Delbridge, A.R., Valente, L.J., and Strasser, A., The role of the apoptotic machinery in tumor suppression. *Cold Spring Harb Perspect Biol*, 2012. **4**(11).
24. Zhang, L. and Yu, J., Role of apoptosis in colon cancer biology, therapy, and prevention. *Curr Colorectal Cancer Rep*, 2013. **9**(4).
25. Fenton, R.G., Hixon, J.A., Wright, P.W., et al., Inhibition of Fas (CD95) expression and Fas-mediated apoptosis by oncogenic Ras. *Cancer Res*, 1998. **58**(15): p. 3391-400.
26. O'Connell, J., Bennett, M.W., Nally, K., et al., Altered mechanisms of apoptosis in colon cancer: Fas resistance and counterattack in the tumor-immune conflict. *Ann N Y Acad Sci*, 2000. **910**: p. 178-92; discussion 193-5.
27. Watson, A.J., Apoptosis and colorectal cancer. *Gut*, 2004. **53**(11): p. 1701-9.
28. Yamamoto, H., Sawai, H., Weber, T.K., et al., Somatic frameshift mutations in DNA mismatch repair and proapoptosis genes in hereditary nonpolyposis colorectal cancer. *Cancer Res*, 1998. **58**(5): p. 997-1003.
29. Huerta, S., Goulet, E.J., and Livingston, E.H., Colon cancer and apoptosis. *Am J Surg*, 2006. **191**(4): p. 517-26.
30. Li, J. and Yuan, J., Caspases in apoptosis and beyond. *Oncogene*, 2008. **27**(48): p. 6194-206.
31. Riedl, S.J. and Shi, Y., Molecular mechanisms of caspase regulation during apoptosis. *Nat Rev Mol Cell Biol*, 2004. **5**(11): p. 897-907.
32. Lavrik, I.N., Golks, A., and Krammer, P.H., Caspases: pharmacological manipulation of cell death. *J Clin Invest*, 2005. **115**(10): p. 2665-72.
33. Parrish, A.B., Freel, C.D., and Kornbluth, S., Cellular mechanisms controlling caspase activation and function. *Cold Spring Harb Perspect Biol*, 2013. **5**(6).
34. Kruidering, M. and Evan, G.I., Caspase-8 in apoptosis: the beginning of "the end"? *IUBMB Life*, 2000. **50**(2): p. 85-90.
35. Fulda, S. and Debatin, K.M., Extrinsic versus intrinsic apoptosis pathways in anticancer chemotherapy. *Oncogene*, 2006. **25**(34): p. 4798-811.
36. Berthelet, J. and Dubrez, L., Regulation of Apoptosis by Inhibitors of Apoptosis (IAPs). *Cells*, 2013. **2**(1): p. 163-87.
37. de Almagro, M.C. and Vucic, D., The inhibitor of apoptosis (IAP) proteins are critical regulators of signaling pathways and targets for anti-cancer therapy. *Exp Oncol*, 2012. **34**(3): p. 200-11.

38. LaCasse, E.C., Baird, S., Korneluk, R.G., et al., The inhibitors of apoptosis (IAPs) and their emerging role in cancer. *Oncogene*, 1998. **17**(25): p. 3247-59.
39. Thompson, C.B., Apoptosis in the pathogenesis and treatment of disease. *Science*, 1995. **267**(5203): p. 1456-62.
40. Cancer Genome Atlas Network, Comprehensive molecular characterization of human colon and rectal cancer. *Nature*, 2012. **487**(7407): p. 330-7.
41. Fleming, N.I., Jorissen, R.N., Mouradov, D., et al., SMAD2, SMAD3 and SMAD4 mutations in colorectal cancer. *Cancer Res*, 2013. **73**(2): p. 725-35.
42. Bellam, N. and Pasche, B., Tgf-beta signaling alterations and colon cancer. *Cancer Treat Res*, 2010. **155**: p. 85-103.
43. Kim, H.S., Lee, J.W., Soung, Y.H., et al., Inactivating mutations of caspase-8 gene in colorectal carcinomas. *Gastroenterology*, 2003. **125**(3): p. 708-15.
44. Dicuonzo, G., Angeletti, S., Garcia-Foncillas, J., et al., Colorectal carcinomas and PTEN/MMAC1 gene mutations. *Clin Cancer Res*, 2001. **7**(12): p. 4049-53.
45. Rodrigues, N.R., Rowan, A., Smith, M.E., et al., p53 mutations in colorectal cancer. *Proc Natl Acad Sci U S A*, 1990. **87**(19): p. 7555-9.
46. Zhang, B., Zhang, B., Chen, X., et al., Loss of Smad4 in colorectal cancer induces resistance to 5-fluorouracil through activating Akt pathway. *Br J Cancer*, 2014. **110**(4): p. 946-57.
47. Li, F., Cao, Y., Townsend, C.M., Jr., et al., TGF-beta signaling in colon cancer cells. *World J Surg*, 2005. **29**(3): p. 306-11.
48. Randhawa, H., Kibble, K., Zeng, H., et al., Activation of ERK signaling and induction of colon cancer cell death by piperlongumine. *Toxicol In Vitro*, 2013. **27**(6): p. 1626-33.
49. Fang, J.Y. and Richardson, B.C., The MAPK signalling pathways and colorectal cancer. *Lancet Oncol*, 2005. **6**(5): p. 322-7.
50. Vlahovic, G. and Crawford, J., Activation of tyrosine kinases in cancer. *Oncologist*, 2003. **8**(6): p. 531-8.
51. Klampfer, L., Cytokines, inflammation and colon cancer. *Curr Cancer Drug Targets*, 2011. **11**(4): p. 451-64.
52. Terzic, J., Grivennikov, S., Karin, E., et al., Inflammation and colon cancer. *Gastroenterology*, 2010. **138**(6): p. 2101-2114 e5.
53. Wajant, H. and Scheurich, P., TNFR1-induced activation of the classical NF-kappaB pathway. *FEBS J*, 2011. **278**(6): p. 862-76.
54. Schutze, S., Tchikov, V., and Schneider-Brachert, W., Regulation of TNFR1 and CD95 signalling by receptor compartmentalization. *Nat Rev Mol Cell Biol*, 2008. **9**(8): p. 655-62.
55. Hamilton, K.E., Simmons, J.G., Ding, S., et al., Cytokine induction of tumor necrosis factor receptor 2 is mediated by STAT3 in colon cancer cells. *Mol Cancer Res*, 2011. **9**(12): p. 1718-31.
56. Mizoguchi, E., Mizoguchi, A., Takedatsu, H., et al., Role of tumor necrosis factor receptor 2 (TNFR2) in colonic epithelial hyperplasia and chronic intestinal inflammation in mice. *Gastroenterology*, 2002. **122**(1): p. 134-44.
57. Ikeda, I., Tomimoto, A., Wada, K., et al., 5-aminosalicylic acid given in the remission stage of colitis suppresses colitis-associated cancer in a mouse colitis model. *Clin Cancer Res*, 2007. **13**(21): p. 6527-31.
58. Lukas, M., Inflammatory bowel disease as a risk factor for colorectal cancer. *Dig Dis*, 2010. **28**(4-5): p. 619-24.

59. Allison, M., Garland, C., Chlebowski, R., et al., The association between aspirin use and the incidence of colorectal cancer in women. *Am J Epidemiol*, 2006. **164**(6): p. 567-75.
60. Arber, N. and DuBois, R.N., Nonsteroidal anti-inflammatory drugs and prevention of colorectal cancer. *Curr Gastroenterol Rep*, 1999. **1**(5): p. 441-8.
61. Din, F.V., Theodoratou, E., Farrington, S.M., et al., Effect of aspirin and NSAIDs on risk and survival from colorectal cancer. *Gut*, 2010. **59**(12): p. 1670-9.
62. Cammarota, R., Bertolini, V., Pennesi, G., et al., The tumor microenvironment of colorectal cancer: stromal TLR-4 expression as a potential prognostic marker. *J Transl Med*, 2010. **8**: p. 112.
63. Luo, J.L., Maeda, S., Hsu, L.C., et al., Inhibition of NF-kappaB in cancer cells converts inflammation- induced tumor growth mediated by TNFalpha to TRAIL-mediated tumor regression. *Cancer Cell*, 2004. **6**(3): p. 297-305.
64. Numata, A., Minagawa, T., Asano, M., et al., Functional evaluation of tumor-infiltrating mononuclear cells. Detection of endogenous interferon-gamma and tumor necrosis factor-alpha in human colorectal adenocarcinomas. *Cancer*, 1991. **68**(9): p. 1937-43.
65. Terzic, J., Grivennikov, S., Karin, E., et al., Inflammation and colon cancer. *Gastroenterology*, 2010. **138**(6): p. 2101-2114.e5.
66. Dalgleish, A.G. and O'Byrne, K., Inflammation and cancer: the role of the immune response and angiogenesis. *Cancer Treat Res*, 2006. **130**: p. 1-38.
67. Kawanishi, S., Hiraku, Y., Pinlaor, S., et al., Oxidative and nitrative DNA damage in animals and patients with inflammatory diseases in relation to inflammation-related carcinogenesis. *Biol Chem*, 2006. **387**(4): p. 365-72.
68. Nakanishi, M. and Rosenberg, D.W., Multifaceted roles of PGE2 in inflammation and cancer. *Semin Immunopathol*, 2013. **35**(2): p. 123-37.
69. Tudek, B. and Speina, E., Oxidatively damaged DNA and its repair in colon carcinogenesis. *Mutat Res*, 2012. **736**(1-2): p. 82-92.
70. Silk, A.W., Schoen, R.E., Potter, D.M., et al., Humoral immune response to abnormal MUC1 in subjects with colorectal adenoma and cancer. *Mol Immunol*, 2009. **47**(1): p. 52-6.
71. Suzuki, H., Graziano, D.F., McKolanis, J., et al., T cell-dependent antibody responses against aberrantly expressed cyclin B1 protein in patients with cancer and premalignant disease. *Clin Cancer Res*, 2005. **11**(4): p. 1521-6.
72. Dunn, G.P., Bruce, A.T., Ikeda, H., et al., Cancer immunoediting: from immunosurveillance to tumor escape. *Nat Immunol*, 2002. **3**(11): p. 991-8.
73. Dunn, G.P., Old, L.J., and Schreiber, R.D., The three Es of cancer immunoediting. *Annu Rev Immunol*, 2004. **22**: p. 329-60.
74. de Visser, K.E., Eichten, A., and Coussens, L.M., Paradoxical roles of the immune system during cancer development. *Nat Rev Cancer*, 2006. **6**(1): p. 24-37.
75. Funada, Y., Noguchi, T., Kikuchi, R., et al., Prognostic significance of CD8+ T cell and macrophage peritumoral infiltration in colorectal cancer. *Oncol Rep*, 2003. **10**(2): p. 309-13.
76. Correale, P., Cusi, M.G., Tsang, K.Y., et al., Chemo-immunotherapy of metastatic colorectal carcinoma with gemcitabine plus FOLFOX 4 followed by subcutaneous granulocyte macrophage colony-stimulating factor and interleukin-2 induces strong immunologic and antitumor activity in metastatic colon cancer patients. *J Clin Oncol*, 2005. **23**(35): p. 8950-8.

77. Correale, P., Tagliaferri, P., Fioravanti, A., et al., Immunity feedback and clinical outcome in colon cancer patients undergoing chemoimmunotherapy with gemcitabine + FOLFOX followed by subcutaneous granulocyte macrophage colony-stimulating factor and aldesleukin (GOLFIG-1 Trial). *Clin Cancer Res*, 2008. **14**(13): p. 4192-9.
78. Berraondo, P., Umansky, V., and Melero, I., Changing the tumor microenvironment: new strategies for immunotherapy. *Cancer Res*, 2012. **72**(20): p. 5159-64.
79. Medina-Echeverz, J. and Berraondo, P., Colon cancer eradication after chemoimmunotherapy is associated with intratumoral emergence of proinflammatory myeloid cells. *Oncoimmunology*, 2012. **1**(1): p. 118-120.
80. Medina-Echeverz, J., Fioravanti, J., Zabala, M., et al., Successful colon cancer eradication after chemoimmunotherapy is associated with profound phenotypic change of intratumoral myeloid cells. *J Immunol*, 2011. **186**(2): p. 807-15.
81. Garrido, F. and Ruiz-Cabello, F., MHC expression on human tumors--its relevance for local tumor growth and metastasis. *Semin Cancer Biol*, 1991. **2**(1): p. 3-10.
82. Goepel, J.R., Rees, R.C., Rogers, K., et al., Loss of monomorphic and polymorphic HLA antigens in metastatic breast and colon carcinoma. *Br J Cancer*, 1991. **64**(5): p. 880-3.
83. Warabi, M., Kitagawa, M., and Hirokawa, K., Loss of MHC class II expression is associated with a decrease of tumor-infiltrating T cells and an increase of metastatic potential of colorectal cancer: immunohistological and histopathological analyses as compared with normal colonic mucosa and adenomas. *Pathol Res Pract*, 2000. **196**(12): p. 807-15.
84. Altieri, D.C., Survivin and IAP proteins in cell-death mechanisms. *Biochem J*, 2010. **430**(2): p. 199-205.
85. Salz, W., Eisenberg, D., Plescia, J., et al., A survivin gene signature predicts aggressive tumor behavior. *Cancer Res*, 2005. **65**(9): p. 3531-4.
86. Belinsky, G.S., Parke, A.L., Huang, Q., et al., The contribution of methotrexate exposure and host factors on transcriptional variance in human liver. *Toxicol Sci*, 2007. **97**(2): p. 582-94.
87. Kuratnik, A., Senapati, V.E., Verma, R., et al., Acute sensitization of colon cancer cells to inflammatory cytokines by prophase arrest. *Biochem Pharmacol*, 2012. **83**(9): p. 1217-28.
88. Rigatti, M.J., Verma, R., Belinsky, G.S., et al., Pharmacological inhibition of Mdm2 triggers growth arrest and promotes DNA breakage in mouse colon tumors and human colon cancer cells. *Mol Carcinog*, 2012. **51**(5): p. 363-78.
89. Verma, R., Rigatti, M.J., Belinsky, G.S., et al., DNA damage response to the Mdm2 inhibitor nutlin-3. *Biochem Pharmacol*, 2010. **79**(4): p. 565-74.
90. Godman, C.A., Joshi, R., Tierney, B.R., et al., HDAC3 impacts multiple oncogenic pathways in colon cancer cells with effects on Wnt and vitamin D signaling. *Cancer Biol Ther*, 2008. **7**(10): p. 1570-80.
91. Inan, M.S., Rasoulpour, R.J., Yin, L., et al., The luminal short-chain fatty acid butyrate modulates NF-kappaB activity in a human colonic epithelial cell line. *Gastroenterology*, 2000. **118**(4): p. 724-34.
92. Belinsky, G.S., Claffey, K.P., Nambiar, P.R., et al., Vascular endothelial growth factor and enhanced angiogenesis do not promote metastatic conversion of a newly established azoxymethane-induced colon cancer cell line. *Mol Carcinog*, 2005. **43**(2): p. 65-74.
93. Goto, H., Yasui, Y., Nigg, E.A., et al., Aurora-B phosphorylates Histone H3 at serine28 with regard to the mitotic chromosome condensation. *Genes Cells*, 2002. **7**(1): p. 11-7.

94. Perez-Cadahia, B., Drobic, B., and Davie, J.R., H3 phosphorylation: dual role in mitosis and interphase. *Biochem Cell Biol*, 2009. **87**(5): p. 695-709.
95. Beg, A.A., Sha, W.C., Bronson, R.T., et al., Embryonic lethality and liver degeneration in mice lacking the RelA component of NF-kappa B. *Nature*, 1995. **376**(6536): p. 167-70.
96. Van Antwerp, D.J., Martin, S.J., Kafri, T., et al., Suppression of TNF-alpha-induced apoptosis by NF-kappaB. *Science*, 1996. **274**(5288): p. 787-9.
97. Wang, C.Y., Mayo, M.W., and Baldwin, A.S., Jr., TNF- and cancer therapy-induced apoptosis: potentiation by inhibition of NF-kappaB. *Science*, 1996. **274**(5288): p. 784-7.
98. Bertin, J., Armstrong, R.C., Ottilie, S., et al., Death effector domain-containing herpesvirus and poxvirus proteins inhibit both Fas- and TNFR1-induced apoptosis. *Proc Natl Acad Sci U S A*, 1997. **94**(4): p. 1172-6.
99. Muzio, M., Salvesen, G.S., and Dixit, V.M., FLICE induced apoptosis in a cell-free system. Cleavage of caspase zymogens. *J Biol Chem*, 1997. **272**(5): p. 2952-6.
100. Gorgun, G., Calabrese, E., Hideshima, T., et al., A novel Aurora-A kinase inhibitor MLN8237 induces cytotoxicity and cell-cycle arrest in multiple myeloma. *Blood*, 2010. **115**(25): p. 5202-13.
101. Lenart, P., Petronczki, M., Steegmaier, M., et al., The small-molecule inhibitor BI 2536 reveals novel insights into mitotic roles of polo-like kinase 1. *Curr Biol*, 2007. **17**(4): p. 304-15.
102. Manfredi, M.G., Ecsedy, J.A., Meetze, K.A., et al., Antitumor activity of MLN8054, an orally active small-molecule inhibitor of Aurora A kinase. *Proc Natl Acad Sci U S A*, 2007. **104**(10): p. 4106-11.
103. Steegmaier, M., Hoffmann, M., Baum, A., et al., BI 2536, a potent and selective inhibitor of polo-like kinase 1, inhibits tumor growth in vivo. *Curr Biol*, 2007. **17**(4): p. 316-22.
104. Tomita, M. and Mori, N., Aurora A selective inhibitor MLN8237 suppresses the growth and survival of HTLV-1-infected T-cells in vitro. *Cancer Sci*, 2010. **101**(5): p. 1204-11.
105. O'Connor, D.S., Grossman, D., Plescia, J., et al., Regulation of apoptosis at cell division by p34cdc2 phosphorylation of survivin. *Proc Natl Acad Sci U S A*, 2000. **97**(24): p. 13103-7.
106. Barrett, R.M., Osborne, T.P., and Wheatley, S.P., Phosphorylation of survivin at threonine 34 inhibits its mitotic function and enhances its cytoprotective activity. *Cell Cycle*, 2009. **8**(2): p. 278-83.
107. Chan, T.A., Morin, P.J., Vogelstein, B., et al., Mechanisms underlying nonsteroidal antiinflammatory drug-mediated apoptosis. *Proc Natl Acad Sci U S A*, 1998. **95**(2): p. 681-6.
108. Giardina, C., Boulares, H., and Inan, M.S., NSAIDs and butyrate sensitize a human colorectal cancer cell line to TNF-alpha and Fas ligation: the role of reactive oxygen species. *Biochim Biophys Acta*, 1999. **1448**(3): p. 425-38.
109. Yin, L., Laevsky, G., and Giardina, C., Butyrate suppression of colonocyte NF-kappa B activation and cellular proteasome activity. *J Biol Chem*, 2001. **276**(48): p. 44641-6.
110. Kaler, P., Sasazuki, T., Shirasawa, S., et al., HDAC2 deficiency sensitizes colon cancer cells to TNFalpha-induced apoptosis through inhibition of NF-kappaB activity. *Exp Cell Res*, 2008. **314**(7): p. 1507-18.
111. Glauben, R. and Siegmund, B., Inhibition of histone deacetylases in inflammatory bowel diseases. *Mol Med*, 2011. **17**(5-6): p. 426-33.
112. Glauben, R., Batra, A., Stroh, T., et al., Histone deacetylases: novel targets for prevention of colitis-associated cancer in mice. *Gut*, 2008. **57**(5): p. 613-22.

113. Glauben, R., Sonnenberg, E., Zeitz, M., et al., HDAC inhibitors in models of inflammation-related tumorigenesis. *Cancer Lett*, 2009. **280**(2): p. 154-9.
114. Shanker, A., Brooks, A.D., Jacobsen, K.M., et al., Antigen presented by tumors in vivo determines the nature of CD8+ T-cell cytotoxicity. *Cancer Res*, 2009. **69**(16): p. 6615-23.
115. Tomonaga, T., Matsushita, K., Ishibashi, M., et al., Centromere protein H is up-regulated in primary human colorectal cancer and its overexpression induces aneuploidy. *Cancer Res*, 2005. **65**(11): p. 4683-9.
116. Tomonaga, T., Matsushita, K., Yamaguchi, S., et al., Overexpression and mistargeting of centromere protein-A in human primary colorectal cancer. *Cancer Res*, 2003. **63**(13): p. 3511-6.
117. Baba, Y., Nosho, K., Shima, K., et al., Aurora-A expression is independently associated with chromosomal instability in colorectal cancer. *Neoplasia*, 2009. **11**(5): p. 418-25.
118. Corn, P.G., Summers, M.K., Fogt, F., et al., Frequent hypermethylation of the 5' CpG island of the mitotic stress checkpoint gene Chfr in colorectal and non-small cell lung cancer. *Carcinogenesis*, 2003. **24**(1): p. 47-51.
119. Ota, T., Suto, S., Katayama, H., et al., Increased mitotic phosphorylation of histone H3 attributable to AIM-1/Aurora-B overexpression contributes to chromosome number instability. *Cancer Res*, 2002. **62**(18): p. 5168-77.
120. Takahashi, T., Sano, B., Nagata, T., et al., Polo-like kinase 1 (PLK1) is overexpressed in primary colorectal cancers. *Cancer Sci*, 2003. **94**(2): p. 148-52.
121. Wang, A., Yoshimi, N., Ino, N., et al., Overexpression of cyclin B1 in human colorectal cancers. *J Cancer Res Clin Oncol*, 1997. **123**(2): p. 124-7.
122. Brandes, J.C., van Engeland, M., Wouters, K.A., et al., CHFR promoter hypermethylation in colon cancer correlates with the microsatellite instability phenotype. *Carcinogenesis*, 2005. **26**(6): p. 1152-6.
123. Burum-Auensen, E., Deangelis, P.M., Schjolberg, A.R., et al., Spindle proteins Aurora A and BUB1B, but not Mad2, are aberrantly expressed in dysplastic mucosa of patients with longstanding ulcerative colitis. *J Clin Pathol*, 2007. **60**(12): p. 1403-8.
124. Baldwin, A.S., Jr., The NF-kappa B and I kappa B proteins: new discoveries and insights. *Annu Rev Immunol*, 1996. **14**: p. 649-83.
125. Boatright, K.M. and Salvesen, G.S., Mechanisms of caspase activation. *Curr Opin Cell Biol*, 2003. **15**(6): p. 725-31.
126. Sherr, C.J., Cancer cell cycles. *Science*, 1996. **274**(5293): p. 1672-7.
127. Chang, F., Lacey, M.R., Bouljihad, M., et al., Tumor necrosis factor receptor 1 functions as a tumor suppressor. *Am J Physiol Gastrointest Liver Physiol*, 2012. **302**(2): p. G195-206.
128. Igaki, T., Pastor-Pareja, J.C., Aonuma, H., et al., Intrinsic tumor suppression and epithelial maintenance by endocytic activation of Eiger/TNF signaling in Drosophila. *Dev Cell*, 2009. **16**(3): p. 458-65.
129. Bell, S.P. and Dutta, A., DNA replication in eukaryotic cells. *Annu Rev Biochem*, 2002. **71**: p. 333-74.
130. Kastan, M.B. and Bartek, J., Cell-cycle checkpoints and cancer. *Nature*, 2004. **432**(7015): p. 316-23.
131. Cooper, G.M., *The Cell: A Molecular Approach*. 2000, Sinauer Associates: Sunderland, MA.
132. Chan, K.S., Koh, C.G., and Li, H.Y., Mitosis-targeted anti-cancer therapies: where they stand. *Cell Death Dis*, 2012. **3**: p. e411.

133. Flatt, P.M. and Pietenpol, J.A., Mechanisms of cell-cycle checkpoints: at the crossroads of carcinogenesis and drug discovery. *Drug Metab Rev*, 2000. **32**(3-4): p. 283-305.
134. Musacchio, A. and Salmon, E.D., The spindle-assembly checkpoint in space and time. *Nat Rev Mol Cell Biol*, 2007. **8**(5): p. 379-93.
135. Meraldi, P., Draviam, V.M., and Sorger, P.K., Timing and checkpoints in the regulation of mitotic progression. *Dev Cell*, 2004. **7**(1): p. 45-60.
136. Schmit, T.L. and Ahmad, N., Regulation of mitosis via mitotic kinases: new opportunities for cancer management. *Mol Cancer Ther*, 2007. **6**(7): p. 1920-31.
137. Rieder, C.L. and Maiato, H., Stuck in division or passing through: what happens when cells cannot satisfy the spindle assembly checkpoint. *Dev Cell*, 2004. **7**(5): p. 637-51.
138. Manchado, E., Guillamot, M., and Malumbres, M., Killing cells by targeting mitosis. *Cell Death Differ*, 2012. **19**(3): p. 369-77.
139. Dujardin, D., Wacker, U.I., Moreau, A., et al., Evidence for a role of CLIP-170 in the establishment of metaphase chromosome alignment. *J Cell Biol*, 1998. **141**(4): p. 849-62.
140. Walczak, C.E. and Heald, R., Mechanisms of mitotic spindle assembly and function. *Int Rev Cytol*, 2008. **265**: p. 111-58.
141. Budman, D.R., New vinca alkaloids and related compounds. *Semin Oncol*, 1992. **19**(6): p. 639-45.
142. Pellegrini, F. and Budman, D.R., Review: tubulin function, action of antitubulin drugs, and new drug development. *Cancer Invest*, 2005. **23**(3): p. 264-73.
143. Wang, T.H., Wang, H.S., Ichijo, H., et al., Microtubule-interfering agents activate c-Jun N-terminal kinase/stress-activated protein kinase through both Ras and apoptosis signal-regulating kinase pathways. *J Biol Chem*, 1998. **273**(9): p. 4928-36.
144. Chari, R.V., Targeted cancer therapy: conferring specificity to cytotoxic drugs. *Acc Chem Res*, 2008. **41**(1): p. 98-107.
145. Chopra, A.S., Kuratnik, A., Scocchera, E.W., et al., Identification of novel compounds that enhance colon cancer cell sensitivity to inflammatory apoptotic ligands. *Cancer Biol Ther*, 2013. **14**(5): p. 436-49.
146. Morrison, K.C. and Hergenrother, P.J., Whole cell microtubule analysis by flow cytometry. *Anal Biochem*, 2012. **420**(1): p. 26-32.
147. Ravelli, R.B., Gigant, B., Curmi, P.A., et al., Insight into tubulin regulation from a complex with colchicine and a stathmin-like domain. *Nature*, 2004. **428**(6979): p. 198-202.
148. Nogales, E., Wolf, S.G., and Downing, K.H., Structure of the alpha beta tubulin dimer by electron crystallography. *Nature*, 1998. **391**(6663): p. 199-203.
149. Ranaivoson, F.M., Gigant, B., Berritt, S., et al., Structural plasticity of tubulin assembly probed by vinca-domain ligands. *Acta Crystallogr D Biol Crystallogr*, 2012. **68**(Pt 8): p. 927-34.
150. Trott, O. and Olson, A.J., AutoDock Vina: improving the speed and accuracy of docking with a new scoring function, efficient optimization, and multithreading. *J Comput Chem*, 2010. **31**(2): p. 455-61.
151. Thomsen, R. and Christensen, M.H., MolDock: a new technique for high-accuracy molecular docking. *J Med Chem*, 2006. **49**(11): p. 3315-21.
152. Cheung, H.T. and Terry, D.S., Effects of nocodazole, a new synthetic microtubule inhibitor, on movement and spreading of mouse peritoneal macrophages. *Cell Biol Int Rep*, 1980. **4**(12): p. 1125-9.

153. Himes, R.H., Interactions of the catharanthus (Vinca) alkaloids with tubulin and microtubules. *Pharmacol Ther*, 1991. **51**(2): p. 257-67.
154. Taylor, E.W., The mechanism of colchicine inhibition of mitosis. I. Kinetics of inihbition and the binding of [^{3}H]-colchicine. *J Cell Biol*, 1965. **25**: p. Suppl:145-60.
155. Franco, D.L., Nojek, I.M., Molinero, L., et al., Osmotic stress sensitizes naturally resistant cells to TNF-alpha-induced apoptosis. *Cell Death Differ*, 2002. **9**(10): p. 1090-8.
156. Tait, S.W. and Green, D.R., Mitochondria and cell death: outer membrane permeabilization and beyond. *Nat Rev Mol Cell Biol*, 2010. **11**(9): p. 621-32.
157. Chan, J.Y., A clinical overview of centrosome amplification in human cancers. *Int J Biol Sci*, 2011. **7**(8): p. 1122-44.
158. Kramer, A., Neben, K., and Ho, A.D., Centrosome replication, genomic instability and cancer. *Leukemia*, 2002. **16**(5): p. 767-75.
159. Gergely, F. and Basto, R., Multiple centrosomes: together they stand, divided they fall. *Genes Dev*, 2008. **22**(17): p. 2291-6.
160. Saunders, W., Centrosomal amplification and spindle multipolarity in cancer cells. *Semin Cancer Biol*, 2005. **15**(1): p. 25-32.
161. Chaturvedi, P., Sudakin, V., Bobiak, M.L., et al., Chfr regulates a mitotic stress pathway through its RING-finger domain with ubiquitin ligase activity. *Cancer Res*, 2002. **62**(6): p. 1797-801.
162. Kang, D., Chen, J., Wong, J., et al., The checkpoint protein Chfr is a ligase that ubiquitinates Plk1 and inhibits Cdc2 at the G2 to M transition. *J Cell Biol*, 2002. **156**(2): p. 249-59.
163. Scolnick, D.M. and Halazonetis, T.D., Chfr defines a mitotic stress checkpoint that delays entry into metaphase. *Nature*, 2000. **406**(6794): p. 430-5.
164. Summers, M.K., Bothos, J., and Halazonetis, T.D., The CHFR mitotic checkpoint protein delays cell cycle progression by excluding Cyclin B1 from the nucleus. *Oncogene*, 2005. **24**(16): p. 2589-98.
165. Privette, L.M. and Petty, E.M., CHFR: A Novel Mitotic Checkpoint Protein and Regulator of Tumorigenesis. *Transl Oncol*, 2008. **1**(2): p. 57-64.
166. Toyota, M., Sasaki, Y., Satoh, A., et al., Epigenetic inactivation of CHFR in human tumors. *Proc Natl Acad Sci U S A*, 2003. **100**(13): p. 7818-23.
167. Barton, N.R. and Goldstein, L.S., Going mobile: microtubule motors and chromosome segregation. *Proc Natl Acad Sci U S A*, 1996. **93**(5): p. 1735-42.
168. Kline-Smith, S.L. and Walczak, C.E., Mitotic spindle assembly and chromosome segregation: refocusing on microtubule dynamics. *Mol Cell*, 2004. **15**(3): p. 317-27.
169. Lodish, H., Berk, A., Zipursky, L., et al., *Molecular Cell Biology*. 2000, W.H. Freeman: New York.
170. Pesin, J.A. and Orr-Weaver, T.L., Regulation of APC/C activators in mitosis and meiosis. *Annu Rev Cell Dev Biol*, 2008. **24**: p. 475-99.
171. Goncalves, A., Braguer, D., Carles, G., et al., Caspase-8 activation independent of CD95/CD95-L interaction during paclitaxel-induced apoptosis in human colon cancer cells (HT29-D4). *Biochem Pharmacol*, 2000. **60**(11): p. 1579-84.
172. Taylor, R.D., Jewsbury, P.J., and Essex, J.W., A review of protein-small molecule docking methods. *J Comput Aided Mol Des*, 2002. **16**(3): p. 151-66.

173. Eum, H.A., Vallabhaneni, R., Wang, Y., et al., Characterization of DISC formation and TNFR1 translocation to mitochondria in TNF-alpha-treated hepatocytes. *Am J Pathol*, 2011. **179**(3): p. 1221-9.
174. Micheau, O. and Tschopp, J., Induction of TNF receptor I-mediated apoptosis via two sequential signaling complexes. *Cell*, 2003. **114**(2): p. 181-90.
175. Schafer, K.A., The cell cycle: a review. *Vet Pathol*, 1998. **35**(6): p. 461-78.
176. Gascoigne, K.E. and Taylor, S.S., How do anti-mitotic drugs kill cancer cells? *J Cell Sci*, 2009. **122**(Pt 15): p. 2579-85.
177. Blagosklonny, M.V., Mitotic arrest and cell fate: why and how mitotic inhibition of transcription drives mutually exclusive events. *Cell Cycle*, 2007. **6**(1): p. 70-4.
178. Yamada, H.Y. and Gorbsky, G.J., Spindle checkpoint function and cellular sensitivity to antimitotic drugs. *Mol Cancer Ther*, 2006. **5**(12): p. 2963-9.
179. Li, F., Ambrosini, G., Chu, E.Y., et al., Control of apoptosis and mitotic spindle checkpoint by survivin. *Nature*, 1998. **396**(6711): p. 580-4.
180. Lara-Gonzalez, P., Westhorpe, F.G., and Taylor, S.S., The spindle assembly checkpoint. *Curr Biol*, 2012. **22**(22): p. R966-80.
181. Rao, C.V., Yamada, H.Y., Yao, Y., et al., Enhanced genomic instabilities caused by deregulated microtubule dynamics and chromosome segregation: a perspective from genetic studies in mice. *Carcinogenesis*, 2009. **30**(9): p. 1469-74.
182. Orth, J.D., Loewer, A., Lahav, G., et al., Prolonged mitotic arrest triggers partial activation of apoptosis, resulting in DNA damage and p53 induction. *Mol Biol Cell*, 2012. **23**(4): p. 567-76.
183. Brady, C.A. and Attardi, L.D., p53 at a glance. *J Cell Sci*, 2010. **123**(Pt 15): p. 2527-32.
184. Zilfou, J.T. and Lowe, S.W., Tumor suppressive functions of p53. *Cold Spring Harb Perspect Biol*, 2009. **1**(5): p. a001883.
185. Ha, G.H., Baek, K.H., Kim, H.S., et al., p53 activation in response to mitotic spindle damage requires signaling via BubR1-mediated phosphorylation. *Cancer Res*, 2007. **67**(15): p. 7155-64.
186. Caspari, T., Checkpoints: How to activate p53. *Curr Biol*, 2000. **10**(8): p. R315-R317.
187. Cheng, Q., Chen, L., Li, Z., et al., ATM activates p53 by regulating MDM2 oligomerization and E3 processivity. *EMBO J*, 2009. **28**(24): p. 3857-67.
188. Muller, P.A. and Vousden, K.H., p53 mutations in cancer. *Nat Cell Biol*, 2013. **15**(1): p. 2-8.
189. Rivlin, N., Brosh, R., Oren, M., et al., Mutations in the p53 Tumor Suppressor Gene: Important Milestones at the Various Steps of Tumorigenesis. *Genes Cancer*, 2011. **2**(4): p. 466-74.
190. Vogelstein, B. and Kinzler, K.W., p53 function and dysfunction. *Cell*, 1992. **70**(4): p. 523-6.
191. Hollstein, M., Sidransky, D., Vogelstein, B., et al., p53 mutations in human cancers. *Science*, 1991. **253**(5015): p. 49-53.
192. Levine, A.J., Momand, J., and Finlay, C.A., The p53 tumour suppressor gene. *Nature*, 1991. **351**(6326): p. 453-6.
193. Chopra, A., Anderson, A., and Giardina, C., Novel piperazine-based compounds inhibit microtubule dynamics and sensitize colon cancer cells to tumor necrosis factor-induced apoptosis. *J Biol Chem*, 2014. **289**(5): p. 2978-91.

194. Davis, T.W., Wilson-Van Patten, C., Meyers, M., et al., Defective expression of the DNA mismatch repair protein, MLH1, alters G2-M cell cycle checkpoint arrest following ionizing radiation. *Cancer Res*, 1998. **58**(4): p. 767-78.
195. Fearnhead, N.S., Britton, M.P., and Bodmer, W.F., The ABC of APC. *Hum Mol Genet*, 2001. **10**(7): p. 721-33.
196. Yang, J., Zhang, W., Evans, P.M., et al., Adenomatous polyposis coli (APC) differentially regulates beta-catenin phosphorylation and ubiquitination in colon cancer cells. *J Biol Chem*, 2006. **281**(26): p. 17751-7.
197. Jiricny, J. and Marra, G., DNA repair defects in colon cancer. *Curr Opin Genet Dev*, 2003. **13**(1): p. 61-9.
198. de Voer, R.M., Geurts van Kessel, A., Weren, R.D., et al., Germline mutations in the spindle assembly checkpoint genes BUB1 and BUB3 are risk factors for colorectal cancer. *Gastroenterology*, 2013. **145**(3): p. 544-7.
199. Dalton, W.B. and Yang, V.W., Mitotic Origins of Chromosomal Instability in Colorectal Cancer. *Curr Colorectal Cancer Rep*, 2007. **3**(2): p. 59-64.
200. Huang, H.C., Shi, J., Orth, J.D., et al., Evidence that mitotic exit is a better cancer therapeutic target than spindle assembly. *Cancer Cell*, 2009. **16**(4): p. 347-58.
201. Tao, W., The mitotic checkpoint in cancer therapy. *Cell Cycle*, 2005. **4**(11): p. 1495-9.
202. Masuda, A., Maeno, K., Nakagawa, T., et al., Association between mitotic spindle checkpoint impairment and susceptibility to the induction of apoptosis by anti-microtubule agents in human lung cancers. *Am J Pathol*, 2003. **163**(3): p. 1109-16.
203. Fodde, R., The APC gene in colorectal cancer. *Eur J Cancer*, 2002. **38**(7): p. 867-71.
204. Rowan, A.J., Lamlum, H., Ilyas, M., et al., APC mutations in sporadic colorectal tumors: A mutational "hotspot" and interdependence of the "two hits". *Proc Natl Acad Sci U S A*, 2000. **97**(7): p. 3352-7.
205. Fearon, E.R. and Vogelstein, B., A genetic model for colorectal tumorigenesis. *Cell*, 1990. **61**(5): p. 759-67.
206. Powell, S.M., Zilz, N., Beazer-Barclay, Y., et al., APC mutations occur early during colorectal tumorigenesis. *Nature*, 1992. **359**(6392): p. 235-7.
207. MacDonald, B.T., Tamai, K., and He, X., Wnt/beta-catenin signaling: components, mechanisms, and diseases. *Dev Cell*, 2009. **17**(1): p. 9-26.
208. Aoki, K. and Taketo, M.M., Adenomatous polyposis coli (APC): a multi-functional tumor suppressor gene. *J Cell Sci*, 2007. **120**(Pt 19): p. 3327-35.
209. Kaplan, K.B., Burds, A.A., Swedlow, J.R., et al., A role for the Adenomatous Polyposis Coli protein in chromosome segregation. *Nat Cell Biol*, 2001. **3**(4): p. 429-32.
210. Mahmoud, N.N., Boolbol, S.K., Bilinski, R.T., et al., Apc gene mutation is associated with a dominant-negative effect upon intestinal cell migration. *Cancer Res*, 1997. **57**(22): p. 5045-50.
211. Sablina, A.A., Agapova, L.S., Chumakov, P.M., et al., p53 does not control the spindle assembly cell cycle checkpoint but mediates G1 arrest in response to disruption of microtubule system. *Cell Biol Int*, 1999. **23**(5): p. 323-34.
212. Fragkos, M. and Beard, P., Mitotic catastrophe occurs in the absence of apoptosis in p53-null cells with a defective G1 checkpoint. *PLoS One*, 2011. **6**(8): p. e22946.
213. Tritarelli, A., Oricchio, E., Ciciarello, M., et al., p53 localization at centrosomes during mitosis and postmitotic checkpoint are ATM-dependent and require serine 15 phosphorylation. *Mol Biol Cell*, 2004. **15**(8): p. 3751-7.

214. Morris, V.B., Brammall, J., Noble, J., et al., p53 localizes to the centrosomes and spindles of mitotic cells in the embryonic chick epiblast, human cell lines, and a human primary culture: An immunofluorescence study. *Exp Cell Res*, 2000. **256**(1): p. 122-30.
215. Lavin, M.F. and Gueven, N., The complexity of p53 stabilization and activation. *Cell Death Differ*, 2006. **13**(6): p. 941-50.
216. Fragkos, M., Jurvansuu, J., and Beard, P., H2AX is required for cell cycle arrest via the p53/p21 pathway. *Mol Cell Biol*, 2009. **29**(10): p. 2828-40.
217. Oricchio, E., Saladino, C., Iacovelli, S., et al., ATM is activated by default in mitosis, localizes at centrosomes and monitors mitotic spindle integrity. *Cell Cycle*, 2006. **5**(1): p. 88-92.
218. Vogel, C., Kienitz, A., Hofmann, I., et al., Crosstalk of the mitotic spindle assembly checkpoint with p53 to prevent polyploidy. *Oncogene*, 2004. **23**(41): p. 6845-53.
219. Yang, C., Tang, X., Guo, X., et al., Aurora-B mediated ATM serine 1403 phosphorylation is required for mitotic ATM activation and the spindle checkpoint. *Mol Cell*, 2011. **44**(4): p. 597-608.
220. Field, J.J., Kanakkanthara, A., and Miller, J.H., Microtubule-targeting agents are clinically successful due to both mitotic and interphase impairment of microtubule function. *Bioorg Med Chem*, 2014. **22**(18): p. 5050-9.
221. Soumerai, J.D., Hellmann, M.D., Feng, Y., et al., Treatment of primary mediastinal B-cell lymphoma with rituximab, cyclophosphamide, doxorubicin, vincristine and prednisone is associated with a high rate of primary refractory disease. *Leuk Lymphoma*, 2014. **55**(3): p. 538-43.
222. Johns Hopkins Medicine. From Polyp to Cancer. *Colorectal cancer* 2015. Accessed 2015 May]. http://www.hopkinscoloncancercenter.org/CMS/CMS_Page.aspx?CurrentUDV=59&CMS_Page_ID=0B34E9BE-5DE6-4CB4-B387-4158CC924084.
223. Sancho, E. Molecular mechanisms involved in colorectal cancer initiation and progression. *Oncology Programme*, 2007.
224. Najdi, R., Holcombe, R.F., and Waterman, M.L., Wnt signaling and colon carcinogenesis: beyond APC. *J Carcinog*, 2011. **10**: p. 5.
225. Behrens, J., The role of the Wnt signalling pathway in colorectal tumorigenesis. *Biochem Soc Trans*, 2005. **33**(Pt 4): p. 672-5.
226. Gregorieff, A. and Clevers, H., Wnt signaling in the intestinal epithelium: from endoderm to cancer. *Genes Dev*, 2005. **19**(8): p. 877-90.
227. Smith, K.J., Johnson, K.A., Bryan, T.M., et al., The APC gene product in normal and tumor cells. *Proc Natl Acad Sci U S A*, 1993. **90**(7): p. 2846-50.
228. Sansom, O.J., Reed, K.R., Hayes, A.J., et al., Loss of Apc in vivo immediately perturbs Wnt signaling, differentiation, and migration. *Genes Dev*, 2004. **18**(12): p. 1385-90.
229. Rubinfeld, B., Albert, I., Porfiri, E., et al., Loss of beta-catenin regulation by the APC tumor suppressor protein correlates with loss of structure due to common somatic mutations of the gene. *Cancer Res*, 1997. **57**(20): p. 4624-30.
230. Barth, A.I., Caro-Gonzalez, H.Y., and Nelson, W.J., Role of adenomatous polyposis coli (APC) and microtubules in directional cell migration and neuronal polarization. *Semin Cell Dev Biol*, 2008. **19**(3): p. 245-51.

231. Zumbrunn, J., Kinoshita, K., Hyman, A.A., et al., Binding of the adenomatous polyposis coli protein to microtubules increases microtubule stability and is regulated by GSK3 beta phosphorylation. *Curr Biol*, 2001. **11**(1): p. 44-9.
232. Siegrist, S.E. and Doe, C.Q., Microtubule-induced cortical cell polarity. *Genes Dev*, 2007. **21**(5): p. 483-96.
233. Giaretti, W., Venesio, T., Prevosto, C., et al., Chromosomal instability and APC gene mutations in human sporadic colorectal adenomas. *J Pathol*, 2004. **204**(2): p. 193-9.
234. Hermsen, M., Postma, C., Baak, J., et al., Colorectal adenoma to carcinoma progression follows multiple pathways of chromosomal instability. *Gastroenterology*, 2002. **123**(4): p. 1109-19.
235. Pino, M.S. and Chung, D.C., The chromosomal instability pathway in colon cancer. *Gastroenterology*, 2010. **138**(6): p. 2059-72.
236. Bordonaro, M., Lazarova, D.L., and Sartorelli, A.C., Hyperinduction of Wnt activity: a new paradigm for the treatment of colorectal cancer? *Oncol Res*, 2008. **17**(1): p. 1-9.
237. Tirnauer, J.S. and Bierer, B.E., EB1 proteins regulate microtubule dynamics, cell polarity, and chromosome stability. *J Cell Biol*, 2000. **149**(4): p. 761-6.
238. Zhu, Z.C., Gupta, K.K., Slabbekoorn, A.R., et al., Interactions between EB1 and microtubules: dramatic effect of affinity tags and evidence for cooperative behavior. *J Biol Chem*, 2009. **284**(47): p. 32651-61.
239. Wen, Y., Eng, C.H., Schmoranzer, J., et al., EB1 and APC bind to mDia to stabilize microtubules downstream of Rho and promote cell migration. *Nat Cell Biol*, 2004. **6**(9): p. 820-30.
240. Nakamura, M., Zhou, X.Z., and Lu, K.P., Critical role for the EB1 and APC interaction in the regulation of microtubule polymerization. *Curr Biol*, 2001. **11**(13): p. 1062-7.
241. Zhang, J., Neisa, R., and Mao, Y., Oncogenic Adenomatous polyposis coli mutants impair the mitotic checkpoint through direct interaction with Mad2. *Mol Biol Cell*, 2009. **20**(9): p. 2381-8.
242. Hughes, S.A., Carothers, A.M., Hunt, D.H., et al., Adenomatous polyposis coli truncation alters cytoskeletal structure and microtubule stability in early intestinal tumorigenesis. *J Gastrointest Surg*, 2002. **6**(6): p. 868-74; discussion 875.
243. LeBrasseur, N., The APC-tumor connection. *J Cell Biol*, 2003. **163**(5): p. 926-927.
244. Tighe, A., Johnson, V.L., and Taylor, S.S., Truncating APC mutations have dominant effects on proliferation, spindle checkpoint control, survival and chromosome stability. *J Cell Sci*, 2004. **117**(Pt 26): p. 6339-53.
245. Kops, G.J., Weaver, B.A., and Cleveland, D.W., On the road to cancer: aneuploidy and the mitotic checkpoint. *Nat Rev Cancer*, 2005. **5**(10): p. 773-85.
246. Caldwell, C.M., Green, R.A., and Kaplan, K.B., APC mutations lead to cytokinetic failures in vitro and tetraploid genotypes in Min mice. *J Cell Biol*, 2007. **178**(7): p. 1109-20.
247. Whitehead, R.H. and Robinson, P.S., Establishment of conditionally immortalized epithelial cell lines from the intestinal tissue of adult normal and transgenic mice. *Am J Physiol Gastrointest Liver Physiol*, 2009. **296**(3): p. G455-60.
248. Life Technologies. Lipofectamine(R) 3000 Reagent Protocol. 2014. Accessed 2015. https://tools.lifetechnologies.com/content/sfs/manuals/lipofectamine3000_protocol.pdf.
249. Barth, A.I., Siemers, K.A., and Nelson, W.J., Dissecting interactions between EB1, microtubules and APC in cortical clusters at the plasma membrane. *J Cell Sci*, 2002. **115**(Pt 8): p. 1583-90.

250. Fodde, R., Smits, R., and Clevers, H., APC, signal transduction and genetic instability in colorectal cancer. *Nat Rev Cancer*, 2001. **1**(1): p. 55-67.
251. Li, L., Bennett, S.A., and Wang, L., Role of E-cadherin and other cell adhesion molecules in survival and differentiation of human pluripotent stem cells. *Cell Adh Migr*, 2012. **6**(1): p. 59-70.
252. Reddig, P.J. and Juliano, R.L., Clinging to life: cell to matrix adhesion and cell survival. *Cancer Metastasis Rev*, 2005. **24**(3): p. 425-39.
253. Stypula-Cyrus, Y., Mutyal, N.N., Dela Cruz, M., et al., End-binding protein 1 (EB1) up-regulation is an early event in colorectal carcinogenesis. *FEBS Lett*, 2014. **588**(5): p. 829-35.
254. Liu, M., Yang, S., Wang, Y., et al., EB1 acts as an oncogene via activating beta-catenin/TCF pathway to promote cellular growth and inhibit apoptosis. *Mol Carcinog*, 2009. **48**(3): p. 212-9.
255. Rowinsky, E., The Vinca Alkaloids. Sixth edition ed. Cancer Medicine
ed. D.W.P. Kufe, R.E.; Weichselbaum, R.R., et al. 2003: BC Decker.
256. Klotz, D.M., Nelson, S.A., Kroboth, K., et al., The microtubule poison vinorelbine kills cells independently of mitotic arrest and targets cells lacking the APC tumour suppressor more effectively. *J Cell Sci*, 2012. **125**(Pt 4): p. 887-95.
257. Smith, K.J., Levy, D.B., Maupin, P., et al., Wild-type but not mutant APC associates with the microtubule cytoskeleton. *Cancer Res*, 1994. **54**(14): p. 3672-5.
258. Bettencourt-Dias, M. and Glover, D.M., Centrosome biogenesis and function: centrosomics brings new understanding. *Nat Rev Mol Cell Biol*, 2007. **8**(6): p. 451-63.
259. Doxsey, S.J., Stein, P., Evans, L., et al., Pericentrin, a highly conserved centrosome protein involved in microtubule organization. *Cell*, 1994. **76**(4): p. 639-50.
260. Fukasawa, K., Centrosome amplification, chromosome instability and cancer development. *Cancer Lett*, 2005. **230**(1): p. 6-19.
261. D'Assoro, A.B., Lingle, W.L., and Salisbury, J.L., Centrosome amplification and the development of cancer. *Oncogene*, 2002. **21**(40): p. 6146-53.
262. Karna, P., Rida, P.C., Pannu, V., et al., A novel microtubule-modulating noscapinoid triggers apoptosis by inducing spindle multipolarity via centrosome amplification and declustering. *Cell Death Differ*, 2011. **18**(4): p. 632-44.
263. Zhang, J., Ahmad, S., and Mao, Y., BubR1 and APC/EB1 cooperate to maintain metaphase chromosome alignment. *J Cell Biol*, 2007. **178**(5): p. 773-84.
264. Grady, W.M., Genomic instability and colon cancer. *Cancer Metastasis Rev*, 2004. **23**(1-2): p. 11-27.
265. Prall, F., Duhrkop, T., Weirich, V., et al., Prognostic role of CD8+ tumor-infiltrating lymphocytes in stage III colorectal cancer with and without microsatellite instability. *Hum Pathol*, 2004. **35**(7): p. 808-16.
266. Holcombe, R.F., Jacobson, J., Dakhil, S.R., et al., Association of immune parameters with clinical outcome in stage III colon cancer: results of Southwest Oncology Group Protocol 9009. *Cancer Immunol Immunother*, 1999. **48**(9): p. 533-9.
267. Correale, P., Cusi, M.G., Micheli, L., et al., Chemo-immunotherapy of colorectal carcinoma: preclinical rationale and clinical experience. *Invest New Drugs*, 2006. **24**(2): p. 99-110.
268. Wiemann, B. and Starnes, C.O., Coley's toxins, tumor necrosis factor and cancer research: a historical perspective. *Pharmacol Ther*, 1994. **64**(3): p. 529-64.

269. Ando, K., Kernan, J.L., Liu, P.H., et al., PIDD death-domain phosphorylation by ATM controls prodeath versus prosurvival PIDDosome signaling. *Mol Cell*, 2012. **47**(5): p. 681-93.
270. Stagni, V., di Bari, M.G., Cursi, S., et al., ATM kinase activity modulates Fas sensitivity through the regulation of FLIP in lymphoid cells. *Blood*, 2008. **111**(2): p. 829-37.

APPENDIX A

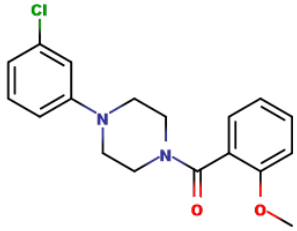

1-(3-chlorophenyl)-4-(2-methoxybenzoyl)piperazine **(AK3)**

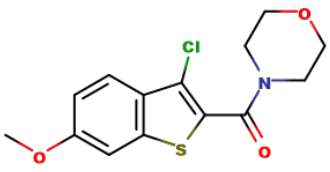

1-(3-chlorophenyl)-4-(2-methoxybenzoyl)piperazine **(AK7)**

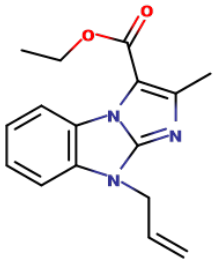

1-(3-chlorophenyl)-4-(2-methoxybenzoyl)piperazine **(AK8)**

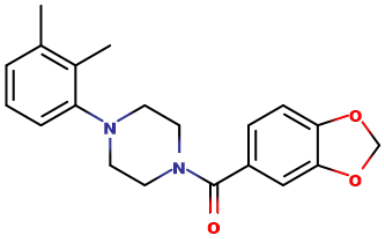

1-(3-chlorophenyl)-4-(2-methoxybenzoyl)piperazine **(AK10)**

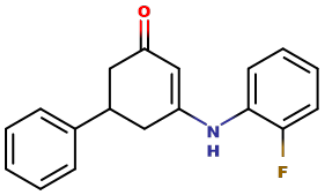

1-(3-chlorophenyl)-4-(2-methoxybenzoyl)piperazine **(AK16)**

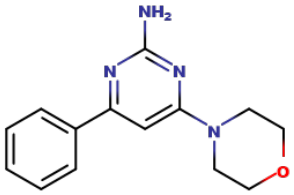

1-(3-chlorophenyl)-4-(2-methoxybenzoyl)piperazine **(AK17)**

Figure A1. Structures of active compounds from the screen.

Structures of the compounds selected out of a screen of 400 compounds from ChemBridge DIVERSet^{TM} library of compounds. These compounds showed the highest levels of caspase-3 activity as suggested by the percentage of cells expressing cleaved caspase-3. The respective IUPAC names of these compounds are listed.

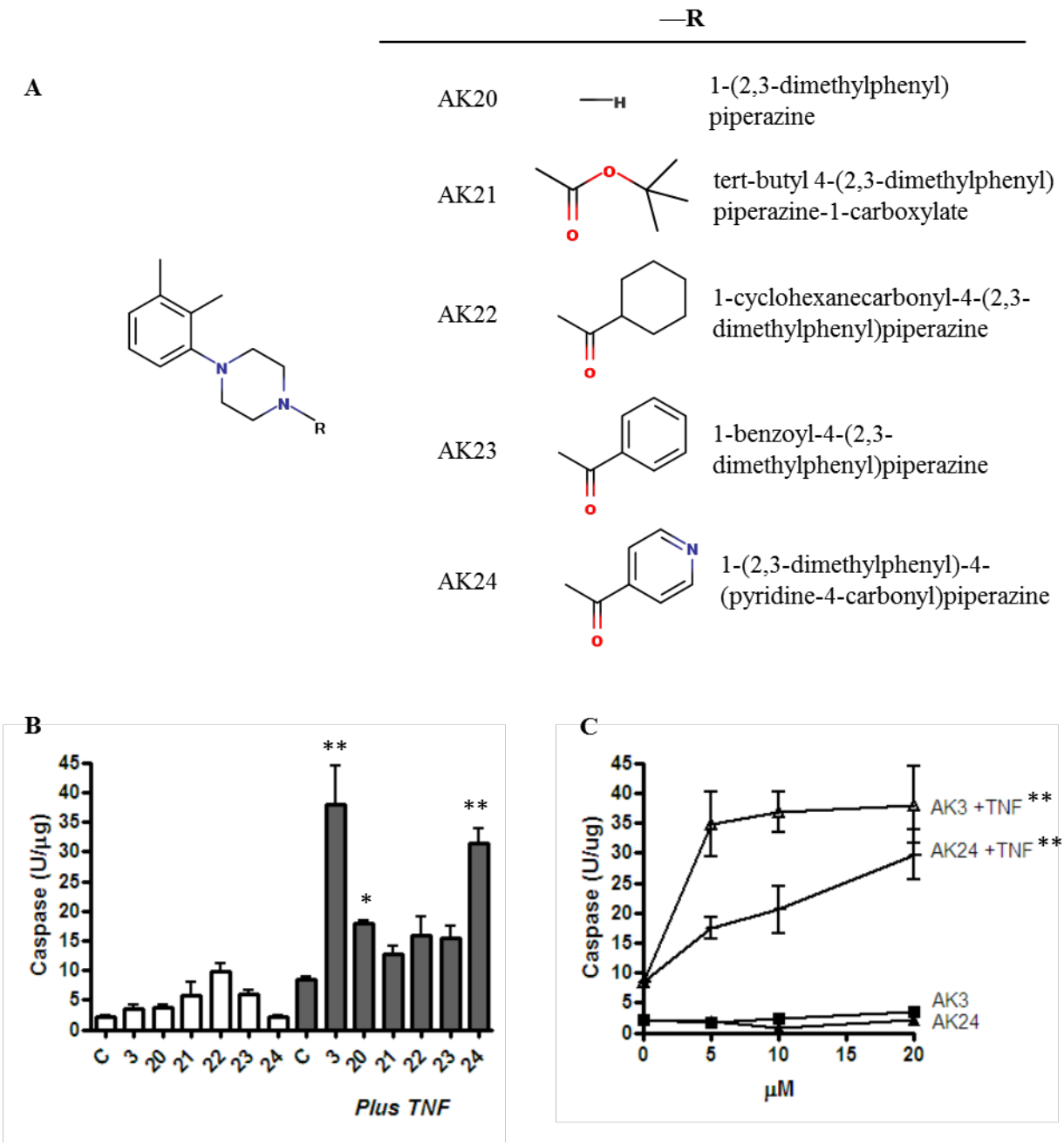

Figure A2. Structure-specific requirement for TNF sensitization of colon cancer cells.

(A) Structural analogs of AK3 and AK10 (AK20-AK24) were prepared with modifications to the benzoyl group and tested for TNF-sensitizing activity. Modifications included removal of benzoyl groups (AK20), substitution with *tert*-butyl (AK21), benzo[1,3]dioxol-5-yl (AK22), phenyl (AK23), and pyridine-4-yl (AK24). (B) Ht29 cells treated with analogs in (A) at 25 µM

and tested for their ability to enhance caspase-3 activation in a TNF-dependent manner using the DEVD-AMC cleavage assay. AK3 and AK24 induced significantly higher caspase activity than the other compounds tested (ANOVA, Tukey's post-doc). (C) Dose-dependent caspase activation with AK3 and AK24 in the presence or absence of TNF was determined using the DEVD-AMC substrate. AK3 was significantly more active than AK24 at lower concentrations (*$P < 0.05$, **$P < 0.01$)

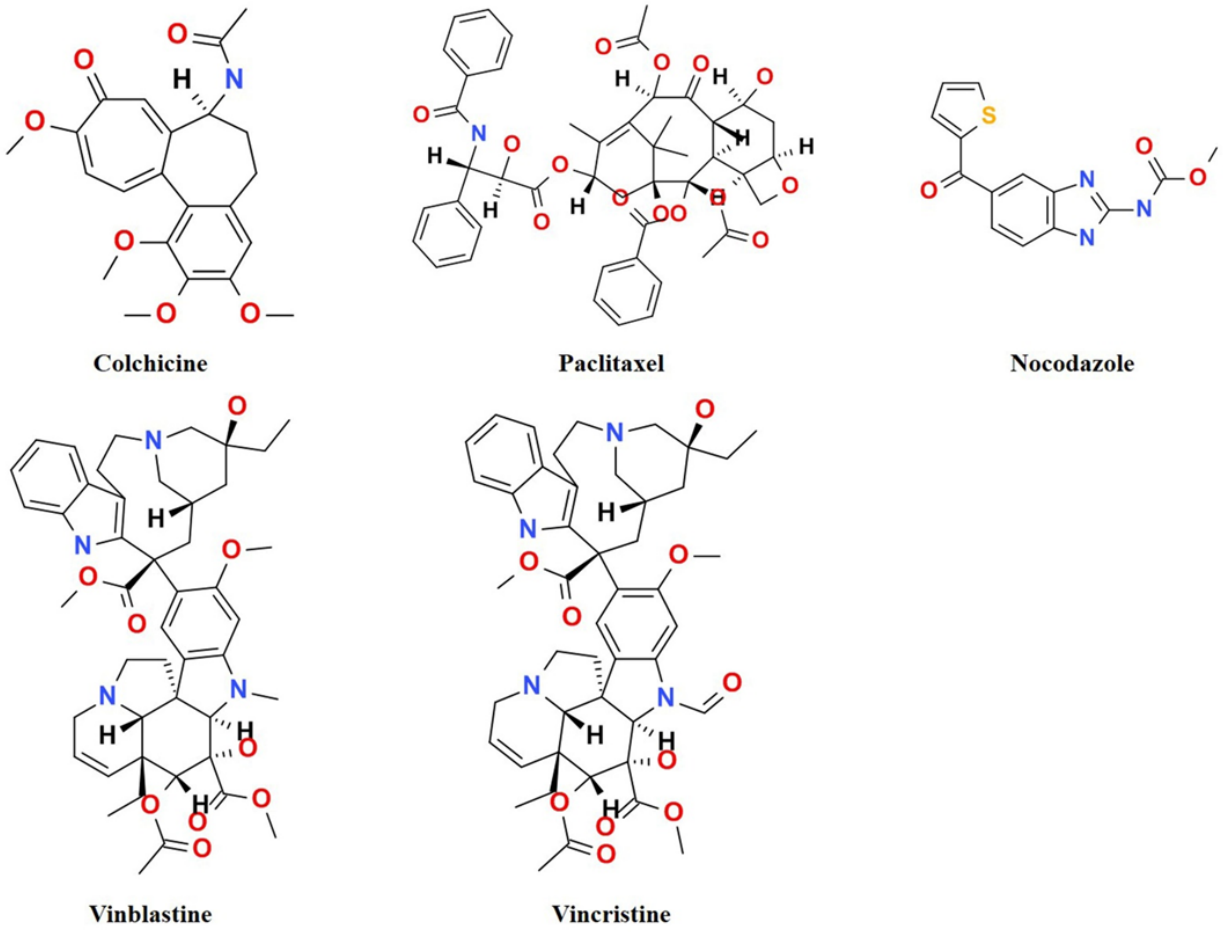

Figure A3. Structures of compounds that alter microtubule dynamics.

Colchicine, nocodazole, and vinca alkaloids (vincristine and vinblastine) are microtubule destabilizers, whereas paclitaxel acts to stabilize microtubules.

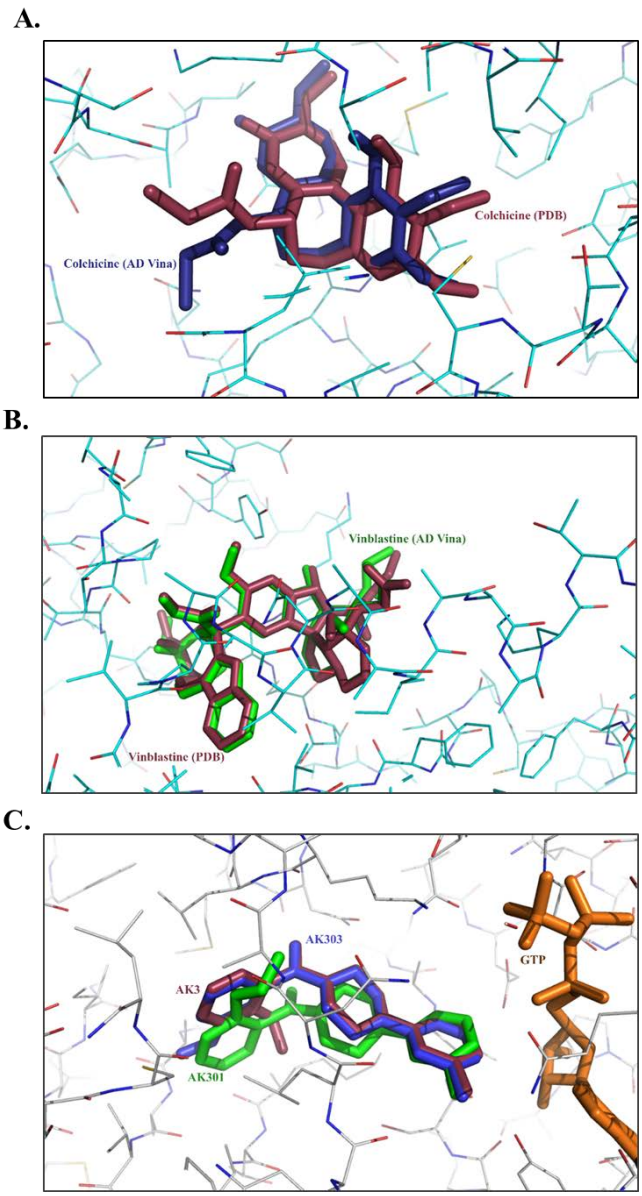

Figure A4. Validation of AutoDock Vina for molecular docking study.

(A) Colchicine, and (B) vinblastine were removed from their respective PDB structures and docked back into tubulin. The lowest energy structural poses obtained from docking were compared to that of the published poses. Both colchicine and vinblastine docked to their respective site with similar poses. (C) Lowest energy poses of AK3, AK301, and AK303. All three compounds bind in the same site on tubulin with similar poses.

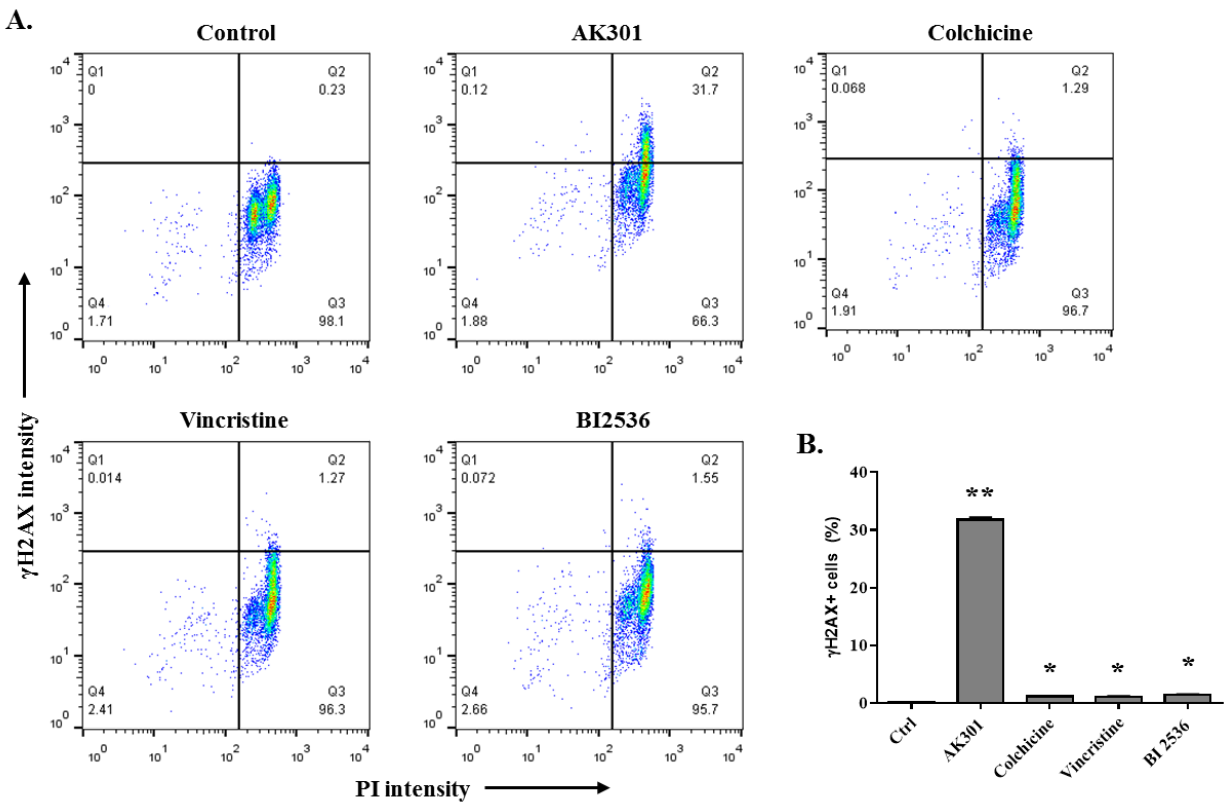

Figure A5. AK301-treated HCT116 cells show activation of γH2AX, but not other mitotic arresting agents.

$p53^{+/+}$ HCT116 colon cancer cells were treated with 500 nM of the indicated mitotic arrest agents. Cells were then fixed and stained for γH2AX and PI as counterstain for DNA. Cells were analyzed by flow cytometry. Analysis was performed on cells that stained positive for PI. (B) Quantification of the flow cytometric data in (A). All agents induced γH2AX activation to some extent (*P < 0.05), but AK301-treated induced a significantly higher (15-fold) (**P < 0.0001) activation of γH2AX.

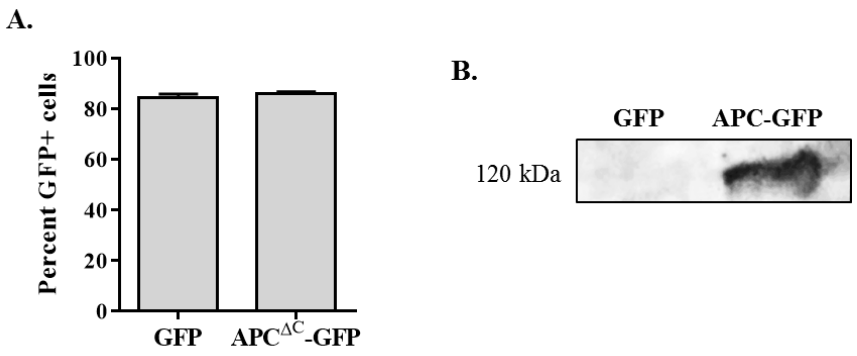

Figure A6. Expression of APC$^{\Delta C}$-GFP in HEK293 cells with high transfection efficiency. (A) HEK293 cells were transiently transfected with GFP or APC$^{\Delta C}$-GFP containing plasmid using Lipofectamine® 3000 Reagent for 24 hrs. Cells were harvested and analyzed by flow cytometry. Transfection of HEK293 cells yielded high transfection efficiencies (> 80%). (B) Protein extracts from transiently transfected APC$^{\Delta C}$-GFP and GFP were prepared using RIPA protein extraction protocol. The lysates were run on polyacrylamide gels, transferred to a nitrocellulose membrane and immunoblotted for N-terminus of APC. APC$^{\Delta C}$-GFP HEK293 showed the expression of truncated APC-GFP fusion protein.